

Rate dependent nonlinear properties of perovskite tetragonal piezoelectric materials using a micromechanical model

Der Fachbereich Maschinenbau & Verfahrenstechnik
der Technische Universität Kaiserslautern
zur Erlangung des akademischen Grades
eines Doktors der Ingenieurwissenschaften
genehmigte Dissertation

von
M.Sc. Mechatronik Ing. Bülent Delibas
aus Malatya, Türkei

Kaiserslautern, September 2005

Hiermit erkläre ich, dass ich die vorliegende Arbeit selbst angefertigt und alle in ihr benutzten Hilfsmittel in der Arbeit angegeben habe; dass ich die Dissertation oder Teile hiervon nicht als Prüfungsarbeit für eine staatliche oder andere wissenschaftliche Prüfung eingereicht habe; dass ich die gleiche oder eine andere Abhandlung nicht bei einem anderen Fachbereich oder einer anderen Universität als Dissertation eingereicht habe.

Kaiserslautern, September 2005

Acknowledgements

I would like to express my deepest appreciation to my advisor, Prof. Dr.-Ing. Wolfgang Seemann for the guidance, encouragement, and feedback he has provided to me during the research and thesis process.

I am also very pleased to acknowledge the financial support of German Research Foundation (Deutsche Forschungsgemeinschaft -DFG "Ingenieurmaterialien auf verschiedenen Skalen: Experiment, Modellierung und Simulation") for this research during the last three years.

I wish to continue my appreciation to Prof. Dr.-Ing. Paul Steinmann and Dr. Andreas Menzel for their continued interest and support in my work.

I am also grateful for the assistance of my colleague Arunachalakasi Arockiarajan during the progression of the research.

I would like to thank my faculty friends Rainer Gaussmann and Andreas Maier for their encouragement in the workgroup Machine Dynamics of Kaiserslautern University of Technology.

I especially would like to thank my mother, brother and sisters, my cousin Arif Yavuz and his wife Suna Yavuz for their support and encouragement.

Finally, I must thank my friends Seda Eden and Ozgün Pelvan for their many hours spent in helping to correct the typescript mistakes in my thesis.

Abstract

Nowadays piezoelectric and ferroelectric materials are becoming more and more an interesting part of smart materials in scientific and engineering applications. Precision machining in manufacturing, micropositioning in metrology, common rail systems with piezo fuel injection control in automobile industry, and ferroelectric random access memories (FRAM) in microelectromechanical systems (MEMS) besides commercial piezo actuators and sensors can be very good examples for the application of piezoceramic and ferroelectric materials.

In spite of having good characteristics, piezoelectric and ferroelectric materials have significant nonlinearities, which limit the applications in high performance usage. Domain switching (ferroelastic or ferroelectric) is the main reason for the nonlinearity of ferroelectric materials. External excessive electromechanical loads (mechanical stress and electric field) are driving forces for domain switching. In literature, various important experiments related to the non-linear properties of piezoelectric and ferroelectric materials are reported. Simulations of nonlinear properties of piezoelectric and ferroelectric materials based on physical insights of the material have been performed during the last two decades by using micromechanical and phenomenological models. The most significant experiments and models are deeply discussed in the literature survey.

In this thesis the nonlinear behaviour of tetragonal perovskite type piezoceramic materials is simulated theoretically using two and three dimensional micromechanical models which are based on physical insights of the material. In the simulations a bulk piezoceramic material which has numerous grains is considered. Each grain has random orientation in properties of polarization and strain. Randomness of orientations is given by Euler angles equally distributed between 0 and 2π . Each element in the micromechanical model has been assumed to have the same properties of the real piezoelectric grain.

In the first part of the simulations, quasi-static characteristics of piezoelectric materials are investigated by applying cyclic, rate independent, bipolar, uni-axial and external electrical loading with an amplitude of 2 kV/mm gradually starting from zero value in virgin state. Moreover, the simulations are undertaken for these materials which are subjected to quasi-static, uni-polar, uni-axial mechanical stress, namely compressive stress. The calculations are performed at each element based on linear constitutive

equations, nonlinear domain switching and a probability theory for domain switching. In order to fit the simulations to the experimental data, some parameters such as spontaneous polarization, spontaneous strain, piezoelectric and dielectric constants are chosen from literature. The domain switching of each grain is determined by an electromechanical energy criterion. Depending on the actual energy related to a critical energy a certain probability is introduced for domain switching of the polarization direction. Same energy levels are assumed in the electromechanical energy relation for different types of domain switching like 90° and 180° for perovskite type tetragonal or 70.5° and 109.5° for rhombohedral microstructures. It is assumed that intergranular effects between grains can be modelled by such probability functions phenomenologically. The macroscopic response of the material to the applied electromechanical loading is calculated by using Euler transformations and averaging the individual grains.

Properties of piezoelectric materials under fixed mechanical stresses are also investigated by applying constant compressive stress in addition to cyclic electrical loading in the simulations. Compressive stress is applied and kept constant before cyclic bipolar electrical loading is implemented.

In the following chapters, a three-dimensional micromechanical model is extended for the simulation of the rate dependent properties of certain perovskite type tetragonal piezoelectric materials. The frequency dependent micromechanical model is now not only based on linear constitutive and nonlinear domain switching but also linear kinetics theories. The material is loaded both electrically and mechanically in separate manner with an alternating electrical voltage and mechanical stress values of various moderate frequencies, which are in the order of 0.01 Hz to 1 Hz. Electromechanical energy equation in combination with a probability function is again used to determine the onset of the domain switching inside the grains. The propagation of the domain wall during the domain switching process in grains is modelled by means of linear kinetics relations after a new domain nucleates. Electric displacement versus electric field hysteresis loops, mechanical strain versus mechanical stress and electric displacement versus mechanical stress for different frequencies and amplitudes of the alternating electric fields and compressive stresses are simulated and presented. A simple micromechanical model without using probabilistic approach is compared with the one that takes it into account. Both models give important insights into the rate dependency of piezoelectric materials, which was observed in some experiments reported in the literature.

Intergranular effects are other significant factors for nonlinearities of polycrystalline ferroelectric materials. Even piezoelectric actuators and sensors show nonlinearities when they are operated with electrical loading, which is much lower than the coercive electric field level. Intergranular effects are the main cause of such small hysteresis loops. In the corresponding chapter, two basic field effects which are electrical and mechanical are taken into account for the consideration of intergranular effects micromechanically

in the simulations of the two dimensional model. Therefore, a new electromechanical energy equation for the threshold of domain switching is introduced to explain nonlinearities stemming from both domain switching and intergranular effects. The material parameters like coercive electric field and critical spontaneous polarization or strain quantities are not implemented in the electromechanical energy relation. But, this relation contains new parameters which consider both mechanical and electrical field characteristics of neighbouring elements. By using this new model, mechanical strain versus electric field butterfly curves under small electrical loading conditions are also simulated. Hence, a rate dependent concept is applied in butterfly curves by means of linear kinetics model. As a result, the simulations have better matching with corresponding experiments in literature.

In the next step, the model can be extended in three dimensional case and the parameters of electromechanical energy relation can be improved in order to get better simulations of nonlinear properties of polycrystalline piezoelectric materials.

Zusammenfassung

Piezoelektrische und ferroelektrische Materialien sind sehr wichtige Komponenten von sogenannten intelligenten Strukturen, die heutzutage in vielfältigen wissenschaftlichen und technischen Anwendungen eingesetzt werden. Kommerzielle piezoelektrische Stapelaktoren und Sensoren, aktive Regelung von Einspritzsystemen in der Automobil Industrie mit Piezo-Aktoren, ferroelektrische Speicher (FRAM) von mikroelektromechanischen Systemen (MEMS) sind sehr bekannte Anwendungen.

Piezoelektrische und ferroelektrische Materialien weisen ein ausgeprägtes nichtlineares Verhalten auf, sofern die Materialien Verwendung im Hochleistungsbereich finden. Hauptursache dieser nichtlinearen Eigenschaften sind Umklappprozesse der ferroelektrischen und ferroelastischen Domänen, welche durch starke äußere elektromechanische Belastungen ausgelöst werden können. In der Literatur finden sich verschiedene experimentelle Untersuchungen in Bezug auf das nichtlineare Verhalten von ferroelektrischen und piezoelektrischen Materialien. Simulationen der nichtlinearen Eigenschaften von ferroelektrischen und piezoelektrischen Materialien wurden in den letzten zwei Dekaden mit mikromechanischen und phänomenologischen Modellen durchgeführt. Die wichtigsten experimentellen und theoretischen Ergebnisse werden im Literaturüberblick angegeben.

In Rahmen dieser Arbeit wird das nichtlineare Verhalten von piezoelektrischen Werkstoffen mit Perovskit-Struktur unter Verwendung zwei- und dreidimensionaler mikromechanischer Modelle simuliert. Der piezoelektrische Werkstoff wird dabei als Summe einzelner Körner aufgefasst, die eine jeweils zufällige spontane Polarisation und Dehnung aufweisen können. Die Orientierung der Polarisation innerhalb der Körner wird zwischen gleichverteilten Eulerwinkeln im Bereich von null und 2π angenommen. Die Elemente im mikromechanischen Modell werden analog zum realen Verhalten der Körner des piezoelektrischen Werkstoffes abgebildet.

In den Simulationen werden zunächst quasistatische Eigenschaften der piezoelektrischen Materialien in Abhängigkeit von zyklischer, bipolarer und einachsiger elektrischer Ladung untersucht, wobei das elektrische Feld am ungepolten Werkstoff schrittweise von 0 bis 2 kV/mm Feldstärke erhöht wird. Darüber hinaus werden auch Simulationen mit quasistatischer, einpoliger und einachsiger mechanischer Druckbelastung durchgeführt.

Die Berechnungen für jedes Element basieren auf linearen konstitutiven Gleichungen, nichtlinearen Umklappprozessen und einem Wahrscheinlichkeitsansatz für das Umklappen der Domänen. Um die Simulationen den experimentellen Daten anzupassen, werden Materialkennwerte, wie zum Beispiel die spontane Polarisierung, die spontane Dehnung, die piezoelektrische und die dielektrische Konstante der Literatur entnommen. Umklappprozesse jeder Domäne werden durch ein Kriterium basierend auf einer elektromechanischen Energiefunktion gesteuert. Die Wahrscheinlichkeit des Umklappens hängt dabei von dieser Energiefunktion ab. Abhängig von der aktuellen Energie im Verhältnis zu einer kritischen Energie wird eine Wahrscheinlichkeit für das Umklappen der Polarisationsrichtung definiert. Dabei werden in der elektromechanischen Energie gleiche Energieniveaus sowohl für das 90° und das 180° Umklappen tetragonaler, bzw. 70.5° und 109.5° für rhombohedrische Mikrostrukturen angenommen. Es wird angenommen, dass interkristalline Effekte zwischen Körnern durch die Wahrscheinlichkeitsfunktionen phänomenologisch modelliert werden können. Die makroskopische Reaktion der Materialien auf die angelegte elektromechanische Last wird durch eine Euler-Transformation und einer Mittelwertbildung der Körner berechnet.

Im weiteren Verlauf werden im Rahmen der Simulationen die Eigenschaften von piezoelektrischen Materialien bei konstanter mechanischer und zyklischer elektrischer Belastung untersucht. Dabei wird zunächst eine mechanische Druckspannung aufgebracht und danach eine zyklische bipolare elektrische Belastung angelegt.

Im weiteren Verlauf wird ein dreidimensionales mikromechanisches Modell verwendet, um die zeit-/geschwindigkeitsabhängigen Eigenschaften bestimmter tetragonaler piezoelektrischer Materialien vom Perovskit-Typ zu untersuchen. Das frequenzabhängige mikromechanische Modell basiert nicht nur auf linearen konstitutiven Gleichungen und nichtlinearen Umklappprozessen, sondern auch auf einer linearen Kinetiktheorie. Der piezoelektrische Werkstoff wird sowohl einem elektrischen Feld als auch einer mechanischen Druckbelastung unterworfen. Beide haben dreieckförmigen Verlauf mit verschiedenen Frequenzen zwischen 0.01 Hz und 1 Hz. Wiederum wird der Beginn der Umklappprozesse über ein Wahrscheinlichkeitskriterium hinsichtlich der elektromechanischen Energie bestimmt. Die Bewegung der Domänenwände während des Umklappens wird mittels einer linearen Kinetiktheorie beschrieben. Mittels Simulationen werden Zusammenhänge zwischen der elektrischen Verzerrung und dem elektrischen Feld, der mechanischen Dehnung und dem elektrischen Feld, der mechanischen Dehnung und der mechanischen Spannung, sowie der elektrischen Verzerrung und der mechanischen Spannung ermittelt.

Des Weiteren wird der Einfluss des Wahrscheinlichkeitsansatzes auf das einfache mikromechanische Modell untersucht. Die Ansätze mit und ohne den Wahrscheinlichkeitsansatz geben beide wichtige Einblicke in das zeit-/geschwindigkeitsabhängige Verhalten von piezoelektrischen Werkstoffen, welches in der Literatur in einigen experimentellen Arbeiten beschrieben wird.

Interkristalline Effekte sind weitere wichtige Ursachen für nichtlineare Eigenschaften polykristalliner ferroelektrischer Materialien. So zeigen auch piezoelektrische Aktoren und Sensoren Nichtlinearitäten, obwohl die elektrische Belastung niedriger als die Koerzitivfeldstärke ist. Interkristalline Effekte sind die Hauptursachen für kleine Hysteresekurven. Im dem Kapitel wird versucht, die elektrischen und mechanischen Einflussfaktoren auf interkristalline Effekte auf mikromechanischer Ebene zu berücksichtigen. Hierzu wird eine neue elektromechanische Energie eingeführt, um sowohl Umklappprozesse als auch intergranulare Effekte zu berücksichtigen. Die Materialkonstanten, wie zum Beispiel die Koerzitivfeldstärke, die spontane Polarisation und die spontane Dehnung, sind nicht in der elektromechanischen Energie enthalten. Es ist jetzt möglich, die kleine Hysteresekurve mit diesem neuen mikromechanischen Modell zu simulieren. Die Simulationsergebnisse des Modells zeigen eine sehr gute Übereinstimmung mit experimentellen Ergebnissen.

Zukünftig kann das Modell auf ein dreidimensionales Modell erweitert werden. Die Parameter der elektromechanischen Energie können verbessert werden, um verbesserte Simulationen der nichtlinearen Eigenschaften polykristalliner piezoelektrischer Materialien zu erhalten.

Contents

Acknowledgements	iii
Abstract	v
Zusammenfassung	ix
Table of contents	1
1 Introduction	5
2 Literature survey	9
2.1 Experimental analysis	9
2.2 Modelling	11
2.2.1 Micromechanical modelling	11
2.2.2 Phenomenological modelling	13
2.2.3 Finite element modelling	16
2.2.4 Rate dependent modelling	17
2.3 Miscellaneous studies	20
3 Concepts of piezoelectric materials	25
3.1 Introduction	25
3.2 Smart structures and properties	25
3.2.1 Ferroelectricity	26
3.2.2 Piezoelectricity	27
3.2.3 Pyroelectricity	31
3.2.4 Electrostrictivity	31
3.2.5 Magnetostrictivity	33
3.2.6 Shape memory effect	33

3.3	Piezoceramic materials	33
3.3.1	Production process of piezoelectric materials	35
3.3.2	Perovskite structures	35
3.3.3	Ferroelectric domains	41
3.3.4	Domain switching	42
3.3.5	Rhombohedral structures	43
3.3.6	Ferroelectric domain switching	44
3.3.7	Ferroelastic domain switching	45
3.3.8	Macroscopic properties	47
4	Quasi-static Models	53
4.1	Structure of the model	53
4.2	Electrical loading	58
4.3	Stress-strain and stress-polarization relations	63
4.4	Electric field and constant compressive stress	70
4.5	Concluding remarks	75
5	Rate dependent model	77
5.1	Relaxation time and frequency	77
5.2	Rate dependent model	77
5.3	Rate dependent cyclic electric loading	79
5.3.1	Simulations	82
5.4	Rate dependent mechanical loading	87
5.4.1	Simulations	88
5.5	Concluding remarks	96
6	Intergranular effects	99
6.1	Concepts	99
6.2	Simulations	102
6.3	Concluding remarks	109
7	Summary	111
	References	113
	Appendix	123

<i>CONTENTS</i>	3
A Theory of piezoelectricity	125
A.1 One dimensional model of piezoelectricity	125
A.2 Thermodynamical relations	129
Resume	135

Chapter 1

Introduction

The motivation of this study is to develop a new micromechanical model for the electromechanical behaviour of polycrystalline piezo- and ferroelectric materials. Despite there are lots of micro- and macromechanical models for the simulations of nonlinear properties of piezoelectric materials, existing models are still suffering to simulate significant characteristics of these materials. The reason of this is as follows. First, the behaviour is getting complicated when electrical and mechanical loading are applied together, so-called electromechanical coupling or linear constitutive behaviour. Secondly, as the applied load is getting higher, the response of the piezoelectric material to mechanical or electrical loading is changing nonlinearly. The microstructure of the materials is distorted spontaneously and temperature is also influencing the lattice structure in a nonlinear manner. Third, such a lattice distortion or phase transformation can give rise to internal stresses in the micro level of the material due to the mismatching of grains or domains. Lastly, the nonlinearity stemming from phase transformation is not irrespective of the rate of the applied loading. Therefore, much more research on piezoelectric materials is still required covering all causes of these nonlinearities both in statical and in dynamical loading cases.

A significant part of applications used in industry are piezoelectric actuators and sensor. Although they are operated in low electromechanical loading conditions, they are still showing nonlinearities, which are the main drawback of these actuators and sensors. Hence, a micromechanical model is also needed for the simulation of nonlinear problems of such applications. Present models have to be extended to cover nonlinearities of both low and high electromechanical loading. Therefore, the suggested model would be robust enough to response in any loading conditions with high correspondence to experimental results.

The content of this paper is as follows: chapter 3 presents principles, concepts, examples and scientific applications of some particular smart structures such as piezoelectric, ferroelectric, electrostrictive and magnetostrictive and shape memory materials. Then,

basic properties of piezoelectric ceramic materials including the types, manufacturing methods, microstructures and mesoscale characteristics are explained in detail. Lastly, the macroscopic nonlinear behaviour of piezoelectric materials, which are subjected to high electromechanical loading is introduced.

Basic piezoelectric linear constitutive relations and their derivations are presented in the first part of the appendix. Linear constitutive equations are first derived from a simple one dimensional electromechanical model. Then, thermodynamical concepts such as first law of thermodynamics are implemented in order to achieve the same piezoelectric constitutive relations.

Chapter 2 is devoted to a literature survey in order to get important insights to experimental and modelling work in the field of piezoelectric materials by different researchers in the past decades. The chapter is divided into subsections like experimental analysis, micromechanical, phenomenological, rate dependent, finite element modelling and miscellaneous works in which more than 130 scientific publications in a wide scale are analysed and summarized.

In chapter 4, a micromechanical model for quasi-static macroscopic properties of perovskite type tetragonal piezoelectric materials under pure electrical, mechanical and electromechanical loading is introduced. The piezoelectric bulk material is assumed to be at the virgin unpoled state in the beginning. First, the model is described and quasi-static properties are given. Then, the material is separately subjected to pure bipolar electrical and unipolar mechanical cyclic loading. During the electromechanical loading case, a cyclic bipolar electrical field together with various constant mechanical stress levels are implemented. The simulation results are illustrated in different macroscopic curves like electric displacement or polarization versus electric field or mechanical strain versus electric field for electrical loading, electric displacement versus mechanical stress or mechanical strain versus mechanical stress with the comparison of corresponding experimental ones.

The focus of chapter 5 is to model and simulate frequency dependent characteristics of polycrystalline piezoelectric materials. The model, which is introduced in chapter 4 is extended to cover the frequency and amplitude dependence for a cyclic loading of these materials. Simulations are performed for various moderate frequencies and amplitude levels of both bipolar electrical and unipolar mechanical (compressive) loading of PZT-PIC 151 (PI Ceramic) material.

Chapter 6 presents another micromechanical model, which takes into account intergranular nonlinearities. New parameters are introduced for characterising the intergranular effects micromechanically. The results are shown in curves for the mechanical strain versus electric field butterfly hysteresis curves not only under high cyclic electric field but also low electric field with different amplitude values for simulating the small hysteresis loops in piezoelectric actuators and sensors. Additionally, the simulations for critical loading cases are also presented.

In chapter 7, conclusion and suggestions for the future work, especially regarding rate dependency and intergranular concepts for polycrystalline piezoelectric materials are given.

Chapter 2

Literature survey

2.1 Experimental analysis

Plenty of experiments have been performed and described in literature in order to observe non-linear properties of ferroelectric materials. For the point of measurements, nearly all the experimental set-up are the same. The sample that is piezoceramic material is usually subjected to both electric and mechanical loading. In order to get a precise measurement generally a rigid servo-hydraulic test frame is used that can exert high compressive stress (figures 2.1 and 2.2). In some experiments a special loading fixture has been used for a correct alignment of the loadings [HLM95], [CE93], [SH96], [Lyn96], [SHF03], [BRB01]. A high electric field is applied to the sample by using high voltage amplifiers. In these experiments mostly strain gauges or non contact measurement instruments (contact-less probe, laser) are involved in order to measure the mechanical strain output. Schaeufele et al. [LFLH99] used inductive displacement transducers instead of strain gauges to get a high repeatability in the strain measurements (figure 2.2). Zhou et al. [ZKM01] used a LVDT (linearly variable displacement transducer) for the strain measurement in their experiments. In addition to strain the electric displacement and the polarization is also monitored by simply adding a capacitor, which is connected to ground. Measurement outputs with strain, electric displacement, stress and electric fields are recorded on a multiple channel data acquisition system via ADC (Analogue to digital converter). In such experiments alternating electric or mechanical loadings are applied. The amplitude of the loading is slowly increased (quasi-static) to observe hysteresis and butterfly loops [HLM95].

The response of piezoelectric materials to more complex, combined electromechanical loading was observed in experiments by Zhou et al. [ZK04]. During the experiments, both electrical and mechanical fields are applied cyclic with various conditions such as in phase and out of phase and different magnitude of mean mechanical pre-stress. One of the significant observations is the slight enhancement of piezoelectric and dielectric

constants for low pre-stress and reduction for higher pre-stress.

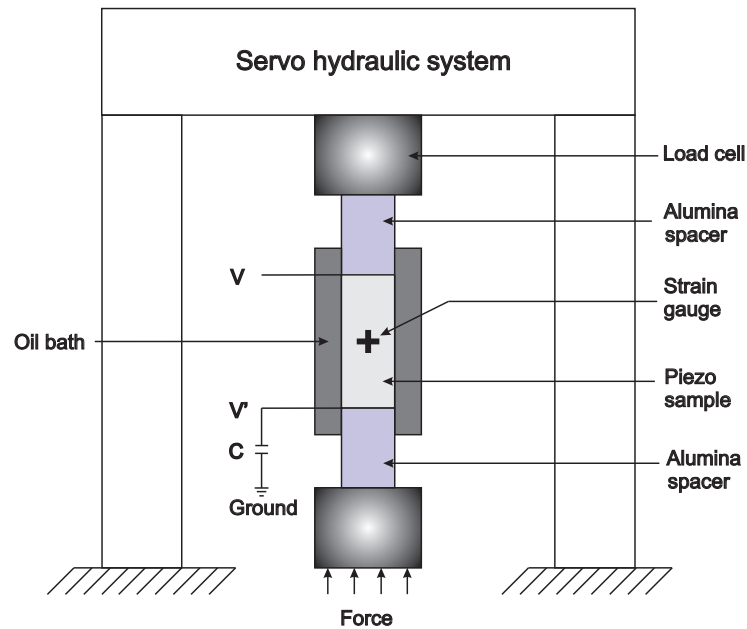


Figure 2.1: Typical experimental set-up 1 (Strain is measured by strain gauges Hwang et al. [HLM95])

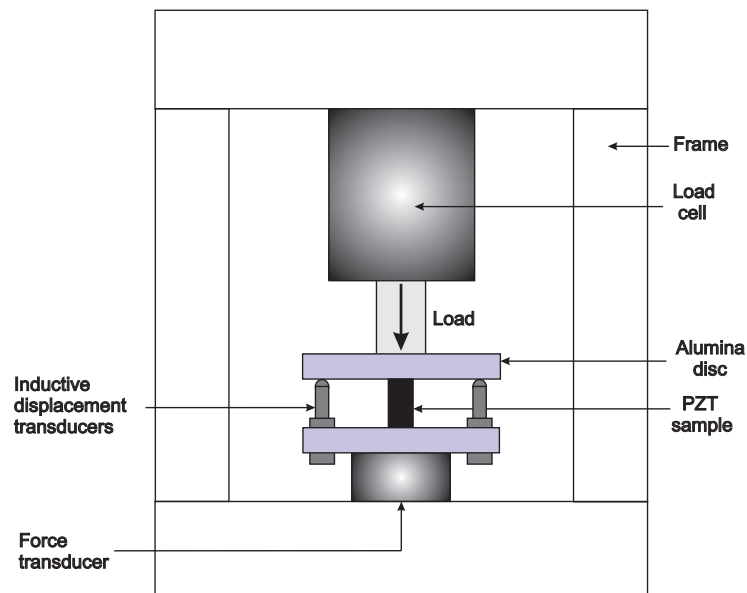


Figure 2.2: Typical experimental set-up 2 (Strain is measured by inductive displacement transducers)

Lynch [Lyn96] made some experiments on soft PLZT material in order to see the effect of nonlinearities of piezoelectric materials on selecting piezoelectric materials. The experiments observed the response of soft piezoelectric materials to the applied electric field and mechanical stress. Basically, the limitations of linear modelling and the limitations of composition of PLZT as an actuator material are investigated for such PLZT materials.

Important contributions by early experimental investigations of ferroelectric materials were presented by Cao and Evans [CE93]. They observed basic stress strain characteristics with linearly changing strain at low and high stress and non linearly changing strain at moderate stress levels of ferroelectric materials. In addition to these, they also observed differences in the responses of the stress strain relationship for hard and soft PZT materials, which have both some similar mechanical properties such as yield strength. In some later experiments, besides the effect of types of PZT (soft or hard), influence of the concentrations of elements and phase changes (tetragonal to rhombohedral and rhombohedral to tetragonal) was also investigated [LFLH99].

Various investigators performed some complex measurements for the assessment of existing multi-axial micromechanical and phenomenological models with experiments, which were done with different loading conditions such as uni-axial compressive stress and coaxial electric field for unpoled BaTiO₃ and PZT ferroelectrics [SHF03].

2.2 Modelling

Computer simulations and modelling are common ways for understanding the characteristics of ferroelectric and piezoelectric materials like in all other research areas. There are two different approaches that have been used in literature. Micromechanical modelling is the one that takes physical insights into account during the simulation. Phenomenological modelling is the other approach that mostly relies on a thermodynamical basis for simulation.

2.2.1 Micromechanical modelling

Simulations of the nonlinear behaviour of piezoelectric materials based on physical insights of the material are performed by using micromechanical models. In these models usually bulk piezoelectric materials are assumed to be composed of domains that are randomly oriented. It is supposed that the behaviour of each element is that of a microcrystal. Linear constitutive equations are used to calculate the effects of the applied electric field and the applied mechanical stress until domain switching occurs. The models assume that the electric field or the mechanical stress in the material is uniform. An energy equation is introduced for the threshold of domain switching. An-

alytical averaging over all elements is implemented in order to get the macroscopic properties according to the micromechanical model.

Several micro-electromechanical models have been developed for the non-linear behaviour of ferroelectric materials. Hwang et al. [HLM95] proposed a similar model like that described above. They use a Preisach hysteresis model to describe the polarization and strain simulation of each grain of the PLZT. In this model the critical energy needed for domain switching is considered to be twice the multiplication of spontaneous polarization and coercive electric field. The model assumes that the macroscopic load is equal to the load on each grain of the PLZT. The simulations are compared with experiments, which were performed with PLZT 8/65/35. The limitation is coming out that this model could not describe the relation between strain and electric field properly. In [MK98], Michelitsch et al. presented an extended analytical approach of the model of Hwang et al. [HLM95]. The model assumes that the material consists of single domain grains which have transversely isotropic micro properties. Macroscopic quantities are derived by a simple analytical averaging. The dielectric hysteresis of the polarization versus electric field, the butterfly hysteresis of strain versus electric field and mechanical depolarization curves under mechanical stress are calculated for the fully poled case.

Chen and co-workers [CFH97] establish a microscopic constitutive relation of single crystal ferroelectric materials by using an internal variable constitutive theory and domain volume fractions. The model is developed for predicting the properties of polycrystalline ferroelectrics based on monocrystalline ferroelectrics. Because of differences between monocrystal and polycrystalline materials, the simulation of the theory does not match exactly.

A self consistent micromechanical model with different sets of switching systems for ferroelectric polycrystals by using some dimensionless micromechanical parameters such as dimensionless piezoelectric constant, polarization and dielectric constants has been presented by Huber et al. [HF04]. Barium Titanate, PZT-4D, and PZT-5H materials are chosen as sample ceramics for the assessment of the model and experiment according to the varying dimensionless material parameters.

Hwang et al. [HM98] presented a simulation for polarization switching to predict electric displacement and strain characteristics of polycrystalline tetragonal ferroelectric ceramics, which are subjected to an electromechanical loading. In their model, the energy required for switching is approximated by using additional parameters to provide the best fit to experimental data that were obtained before. The simulations are carried out for different electrical and mechanical loadings. Though they get reasonable simulations for especially electric displacement and strain versus electric field curves, the simulations are limited in approximating the gradual process of switching.

In an other model, in order to estimate the interaction of the electromechanical field due to the domain switching, an Eshelby inclusion method is provided [HHMF98]. An

ellipsoidal piezoelectric inclusion model in an isotropic matrix, which is derived for domain switching is implemented in the simulations [MH97].

Different types of micromechanical simulations of tetragonal ferroelectric ceramics were performed by Lu et al. [LFLH99]. Using an orientation distribution function for describing the domain patterns of ferroelectrics in micromechanical model was the basic difference of the model from others. Various simulations were performed by using combined electromechanical loadings. The change of the curves were observed while using different stress and electric field values. Their basic limitation was the assumption that the macroscopic load is equal to the load on each grain of the ferroelectric material. Another similar approach was used by Chen and Lynch [CL98]. The model mentioned some other phenomena such as differences between tetragonal and rhombohedral structures, different energy levels associated with switching criteria of these structures (90° and 180° for tetragonal, 70.5° , 109.5° and 180° for rhombohedral), interaction effects between grains and phase transitions (rhombohedral to tetragonal, tetragonal to rhombohedral). Additionally, they applied a linear saturation model to their calculations in order to match simulations with experimental data. Their results show that the interaction energy between grains influences the hysteresis and butterfly curves, but the difference of the crystal structure has no significant effect on the material nonlinearity. Another model tried to explain polarization switching under various loading conditions with non 180° domain switchings [CC01]. It is assumed that there occur only non 180° domain switchings during loading and unloading of piezoelectric ceramics. With this assumption, there need to be two consecutive non 180° domain switchings in order to switch the dipoles in opposite direction. The butterfly and hysteresis curves which are simulated in this model are not so symmetric. This is the basic drawback of the model.

2.2.2 Phenomenological modelling

Phenomenological macroscopic modelling is the other approach that mostly relies on a thermodynamical basis for simulation. Some different phenomenological constitutive models are developed for simulating the behaviour of piezoelectric and ferroelectric materials. Because of having less time requirement for calculations, phenomenological models are in this sense more advantageous than micromechanical models.

Recently, some macroscopic constitutive models were developed to predict the behaviour of ferroelectric and piezoelectric materials. Bassiouny et al. [BGM881], [BGM882] and Bassiouny and Maugin [BM891], [BM892] are the first researchers to develop a nonlinear phenomenological model, which was built within the scheme of a thermodynamical theory. Their model uses plastic deformation and residual polarization as internal variables, which define both reversible and irreversible electromechanical behaviours of ferroelectric media. The model tries to explain the electric effects by using viscoelasticity concepts in mechanics. Most of the recent phenomenological attempts

have been taking this model as a starting point for developing their model. Another early macroscopic model successfully implemented basic hysteresis and butterfly curves with the assumption of delay in domain switching response due to the applied electric field [CM80].

Kamlah et al. [KT99], [KBMT97] presented a simple phenomenological model for ferroelectric materials to simulate the basic dielectric hysteresis, butterfly hysteresis, ferroelectric hysteresis, mechanical depolarization and polarization induced piezoelectricity curves. This model is simple enough to be implemented in a finite element code for the case of uni-axial loadings. The basic assumption of this model is to take the internal state variables as irreversible strain and polarization in addition to stress, strain, electric field and polarization. They take into account the history dependence of the material behaviour by introducing certain internal variables representing the history knowledge of the material. In this model a three dimensional formulation was also presented. Another different phenomenological model is also presented by Kamlah et al. [KJ97], [Kam01]. The model presented macroscopically not only history dependent nonlinearities and dielectric butterfly hysteresis due to switching, but also thermo-electromechanical coupling properties and rate dependent effects in the simulations. In spite of being effective to simulate important properties of ferroelectric materials, the model is too complicated to be solved analytically. Therefore, some numerical methods such as numerical integration is used to model the system.

McMeeking et al. [ML02] propose a phenomenological constitutive model for ferroelectric switching under multi-axial mechanical and electrical loadings. The basis of the model is taking a one-to-one relationship between remnant polarization and remnant strain. Remnant polarization is taken as the only internal variable relating the kinematic effects of the model. This property gives a significant shortcoming to the model that cannot get compressive strains parallel to the polarization direction. Furthermore, it does not produce remnant strain during zero polarization. But it is satisfactory enough for mechanical stresses which are relatively small compared to electrical loadings.

A similar one dimensional phenomenological model based on potential energy equations of different types of domain switching for perovskite type tetragonal piezoelectric material is presented by Harsimar [Har04]. The simulation results are presented with thermal characteristics as well as electromechanical loading. Fully symmetric phenomenological simulation curves are obtained by addition of corresponding dielectric, piezoelectric and elastic properties of piezoelectric materials into domain switching criterions [Lan01].

A constitutive model for non-linear switching of ferroelectric materials is developed by Huber et al. [SH96]. The model uses a single crystal constitutive law that is analogous to slip systems of crystal plasticity theory. Although the model captures the smooth shapes of dielectric hysteresis and butterfly hysteresis loops under electromechanical loads and depolarisation of polycrystalline materials under compressive loads, the higher

computational time is the basic drawback.

A more general multi-axial constitutive model based on thermodynamic formulations for ferroelectric ceramics is presented by Landis [Lan02]. The model is derived from Helmholtz free energy equations. The internal variables used in the model are remnant polarization and remnant strain. The constitutive laws derived from internal variable theories are symmetric. Regarding the computational time, the symmetric model is advantageous for finite element calculations. Landis et al. [LM99] also presented another constitutive model for non-piezoelectric polycrystalline ferroelectrics based upon the domain wall motion through crystals. For predicting the polycrystalline case, a self-consistent scheme is implemented. The model is not able to account for local interactions of neighbouring grains of the polycrystalline material.

Researchers are also trying to compare experimental curves, which are performed under multi-axial loading, with the existing models such as rate independent crystal plasticity model, viscoplastic crystal plasticity model and phenomenological models concerning the dielectric behaviours [HF01]. Experimental curves are presented in electric displacement versus electric field curves for a selection of different loading angles ($0^\circ, 45^\circ, 90^\circ, 135^\circ, 180^\circ$). Among these models, a self consistent model is found to match more accurately to multi-axial loading experiments than others. On the other hand, a self consistent model is the slowest one from the computational point of view. Therefore, sometimes it is required to reduce the number of internal variables used in the model for increasing the efficiency of the computation. Ferroelectric domain evolution is modelled with the help of grain growth theory by Loge and Suo [LS96]. They use variational principles in order to model domain wall motions in a thermodynamic non-equilibrium process.

There are plenty of similar phenomenological models like the one presented by Cocks and McMeeking [CM99]. Their model is akin from the point of view of taking remnant polarization and remnant strain as internal state variables in Helmholtz free energy relation.

Zhang et al. [ZR93] also formulated a 1-D macroscopic model based on the first and second laws of thermodynamics applying a continuum mechanics concepts. Detailed analysis of the energy release, which depends on the local electromechanical fields before and after domain switching, is investigated by Kessler et al. [KB01]. The analyses were applied for the modelling of switching stability and re-polarization.

An extensive basic knowledge of piezoceramic and ferroelectric materials is given by Jaffe et al. in [JCJ71]. The constitutive relations can also be extended to finite strain piezoelectric polymers [LM94].

2.2.3 Finite element modelling

The finite element method is also an effective approach for the simulation of piezoelectric materials. It can be implemented to both micromechanical and phenomenological modeling. General finite element formulation with the basic principle was given by Allik et al. [AH70]. Linear properties of piezoelectric materials for statical loading with the examples of various geometrical shapes are implemented by Peelamedu et al. [PBDN01] with the help of a finite element model.

Finite element methods for analyzing and simulating such nonlinear problems have been known as their increased computational burdens in the models. In spite of taking much more time for simulation, the finite element method can also be implemented in micromechanical approaches [TWSK02]. Therefore, it is becoming inefficient from a calculation point of view especially in some large scale application problems such as nonlinearities of piezoceramics near crack tip. Cao et al. [CG01] presented a modified micromechanical finite element method for fully coupled piezoceramic materials in order to decrease the computational efforts. They used analytical methods instead of a finite element solution in one part of the simulations for both single crystallite and polycrystalline piezoceramic materials.

Li et al. [LF04] developed a three dimensional finite element model for the non-linear modelling of ferroelectric materials with tetragonal microstructures. Due to the assumption of boundary conditions of the model, elements in the free faces of the material undergo domain switching in a less electrical loading than the ones in the constrained faces. In the model the energy barrier for 90° domain switching is assumed to be one quarter of 180° domain switching. Therefore, for all elements there occur two successive 90° domain switchings instead of one 180° domain switching. In addition to a constant uni-axial loading there have been multi-axial loadings for the investigation of the change of butterfly and hysteresis curves. It is shown that the initial poling directions have little effect on hysteresis loops. Simulation results are given not only with electric displacement-electric field and strain-electric displacement curves for an electrical loading but also stress-strain and stress-electric displacement curves.

A study of polarization switching in polycrystalline ferroelectric materials with internal electrical and mechanical contributions has been given by Hwang et al. [HW00], [HW00] using the finite element method. The simulation shows that domain switching occurs for an electrical loading of less than 5 % of the coercive electric field. The model explains the polarization switchings and probability of possible switching of neighbouring regions at low loadings with the explanation of the Rayleigh law. This is the prediction of propagating polarization switching sequence forming a parabolic shape with the major axis which is parallel to the applied electric field direction for low loading range. They use a phenomenological parameter called weighting factor for the mechanical and electrical contribution to polarization switching to simulate hysteresis and butterfly curves. When the electrical contribution is higher, which is given by the

lower values of weighting factor, 90° domain switching is more encouraged than 180° domain switching or vice versa. Grain size effects of the materials to the electric displacement versus electric field curve have been also discussed and confirmed by finite element simulations and show that polarization switching is not dependent on the size [HW00].

Unlike using a scalar electric potential to nodal points of a standard finite element calculation, Landis [Lan02] implemented a vectorial electric displacement derived from an electric potential, which is more advantageous for the numerical stability of the nonlinear behaviour of piezoelectrics. However, the number of nodal degrees of freedom is increased in 3-D problems. Ghandi et al. [GH97] proposed a hybrid finite element model which increases the numerical efficiency of modelling the nonlinear behaviour of PZT ferroelectrics. By means of eliminating some internal iterations in finite element calculation, the hybrid finite element model is more successful than conventional models especially in computational time.

Arockiarajan et al. [ADMS1],[ADS04],[ADSM04] present a three-dimensional nonlinear finite element micromechanical model based on a free energy equation, which covers a domain switching criterion and a probabilistic model. The model is also extended for rate dependent properties of piezoceramic materials by means of linear kinetics theory in addition to quasi-static electromechanical loading. Simulations are performed not only for pure cyclic electric and mechanical stress but also for constant compressive stress with cyclic electric loading.

2.2.4 Rate dependent models

In experiments it has been observed that the mechanism of domain switching in grains of piezoelectric materials is dependent on the rate of the loading. Therefore, the process becomes more nonlinear when the macroscopic alternating loading is applied with different frequencies. In some applications of piezoelectric materials, rate dependent characteristics are important and have to be studied.

Early experiments about determination of electric field and temperature dependence of switching time and current were performed by Merz [Mer54] for BaTiO_3 single crystals. Additionally, he explained the switching mechanism as nucleation of new domains and a growth process with domain wall motion. At the constant applied electric field, reduction of switching time and thus increasing switching current were observed when the temperature is increased. Thus, the nucleation of domains and the growth process are becoming faster at higher temperatures. Likewise, the dependence of the switching time and current with respect to the applied electric field and the coercive field at a fixed temperature is observed. One of the first discussion for simulating the rate dependence of the polarization curve of BaTiO_3 is given by Landauer et al. [LYD56] with the help of Merz's [Mer54] observations, in which the rate of switching was basically related to

the exponential function of the applied electric field. Although the mechanism of the switching process is not determined clearly as nucleation and a domain expansion, they manage to illustrate the change of the coercive field during the application of an electric loading with different rates. Then minimum coercive electric field is found for the minimum loading rate. According to his experiments Drougard [Dro60] proposed that rate dependent properties of BaTiO₃ are dominated by domain wall motion governed by a nucleation process of polarization switching and he argues that nucleation does not disappear completely during the starting and end of the polarization switching.

Extensive analysis of rate dependent domain switching mechanisms both nucleation and growth of the switching microstructure in ferroelectric materials based on thermodynamics and kinetics is presented by Kukushkin et al. [KO02].

Behaviours of domain wall motion for BaTiO₃ and electrostrictive strain response are experimentally analysed under both quasi-static and frequency dependent cyclic electric loading in addition to a constant mechanical stress [BRB02]. The measurements are performed in real time with the help of a microscope and CCD (charge coupled device) camera in the experimental set-up. A high resolution LVDT is used for measuring displacements of the sample.

Mukherjee et al. [MRLMY01] measured dielectric, elastic and piezoelectric constants of both soft and hard piezoelectrics as a function of not only electric field and mechanical stress but also temperature and frequency of the loading by using a laser interferometer system which makes measurements very easy and effective both in longitudinal and transverse directions. According to these experiments piezoelectric constants are not changing dramatically as the frequency of the alternating loading is increased. The response of the piezoelectric constants for hard piezoelectrics (PZT EC-69) is nearly the same with respect to loading frequency. However, they are decreasing in values (5-15 %) for soft materials (PZT EC-65) as the frequency is increased from 10⁻² Hz to 10³ Hz.

The influence of rate dependence on the polarization and strain is investigated by Zhou et al. [ZKM01]. The experiments are performed in a low frequency range between 0.01 Hz to 1.0 Hz. In their experiment the coercive electric and stress fields are found to increase with increasing frequency in polarization and strain versus electric field curves. The saturation polarization and strain values are not detected any more when the frequency is increased. Besides, the change in the characteristics of the strain versus polarization graph is also detected. It is claimed that the different rate orientation of switching types (90° and 180°) is supposed to be the reason of experimental results. Burcsu and co-workers [BRB01] investigate also the rate dependent response of mechanical strain of BaTiO₃ in their experiments. They observe the increase in coercive electric field level when the frequency is increased (0.05 Hz to 1 Hz) as well. But surprisingly, increments of saturation or remnant strain value are observed so high, when the loading frequency is increasing from 0.05 Hz to 1 Hz. Thus, experimental results

are not matching exactly to Zhou's [ZKM01] observations. However, they are both performing the experiments at the same loading rate level. The basic reason for such different behaviours can be explained by using different piezoelectric sample types, which are used in the experiments

A nucleation and growth mechanism in phase transformation of materials and kinetics relations is first proposed by Avrami [Av39], [Av40], [Av41]. There are some modifications to this theorem to get best fitting of polarization switching versus time for ferroelectric materials by taking into account the geometrical boundary criteria and an anisotropic size and growth mechanism [SRM98]. Cao et al. [CTX99] present a simulation of ferroelectric phase transition to emphasize the effects of boundary conditions using a time dependent Ginzburg-Landau model. It is verified in the model that surfaces are the favourable nucleation places for polarization switching. Wang et al. [WSCLZ04] simulate the polarization switching using a phase field model, which is based on an extensional version of the Ginzburg-Landau model with taking into consideration the effects of bulk free energy, electric and elastic energies, domain wall energy, dipole-dipole electric and elastic interaction energy components. Although the model results in an asymmetric behaviour for the mechanical strain versus electric field curve, the simulations have shown the proof of the kinetics process of nucleation and growth of new domains in domain switching.

A macromechanical model for time dependent hysteresis of PZT5A piezoelectric material at low range frequencies is given by Smith et al. [SOW01]. The model incorporates rate dependency to the basic quasi-static hysteresis model in which the effect of inclusions to the domain wall motion is considered as well. Although the model does not accurately predict the change in coercive field, it catches the reduction in remnant polarization during an increase of the loading frequency in a low regime.

A 3-D continuum model, covering switching criterion and kinetics of polarization switching has been successfully applied to 2D ferroelectric ceramics using a finite element method by Kim et al. [KJ02]. The model assumes that the material consists of various types of ferroelectric variants the behaviour of which is characterized by Helmholtz free energy. Nucleation of domains and kinetics of switching are determined by the value of the electromechanical energy and driving force between variants respectively. A simple linear kinetic relation is used for the propagation of the new variant. The model explains the rate-dependent behaviour in terms of the changes in mass fractions of different types of variants. The simulations are performed for hysteresis and butterfly curves for cyclic loadings of various frequencies. The model shows the enlarging of the hysteresis curve when the loading frequency is increased.

Viehland et al. [VC00] present an experimental investigation of the frequency dependent characterisation of ferroelectric material with chemical name $0.7\text{Pb}(\text{Mg}_{1/3}\text{Nb}_{2/3})\text{O}_3-0.3\text{PbTiO}_3$. Additionally, a random field model based on the creation of polar clusters with a reversed polarization within ferroelectric domains is introduced for the kinetics

of domain switching and domain dynamics. The results of experiments and simulations can be well understood for such types of ferroelectrics. However, there are some missing points for different ferroelectric materials such as increasing of the macroscopic polarization during the early unloading stage of the electric field up to the coercive field at higher frequencies. The validity of heterogeneous nucleation in the environments of quenched random fields in soft ferroelectric materials is demonstrated and nucleation processes which are not restricted to be on domain walls are given to be related to the impurity density of inhomogeneous polycrystalline materials [VL01].

Omura et al. [OAI91] propose a simple 1-D lattice model for the explanation of delay during polarization switching by a so-called viscosity constant. In their model, as the viscosity constant is increased, the coercive field of the hysteresis curve simulation increases like in the case of a high frequency cyclic loading of piezoelectric materials.

Another time dependent property of piezoelectric materials is ageing, which is the change of material parameters such as remnant polarization and strain with time after completion of the loading and the unloading process at long term loading. Zhou [Zho03] observed a reduction of the absolute magnitude of the electric displacement and strain with different loading rates during relaxation time duration of PIC 151 soft PZT in his experiments.

2.3 Miscellaneous studies

Rayleigh law which is used basically for magnetic equations can also be applied to some ferroelectric materials showing piezoelectric property such as PZT and BaTiO₃ under low electromechanical fields. Damjanovic [Dam97] showed the applicability of Rayleigh rule by presenting quadratic relation between the charge density and the applied alternating mechanical stress and a linear relation between the piezoelectric constant and the frequency and amplitude of the applied alternating mechanical stress for such materials. It is indicated that the dependence of the piezoelectric constant on the mechanical stress and small piezoelectric hysteresis loops can be explained by pinning of domain walls different than 180°. But still there are some properties of ferroelectric materials which do not obey this principle. It is proposed that there are still many non-180° domain walls at the fully poled state of polycrystalline ferroelectric materials [Dam98]. Therefore, the mechanical strain versus electric field curve characteristics is explained by these non switched non-180° domain walls. The domain switching process in both fine and coarse grained perovskite type tetragonal elements has been investigated by Arlt et al. [Arl96S], [Arl97], [Arl96A]. It is proposed that during a 180° domain switching of the grain a new transient highly mobile 90° domain wall is generated inside the grain for electrical loading, which is higher than the coercive level. As it can be seen in figure 2.3 that 180° domain switching is achieved for the complete domain by having only 90° domain switching in sub-domains with domain wall motion

beginning at the grain boundary. Propagation of new domains is dominated by the phase boundary between old and new nucleated phases. Although sub-domains have completely 90° domain switchings, the total domain undergoes an overall 180° domain switching. Hysteresis curves that are using one critical electrical switching field have been simulated with the described model. The model can explain nonlinear dielectric phenomena, although it deviates from the other models which assume two successive 90° switchings in order to achieve a 180° switching. Additionally, the model fails to explain the 90° switching of the overall grain.

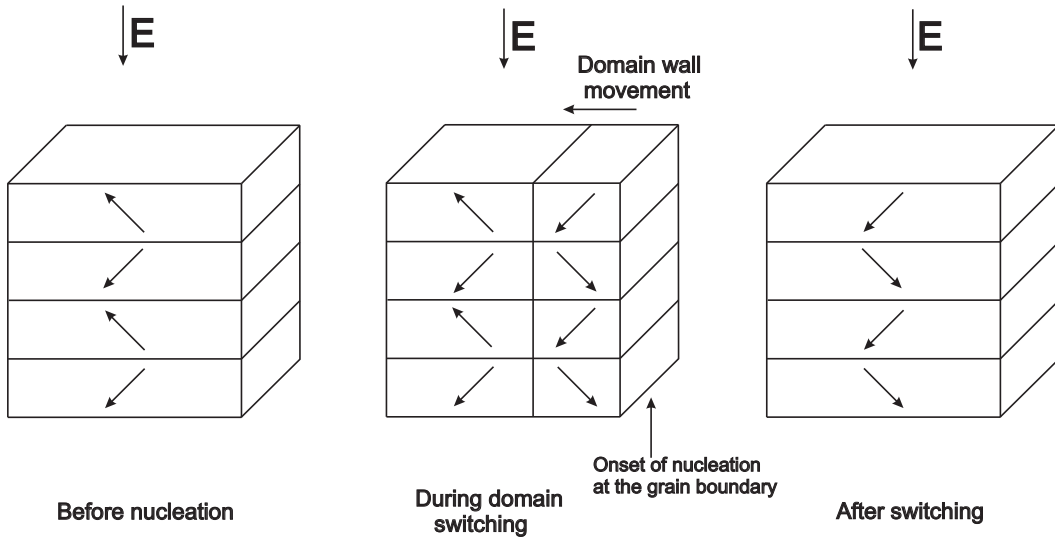


Figure 2.3: Domains inside one grain under electrical loading, before, during and after the switching process (Arlt et al. [Arl96S], [Arl97], [Arl96A], [AN88])

Different orientation distributions between grains or microstructures inside bulk piezoelectric materials have been taken as a basic assumption for modelling of polycrystalline piezoelectric materials. Effects of different orientation distributions on the macroscopic behaviour of piezoceramics are investigated by Fotinich et al. [FC00S] using a micro-mechanical finite element model. They use two types of crystalline distributions. One type is a regularly changing distribution where each element has an orientation difference of an angle of 2° from the neighboring element through the layers of the material. The second type is a random distribution. It is observed in the simulations that macroscopic curves are sharper for a regularly changing distribution than for a random one. The authors used different domain switching criteria based on electric displacement with stability arguments instead of free energy criteria in their other finite element model of monocrystalline piezoceramics [FC00J]. The model is applied in characteristics of fatigue behaviour near a crack in piezoelectric materials under electromechanical loading. The influence of parameter data to the macroscopic behaviour is investigated analytically by varying permittivity and piezoelectric coefficients in the model [FC02].

Gerthsen et al. [GK76] try to formulate the coercive field of fine grained PLZT materials with respect to some material parameters such as spontaneous polarization, spontaneous strain and elastic modulus by characterizing predominantly a non 180° domain switching process in grains. For tetragonal elements the formulation of the coercive field for the displacement of 90° domain walls is also presented with respect to basic piezoelectric material parameters [Sch81], [Kr76].

A domain switching criterion based on internal-energy density has good prediction of 180° and 90° domain switching parameters especially at the point of mechanical loading [SA04].

The influence of interactions of domains to the macroscopic behaviour of piezoelectric materials according to thermodynamic approach and internal variables is presented by Elhadrouz et al. micromechanically [EZP05]. Interaction concepts stem from the incompatibilities of the spontaneous strain and electric displacement fields between domains. Nevertheless, simulations under a compressive loading are given with the assumptions, they are not successfully illustrated due to the inaccurate implementations of the interaction energy in the simulations. Ball et al. [BSKS05] develop a ferroelastic switching model for lead zirconate-titanate (PZT) which quantifies the internal and electrostatic energy associated with 90° and 180° dipole orientations. In order to incorporate inhomogeneities of domains, interaction energy implemented in the energy equations is assumed to be related to exponential functions and variances of experimentally measured values. The results are shown in hysteresis and butterfly curves under various constant compressive stresses with corresponding experimental ones. A statistical theory of ferroelectric materials like BaTiO_3 doped with Fe are analyzed in order to understand the random interactions of such dopants in ferroelectric materials [Bos87]. Chen et al. [CW98] study ferroelectric domain wall motion formulated in analogy with dislocation theory in plasticity.

A constitutive model for the nonlinear effective behaviour of piezoceramic materials is presented in [RK00], [RK00F]. The model is restricted to a small electromechanical loading so that the nonlinearity due to domain switching is assumed to be negligible. The basic aim of the study is to model the effect of interaction of the microcrystals in a statistical method using effective medium approximation. Lateral domain wall motion is taken as the dominating cause of the nonlinearity for small loads. The criterion for domain wall motion is based on the thermodynamic energy difference for changing domain volume fractions. In [RK99], the only effect of orientation distributions of grains in a polycrystal on the linear electro-elastic properties of piezoceramic materials using effective medium approximation is presented. The effective medium approximation method is also applied in ferroelectric composite materials for calculating thermo-electro-elastic properties [KR98].

There are some approaches for deriving effective piezoelectric material constants. Effective linear dielectric, elastic and piezoelectric constants of piezoceramic are determined

by using a numerical method for random volume elements [FBW00]. In this work, the polycrystalline material is assumed to consist of single domain crystals generated by random Voronoi tessellation. The basic addition of this model is taking into account the effect of interactions between grains.

Meyer et al. [MV02] investigated the properties of 180° and 90° domain walls in PbTiO_3 in order to prove that the energy required to create a 180° domain wall is higher than for a 90° domain wall for defect free structures. They use an atomistic approach and calculate the fully relaxed atomic structure, polarization profile across the domain wall and barrier level for a domain wall motion. The calculations of energy requirements result in 35 mJ/m^2 for 90° domain wall, about a factor of 4 lower than the energy of 180° domain wall creation, which is found to be 134 mJ/m^2 .

Haug et al. [HOG05] demonstrated a two dimensional multi-grain model, which predicts internal stresses during poling as a consequence of a mismatch in crystal orientations of a ferroelectric polycrystal by using the micromechanical model of Huber et al. [HFLM99]. The results are presented in macroscopic butterfly and hysteresis curves for an unpoled single and polycrystals by applying an electric field. However, they manage to fit their simulations to experimental hysteresis curves. The difference in mechanical strain is found to be smaller during a cyclic loading than during the poling from the virgin state in the butterfly curve.

It is experimentally found that the porosity of the material structure significantly influences the material constants of piezoelectric materials such as piezoelectric and elastic constants [Kah85], [NIOB80], [BW89]. Dunn [Dun95] proposed a theoretical self-consistent approach for the estimation of grain shape anisotropy and the influence of porosity which is found to have a strong effect on the dielectric constant.

Effects of mechanical stress under cyclic electric loading for heterogeneous electro-mechanically coupled ferroelectric materials using Eshelby's method to the inclusion problem are presented by related authors [LW02].

Chapter 3

Concepts of piezoelectric materials

3.1 Introduction

The aim of the present chapter is to introduce the basic concepts of piezoelectrics and ferroelectrics with other categories of smart materials, which are magnetostrictive, electrostrictive, shape memory and pyroelectric. Definitions of such smart materials including piezoelectricity are provided with additional examples of scientific and engineering applications. Then, piezoelectric ceramic materials are explained in more detail in a wide range like manufacturing processes, microstructures in micro- and mesoscale, linear and nonlinear properties and macroscopic analysis.

3.2 Smart structures and properties

Materials which sense a change in the environment and give a useful response by using a feedback system are called intelligent or smart materials. Input sensing and output responses for smart materials are basic natural quantities such as electric field, mechanical stress, magnetic field and heat. The principle of actuators and sensors are explained in this concept. Figure 3.1 shows the responses of smart materials to input conditions. Electrical polarization can be the output of heat and mechanical loading. Likewise, material senses electrical loading change by distorting its geometrical shape resulting a mechanical strain as an output. The definition of such materials can be extended to "very smart" materials which exhibit adaptive response according to conditions of these natural quantities by changing their property coefficients (piezoelectric constant, elastic constant, dielectric constant). Therefore, macroscopic properties of "very smart" materials are highly nonlinear [NXKC90], [Uch00].

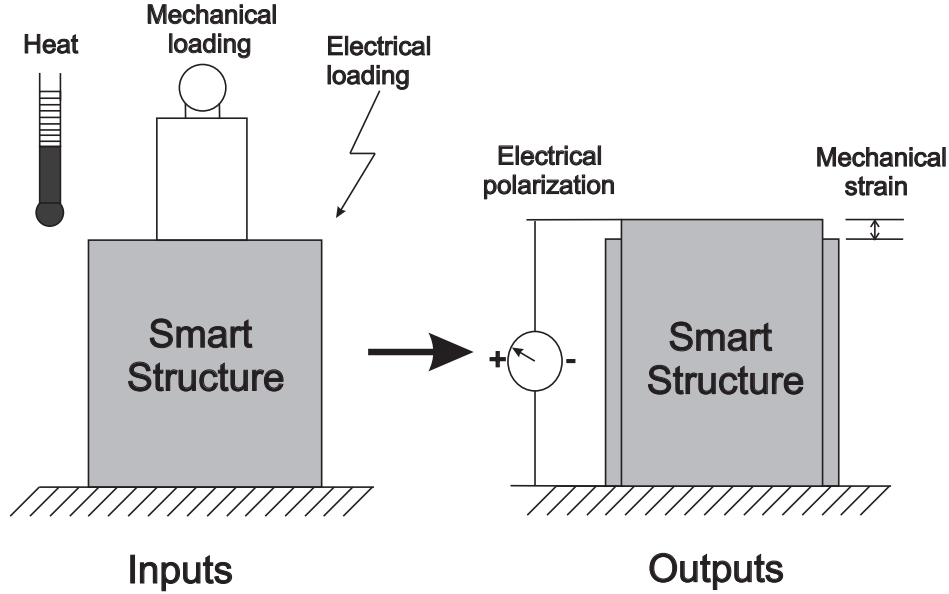


Figure 3.1: Concept of smart structures (Inputs, Outputs)

3.2.1 Ferroelectricity

In order to understand ferroelectricity, one should know the basics of dielectric properties and lattice structures of materials. Dielectricity is the ability to have electricity through the separation of positive and negative charges without any current flow when an electric field is applied. Movements of charges lead to electric dipoles which is called polarization with the units of $[\text{C}/\text{m}^2]$. It is nothing but charge per unit area or electric dipole moment per unit volume. Dielectric materials are widely used in capacitors due to their high material properties and superior insulating behaviours [Mur].

Electric displacement or electric flux density is the physical name of total electric charge per unit area of capacitors. Equation (3.1) shows linear relation of electric displacement (D) with respect to electric field (E) in terms of material dependent dielectric constant (ϵ) for dielectric materials.

$$D = \epsilon E \quad (3.1)$$

Dielectric constants of some materials with respect to vacuum are given in Table 3.1. [ZKM01], [SZY82].

In crystallographic structures of some materials, polarization can be observed even when they are not subject to electrical loading. Polarization which occurs under some conditions except electrical loading is called spontaneous polarization. For instance, a drastic change in temperature can lead to a spontaneous polarization of these materials in their lattice structure. If the direction of this spontaneous polarization can be changed by the application of an electric field the crystals are said to be ferroelectric.

Material	Dielectric constant [F/m]	Relative dielectric constant
Vacuum	$8.854 \cdot 10^{-12}$	1
Benzene	$2.022 \cdot 10^{-11}$	2.284
Barium Titanate	$(8.854-110.68) \cdot 10^{-10}$	100-1250
Glass	$(4.427-8.854) \cdot 10^{-11}$	5-10
Iron Oxide	$1.257 \cdot 10^{-10}$	14.2
Plexiglas	$3.010 \cdot 10^{-11}$	3.4
Polyethylene	$1.992 \cdot 10^{-11}$	2.25
PZT(PIC 151)	$2.125 \cdot 10^{-9}$	2400
Teflon	$1.859 \cdot 10^{-11}$	2.1

Table 3.1: Typical dielectric constants of some materials in nature

Rochelle Salt ($\text{KNaC}_4\text{H}_4\text{O}_6 \cdot 4\text{H}_2\text{O}$) was discovered as the first material showing ferroelectric behaviour at the end of 19th century. In the first half of 20th century, Potassium dihydrogen phosphate (KH_2PO_4) and Barium titanate (BaTiO_3) were found. Other important ferroelectric materials are Lead titanate (PbTiO_3), lead zirconate (PbZrO_3), lead zirconate titanate (PZT), lead lanthanum zirconate titanate (PLZT), lead magnesium niobate (PMN), lithium tantalite (LiTaO_3), and lithium niobate (LiNbO_3). $\text{Pb}(\text{Mg}_{1/3}\text{Nb}_{2/3})\text{O}_3$, $\text{Pb}(\text{Fe}_{1/2}\text{Nb}_{1/2})\text{O}_3$ and $\text{Pb}(\text{Ni}_{1/3}\text{Nb}_{2/3})\text{O}_3$ show ferroelectric characteristics with high rate or frequency dependency on dielectric constants. Therefore, they are known as relaxor ferroelectrics.

Ferroelectric materials, which are commonly made of ceramics are becoming a more interesting part of smart materials due to their applications in scientific and engineering area. MLC (Multilayer ceramic capacitors) which are widely used in electronics engineering have advantageous properties for high capacitance due to their high dielectric constant of ferroelectric materials such as PMN. Ferroelectric memories are another significant implementation of ferroelectric ceramics such as FRAM (Ferroelectric random access memories). Although they have some manufacturing difficulties, ferroelectric microelectromechanical systems (MEMS) are also used in ferroelectric thin films, accelerometers and micro-mirrors [YNLBLE01].

3.2.2 Piezoelectricity

Piezoelectric phenomena are directly related to the microstructural properties of materials. There are thousands of crystals in nature, which can be categorized with 230 different microscopic symmetries. There are 32 point groups or macroscopic symme-

tries if only symmetry elements are taken into account. Table 3.2 shows crystal structures with corresponding point groups. Among these 32 point groups, there are 11 point groups, which have center of symmetry in their lattice structures. There is one point group, which has no center of symmetry but an other symmetry condition holds. The remaining 20 point groups, which do not possess center of symmetry, are known as piezoelectric materials, because these point groups show polarity in their crystals [Nye85]. Figures 3.3, 3.2 illustrate crystals with and without center of symmetry when they are loaded with compressive stress.

Crystal system	Point groups	Non-center of symmetry
Cubic	<i>23,m3,432,43m,m3m</i>	<i>23,43m,432</i>
Hexagonal	<i>6,6,6/m,622,6mm,6m2,(6/m)mm</i>	<i>6,6,622,6mm,6m2</i>
Trigonal	<i>3,3,32,3m,3m</i>	<i>3,32,3m</i>
Tetragonal	<i>4,4,4/m,422,4mm,42m,(4/m)mm</i>	<i>4,4,422,4mm,42m</i>
Orthorhombic	<i>222,mm2,mmm</i>	<i>222,mm2</i>
Monoclinic	<i>2,m,2/m</i>	<i>2,m</i>
Triclinic	<i>1,1</i>	<i>1</i>

Table 3.2: Categorization of crystallographic point groups (point groups given in italic are piezoelectric)

In 1880, Curie brothers (Jacques and Pierre Curie) observed piezoelectricity, the definition of which was given at that time by having an ability of certain materials to produce proportional electrical charge with respect to the applied mechanical stress. This definition is later used for only direct piezoelectricity, because such materials also show the ability of developing linear dependent mechanical strain or deformation when an electric field is applied. This is used for the terminology of converse piezoelectricity [JCJ71]. Figures 3.4 and 3.5 illustrate the reverse and direct piezoelectricity. The expressions of direct and reverse piezoelectricity without adding dielectric and elastic properties are

$$D_k = d_{klm}\sigma_{lm} \quad (3.2)$$

$$S_{ij} = d_{nij}E_n \quad (3.3)$$

Here, D_k denotes the electric displacement, S_{ij} is the mechanical strain, E_n is the electric field, σ_{lm} is the mechanical stress and d_{klm} is the piezoelectric tensor.

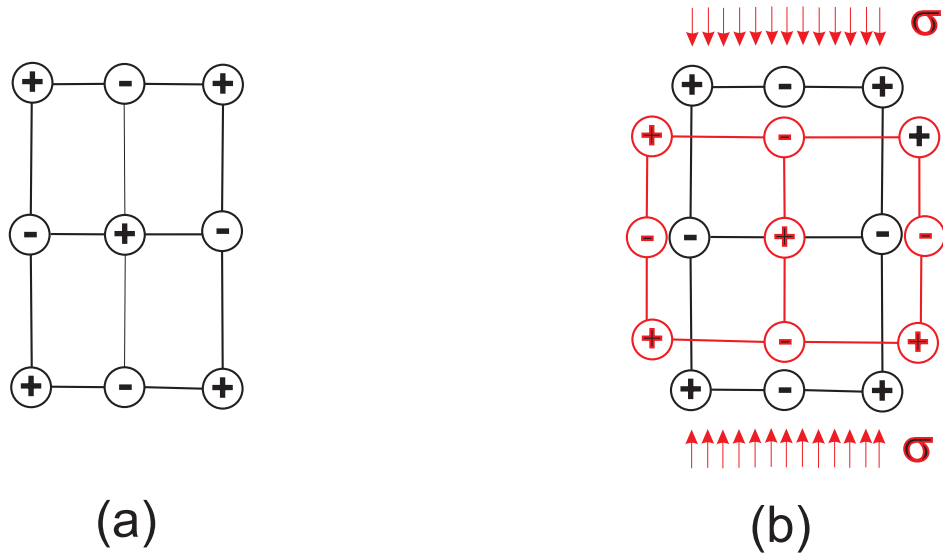


Figure 3.2: Tetragonal structure with center of symmetry (a) and under compressive stress (b)

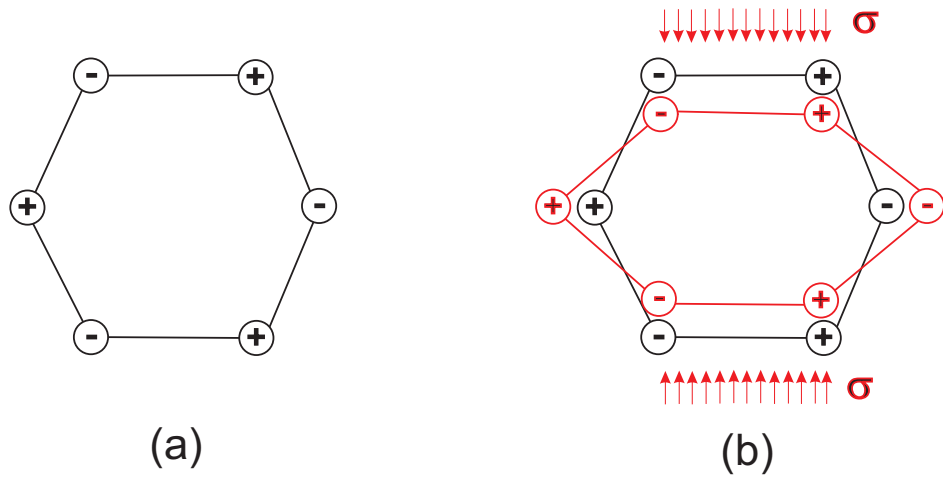


Figure 3.3: Hexagonal structure without center of symmetry (a) under compressive stress (b)

If elasticity and dielectric properties are inserted, equations (3.4) and (3.5) in tensor form become

$$D_k = d_{klm}\sigma_{lm} + \epsilon_{kn}^{\sigma}E_n \quad (3.4)$$

$$S_{ij} = s_{ijlm}^E\sigma_{lm} + d_{nij}E_n \quad (3.5)$$

where ϵ_{kn}^σ is the dielectric constant and s_{ijlm} is the compliance tensor. Superscripts σ on ϵ and E on ϵ illustrate the conditions of constant mechanical stress and electric field respectively.

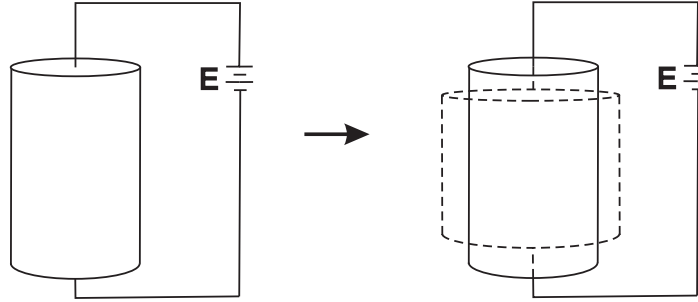


Figure 3.4: Illustration of reverse piezoelectricity

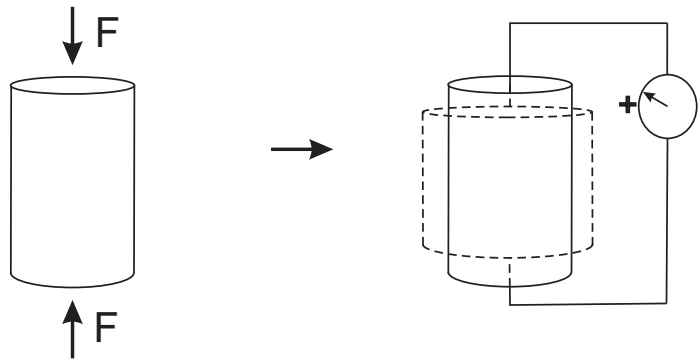


Figure 3.5: Illustration of direct piezoelectricity

Examples of some common piezoelectric materials are Quartz (SiO_2), polyvinylidene fluoride (PVDF), zinc oxide (ZnO) and lead zirconate titanate ($\text{Pb}(\text{Zr},\text{Ti})\text{O}_3$).

Piezoelectric actuators are one of the important parts of atomic force microscopes (AFM), which have been widely used in deriving topographic images of materials' surfaces or providing pictures of atoms in the materials. Piezoelectric stages are integrated in such applications in order to be able to realize micro- and nano-positioning of the samples to be analysed. Various $x - y - z$ or $x - y - \theta$ rotational piezoelectric stages have been implemented in precision measurement devices especially in optics due to their high precise movements and senses under control units.

When a low electric field is applied to piezoelectric materials in the linear range but with high frequency, large mechanical strain can be achieved due to resonances of the system. High amplitude of mechanical vibration will be generated by the application of alternating electric field with the operating frequency of resonance which can be

in kHz and even in MHz range. There has been an enormous increase in the ultrasonic application of piezoelectric materials, especially in the area of biomedical science [Chr88]. Ultrasonic imaging is one of the significant developments, which has been used for the easy diagnosis of illness with very low adverse reaction compared to other medical methods like x-rays. Piezoelectric resonators, vibrators, oscillators and buzzers are other important examples of piezoelectric applications which are operated in resonance frequency modes.

When piezoelectric devices are implemented in order to transform low voltage input into high voltage output by inserting two pairs of electrodes on the surfaces of two differently operated piezoelectric materials, these devices are named as piezoelectric transformers which were first invented by Rosen [Ros56]. They are simply converting electrical signals in high dynamical mechanical motions and then reconvert them into electrical output. Recent applications are mainly concentrated on laptops, where a high power density is required.

3.2.3 Pyroelectricity

There are certain crystals whose spontaneous polarization values are sensitive to changes in temperature values. Such materials are designated to have pyroelectric properties. Change of spontaneous polarization with respect to temperature difference can be shown by equation

$$\delta D = p\delta T \quad (3.6)$$

Here, p is the pyroelectric constant. δD and δT are corresponding changes in electric displacement and temperature. Pyroelectric coefficients can have a negative value, so that the spontaneous polarization decreases when the temperature is increased for such materials. As explained above, among 20 piezoelectric point groups 10 of them have a dipole in their lattice structure which show thermal deformation namely pyroelectricity. That is why all pyroelectric materials show also piezoelectric properties, but a piezoelectric material is not necessarily pyroelectric. Some examples of pyroelectric material groups are CH_2CF_2 , ZnO and $\text{Pb}(\text{Zr}, \text{Ti})\text{O}_3$ [Dam98].

3.2.4 Electrostrictivity

As described above, converse piezoelectric materials have linear proportional strain response to an electric field. Sometimes a linear correlation is not observed for some crystalline materials. Mechanical strain is found to be proportional to the square of the electric field for electrostrictive crystals (figure 3.6). In contrast to piezoelectric materials, electrostrictive materials do not possess spontaneous polarization. According to Cady's definition, the sign of the deformation, which occurs with an applied electric

field, is proportional to a power function of the electric field [JCJ71], [Cad46]. The electrostrictive phenomenon can be seen for all crystals although the effect may be very small. Then mechanical strain (S) can be approximated by a quadratic function of the electric field (E) with the electrostrictive coefficient (M) as factor

$$S = ME^2 \quad (3.7)$$

$\text{Pb}(\text{Mg}_{1/3}\text{Nb}_{2/3})\text{O}_3\text{-PbTiO}_3$ (PMN-PT) and $\text{Pb}(\text{Ni}_{1/3}\text{Nb}_{2/3})\text{O}_3\text{-PbTiO}_3$ (PMN-PT) solutions show electrostrictive behaviour with high mechanical strain under an electrical field. Actually, the lattice structure of PMN has center of symmetry at zero electric field. By the application of electric field, positive and negative charges separate which leads to a strain which is dependent on the electric field quadratically. However, these materials have thermal limitations. Thereby, they cannot be used in high performance applications. Additionally, some piezoelectric materials like PLZT are often called electrostrictive [Kkaj]. These are some displacement transducers made of PMN electrostrictive materials. Since such materials have less hysteresis nonlinearity in strain compared to piezoelectric materials, they are more advantageous in applications. Furthermore, electrostrictive materials are included in some intelligent applications like robotics, sonars and biotechnology.

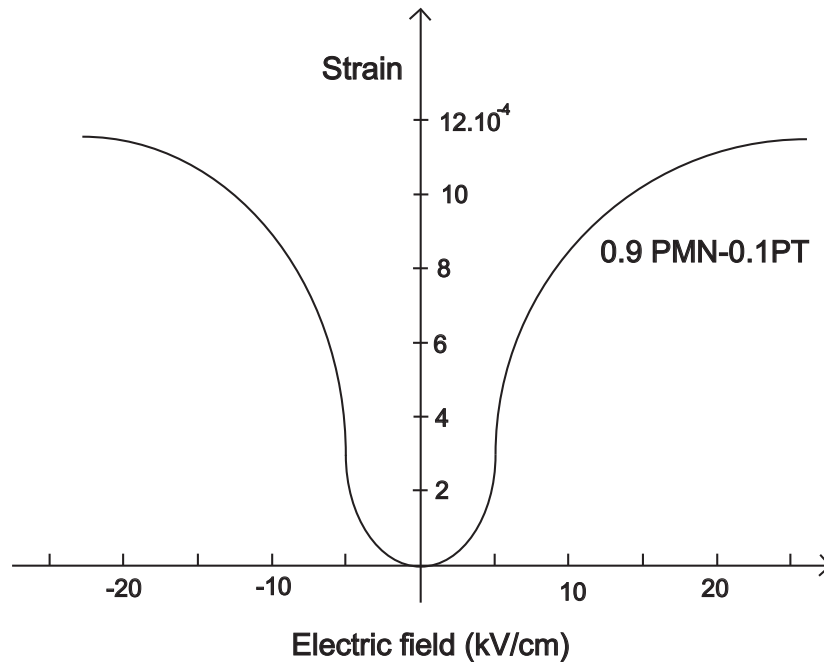


Figure 3.6: Mechanical strain versus electric field curve, Newham et al. [NXKC90] for (0.9 PMN-0.1PT) electrostrictive material

3.2.5 Magnetostrictivity

Magnetostrictive materials change shapes or dimension under the influence of a magnetic field. Magnetostriction was first investigated by Joule in 1842. He observed the deformation in Iron materials when they are subject to magnetization. The principle is the same as reverse piezoelectricity. The only difference between them is the applied loading, which is a magnetic field in magnetostrictivity unlike an electric field in reverse piezoelectricity. The relation between the mechanical strain and the magnetic field is generally quadratic similar to the electric field dependence of electrostrictive materials [Smi05], [DSFF00] (figure 3.7). Like direct piezoelectricity, magnetic properties (magnetization and permeability) of such materials change when they are loaded mechanically as well. Terfenol ($Tb_xDy_{1-x}Fe$) are well known magnetostrictive alloys, which are widely used in vibration and noise control, high precise milling, thin film technology and as torque transducers in engineering applications [Dap02], [Smi05].

The linear governing equations for magnetostrictive materials are

$$S = \frac{\sigma}{E_y} + qH \quad (3.8)$$

$$B = \mu H \quad (3.9)$$

Here, E_y is Young's modulus, q denotes magnetostrictive coupling coefficient, H refers to magnetic field, B is magnetic induction and μ is magnetic permeability.

3.2.6 Shape memory effect

Shape memory effects are observable for some alloys which try to recover their strain via phase change of lattice structure at a certain temperature after being deformed mechanically. Shortly, they have the ability to get their original shape before being strained by temperature increase. Most widely used shape memory alloys are Nickel-Titanium (Ni-Ti), Copper-aluminum-nickel (CuAlNi), Copper-zinc-aluminum (CuZnAl) and Iron-manganese-silicon (FeMnSi). Basic applications of them are in aerospace engineering for increasing the performance of wing properties (lift, drag), and in medical technology for micro-instruments (grasper).

3.3 Piezoceramic materials

Ferroelectric and piezoelectric materials, which are commonly made of ceramics, have become a highly interesting part of smart materials due to their applications in intelligent systems, especially in electronics and mechatronics engineering area [TKU01].

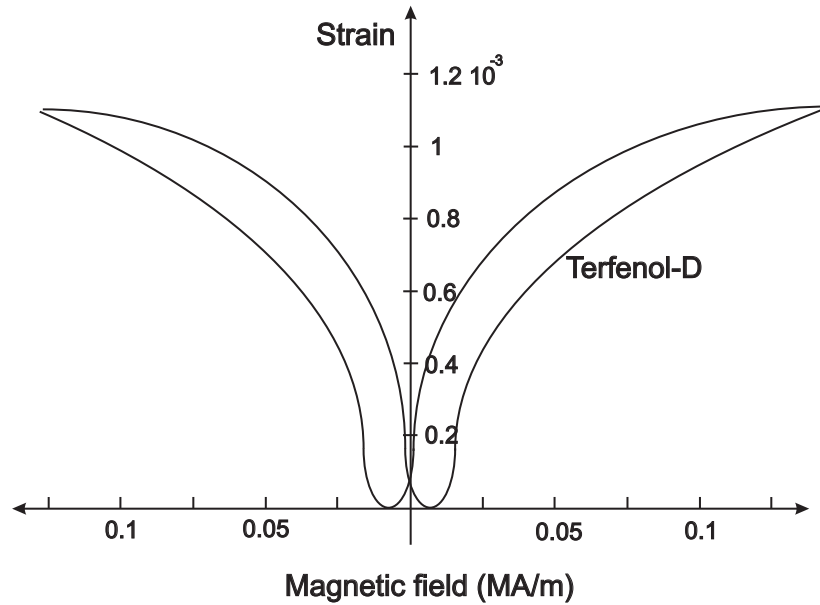


Figure 3.7: Mechanical strain versus magnetic field hysteresis curve for Terfenol-D magnetostriuctive material [Smi05], [DSFF00].

Vibration damping and noise control [BHY98], precision positioning, micro-machining [Del02], [YNG03], [CBKHSB02], injection mechanisms in common rail systems with piezo control in automobiles, ink-jet printers, thin films [RMBG04], commercial stack actuators and sensors and microelectromechanical systems (MEMS) are some examples of usage of these materials in recent years.

Piezoceramic materials can be classified into two types as soft and hard piezoceramics. Soft and hard piezoelectricity can be characterised by the stability of domain walls during electromechanical loading. When domain walls move and domain switchings occur well below 1 kV/mm electrical loading, the piezoceramic material is defined as soft. For such soft piezoceramics, domain walls are very unstable. On the other hand, some piezoceramics whose lattice structure undergoes domain switching only above 1 kV/mm are called hard [Uch00]. Soft piezoceramics have higher dielectric constants, piezoelectric constants and elastic constants than hard ones. In PZT materials, donor-type ion doping leads to piezoceramic soft characteristics. Therefore, such PZT materials have large piezoelectric constants. On the contrary, lower-valent substituents provide rather hard behaviour to PZT. Commercial sensors and actuators are basic applications of hard piezoelectrics.

3.3.1 Production process of piezoelectric materials

In this part, the main manufacturing process of piezoceramic materials, which are often made up of polycrystalline ceramics, are shortly explained. It is clearly expected that types and conditions of the process have strong influence on the characteristics of piezoceramic material.

Firstly, raw material powders should be in fine particle size (sub-micrometer range) in order to have better mixing. Compositional elements should have high homogeneity and exact amount for perfect solid solution. BaTiO_3 is produced from raw material powders of BaO and TiO_2 . Likewise, PbO , ZrO_2 and TiO_2 should be starting raw solutions for preparation of PZT ceramics. The mixing process can generally be accomplished by using ball milling.

Mixed powders are then heated up to $800\text{ }^\circ\text{C}$ to remove impurities and obtain the desired chemical reaction and homogeneity for the solution. After the calcination process, milling and/or grinding methods of machining are used for shape forming.

Production of various special piezoceramic materials requires additional processes such as precipitation, which is needed for better homogeneity of the final piezoceramic by inserting an additional solution called precipitant into mixing [JCJ71], [Uch00], [Cer].

After forming the material into the desired shape, the solution is fired again under the melting point ($1200\text{ }^\circ\text{C}$ - $1400\text{ }^\circ\text{C}$). The aim of such firing which is known as sintering is to increase the ceramic density by the elimination diffusion of the vacancies and pores at the microstructural level.

The last process is electroding for the application of poling. Generally, layer of silver materials are bonded to the piezoceramic surface to which the electric field will be applied. The silver layers should be adhered strongly without allowing any gaps that can reduce the effectiveness of piezo actuators and sensors. Other electrode materials which are commonly used as electrodes are gold, nickel, copper and platinum elements [JCJ71]. In figure 3.8 a flowchart of the manufacturing process of piezoceramic materials is illustrated.

3.3.2 Perovskite structures

The microstructures of piezoelectric materials like ferroelectrics contain spontaneous polarization. Therefore, all piezoelectric materials are also considered to be ferroelectric materials. Since some of the ferroelectric materials do not show a linear electromechanical behaviour, all ferroelectric materials cannot be regarded as piezoelectric materials. Most of the commercially used piezoelectric materials are polycrystalline ferroelectrics such as BaTiO_3 , PZT and PLZT. These types of ferroelectric materials are in the group of perovskite lattice structures which is in the form of ABO_3 . The microstructure of such perovskites is shown in figure 3.9. All piezoelectric materials are existing with a

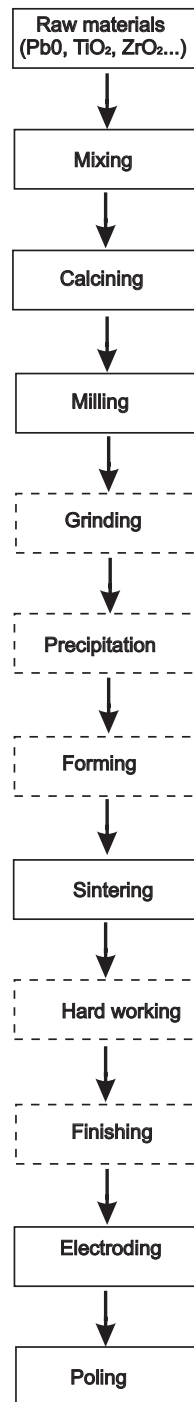


Figure 3.8: Flowchart of the manufacturing process of piezoceramic materials (Rectangles with dashed lines are processes that are required for various piezoceramics.)

cubic crystal structure as long as they are above a certain temperature called Curie temperature (T_c). This is the transition temperature for such materials to change the microstructure from cubic to non-cubic (tetragonal or rhombohedral) when reducing the temperature. Most typical perovskite ferroelectric structures have a Curie temperature between 120 °C and 300 °C. For example for BaTiO_3 , this is 130 °C for and for PIC 151 it is 250 °C. As it can be seen on the left side of figure 3.9, positive barium atoms are located at the corner of cubic elements. At the face centers six negative oxygen atoms are placed. A positive titanium atom, which can move in the directions of one of the negative oxygen atoms, is situated at the center of the cubic element. Such positions of atoms inside cubic elements bring out equally located positive and negative charges which means that the distance between the center of negative charges and the center of positive charges is zero. On the other hand, on the right hand side of figure 3.9 the positive titanium atom is no more at the center of the lattice for the case of a temperature level which is less than the Curie temperature. This titanium atom is now much nearer to one of the oxygen atoms than to the others.

In the lower part of figure 3.9 internal energies for both cubic and tetragonal elements are illustrated. The internal energy of the cubic element has a minimum value when the positive titanium atom is at the center of the lattice structure. The energy is increasing for any other position of the titanium atom along the z axis. On the other hand, there are two minimum energy levels for tetragonal elements. In contrary to the cubic structure, the energy of the tetragonal structure has no minimum energy if the titanium atom is at the center of the lattice.

In order to find the polarization characteristics of both the cubic and the tetragonal microstructure one should calculate the dipole moment, which is the total magnitude of the charge times distance between atoms with a direction from negative charge towards positive charge. Figure 3.10 illustrates positions of charges inside a tetragonal perovskite element. Since b_c and a are the longitudinal and transverse dimensions of the unit cell, d is the distance from the positive titanium atom (Ti) to the center of the lattice and q is the electrical charge of titanium and oxygen atoms, dipole moment in the positive z direction of negative oxygen and positive titanium atoms can be calculated as

$$M_z = q\left(\frac{b_c}{2} + d\right) - q\left(\frac{b_c}{2} - d\right) + 2aq \tan(\alpha) + 2aq \tan(\alpha) \quad (3.10)$$

$$M_z = 6qd \quad (3.11)$$

The resulting dipole moment is directed along the positive z direction. The summation of dipole moments cancels for x and y directions. The polarization, which is the result of the net dipole moment per volume of the microstructure in the lattice structure during the phase transition, is called the spontaneous polarization (P_0). Due to the

equally located charges inside cubic elements, dipole moments cancel each other in all x , y and z directions. Therefore, there is no polarization inside a cubic lattice structure.

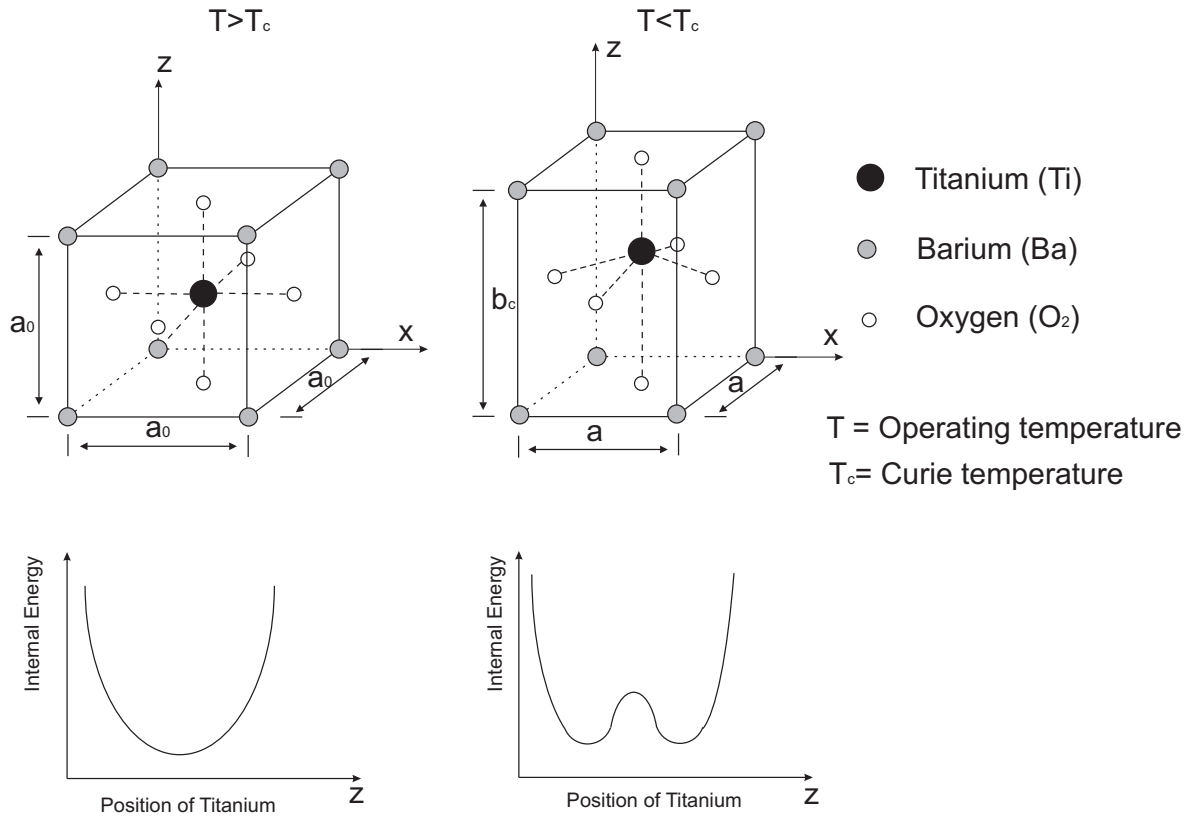


Figure 3.9: Lattice structure of cubic and tetragonal elements of perovskite type ferroelectrics (BaTiO_3) and corresponding internal energies

As explained above piezoceramic materials at room temperature mostly exist in a phase with tetragonal or rhombohedral lattice structure depending on the constitutional elements of the material. The Curie temperature is the transition temperature for ferroelectric and piezoelectric materials at which they start to change their lattice structure. When the temperature is above the Curie temperature, the lattice structure is in the form of cubic elements, in which the net dipole moment is zero due to the equally spaced locations of atoms inside the lattice. This phase is called the paraelectric phase. The microstructure of these materials transforms into a different type when the temperature is reduced below the Curie temperature. The new phase occurring after this transition is called the ferroelectric phase, in which there is a net non-zero dipole moment (figure 3.10). In the ferroelectric phase, the lattice structure actually distorts from cubic to tetragonal. This leads to a mechanical strain, which is called the spontaneous strain (S_0). The spontaneous strain for a tetragonal structure in the direction

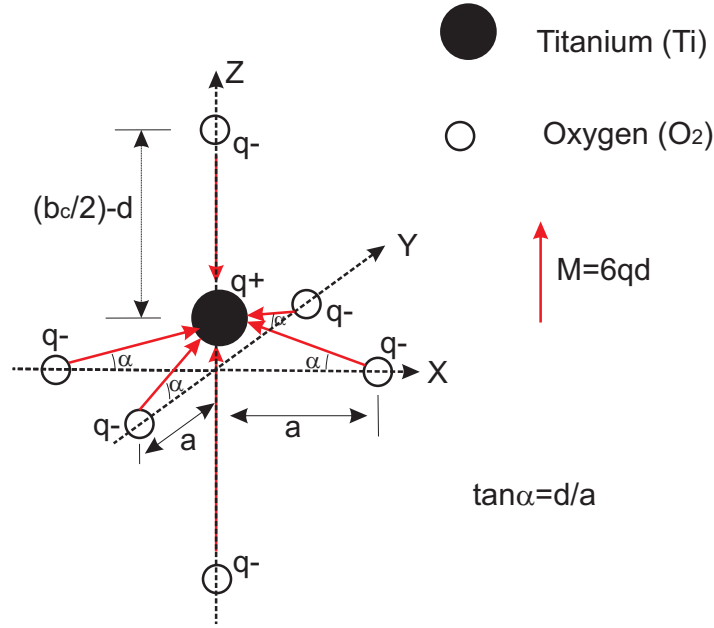


Figure 3.10: Locations of atoms and dipole moment calculation for perovskite type tetragonal BaTiO₃ structures.

of moving positive titanium atom (+z direction in figure 3.10) can be calculated by

$$S_0 = \frac{b_c - a_0}{a_0} \quad (3.12)$$

The positive atom in the center of the unit cell can move in direction of one of the negative atoms which are located at the face center of the tetragonal element. In the case of BaTiO₃, the titanium atom can move in direction of one of six oxygen atoms. This is the reason for the possible orientations of the spontaneous polarization direction inside a perovskite tetragonal element (figure 3.11).

A typical phase diagram of ferroelectric materials is shown in figure 3.12 for the example of a PZT solid solution. There are 3 possible phase changes according to the compositional percentage of PbZrO₃ and PbTiO₃ solutions. As seen in the diagram, Zirconium elements lead to a microstructure which is mostly a non-tetragonal structure below the Curie temperature. In the case of a low percentage of titanium (from I to II) the lattice structure is highly orthorhombic. When the amount of titanium is increased namely between 5 % to 45 % (from I to III), the microstructure changes to rhombohedral. Finally, tetragonal lattice structures are mostly available when the solution contains more titanium than zirconium (from I to IV). Commercially used PZT materials are usually chosen from the region of IV due to its highly concentrated tetragonal structures.

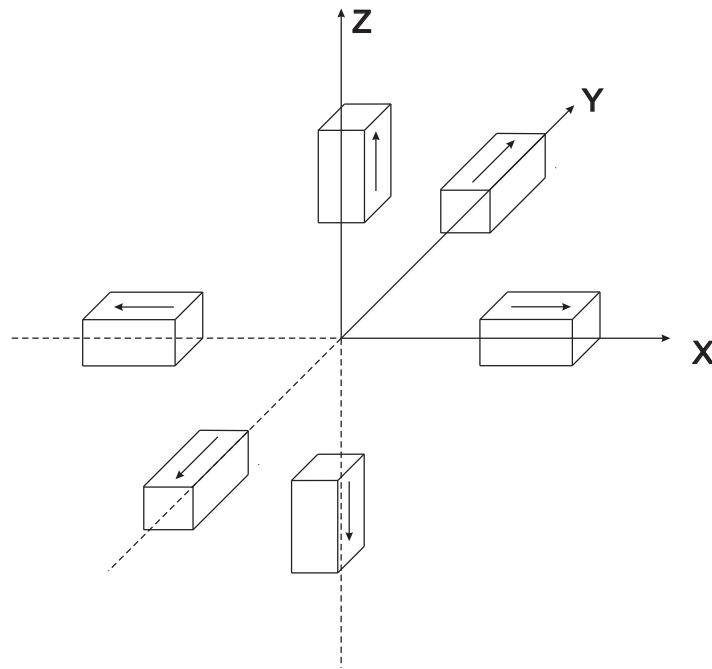


Figure 3.11: Six possible domain orientations in 3-D illustration

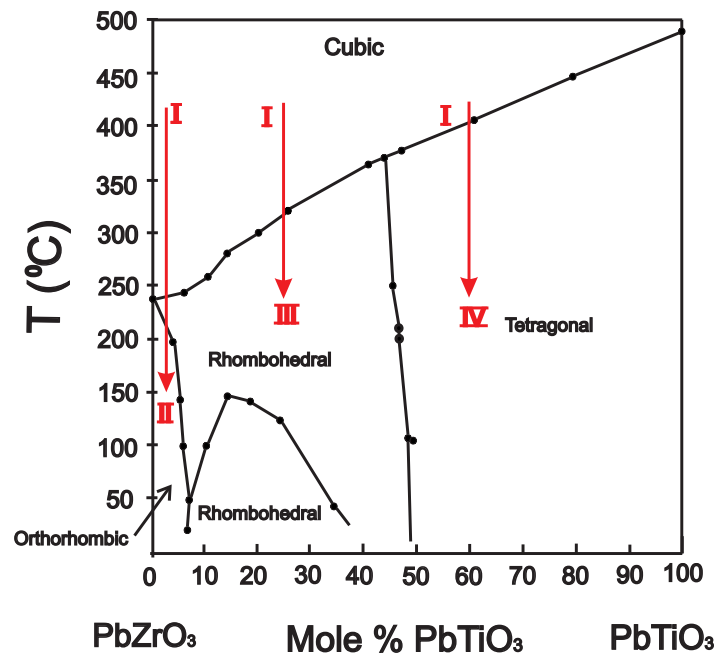


Figure 3.12: Phase diagram of PZT and ferroelectric phases [JCJ71]

3.3.3 Ferroelectric domains

In micro scale of ferroelectric materials, lattice structures which have the same spontaneous polarization orientations form homogeneous regions. Such uniformly distributed accumulated lattice structures are called ferroelectric domains. Many of these domains constitute the grains of the material. The boundary between two neighboring domains is referred to as a domain wall. There exist two types of domain walls for perovskite type ferroelectric materials. The domain wall separating oppositely oriented domains are called 180° domain wall. The second type of domain walls is separating domains which have perpendicular orientation to each other. Therefore, they are called 90° domain wall (figure 3.13). There are also ferroelastic domain walls between domains with different spontaneous strain characteristics. Unlike 180° domain walls, 90° domain walls can be both ferroelectric and ferroelastic. For the case of rhombohedral structures, there occur three different domain walls which are 180° , 70.5° , 109.5° [Dam98].

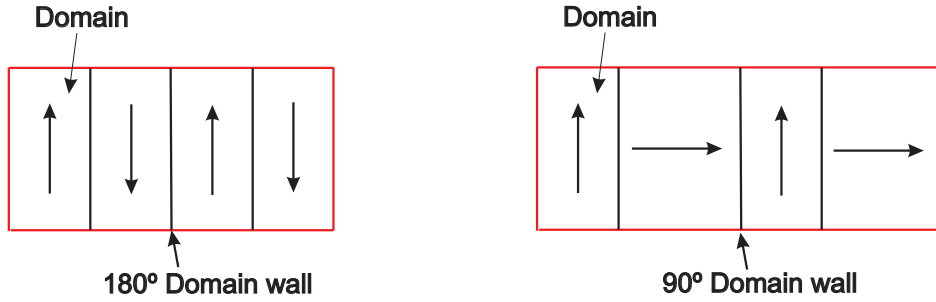


Figure 3.13: Illustration of 90° and 180° domain walls

Looking closely at the micro-level of both piezoelectric and ferroelectric materials, it can be seen that the unpoled material is composed of randomly oriented grains due to the complex electromechanical conditions in micro-level (figure 3.14). Since the direction of the polarization is more or less equally distributed in the virgin state, the average polarization or mechanical strain of the bulk material is approximately zero. When the material is subject to a high external electric field, the directions of all spontaneous polarization vectors are aligned in the direction of the electric field by means of domain switching of the grains. Since the direction of the polarization vector after domain switching has to be in one of the local lattice axes, the polarization in general is not parallel to the electric field locally but has a component in direction of the electric field. The process of applying a strong electric field to ferroelectric materials in order to align domains in the direction field is called poling. Figure 3.14 illustrates the grains and domains for polycrystalline ferroelectric materials before and after poling. As it can be observed in the figure there are still some domain walls inside grains which do not have completely the same spontaneous polarization direction. Due to the different mechanical and electrical boundary conditions of grains of polycrystalline ferroelectric

materials, directions of spontaneous polarization vectors can not be aligned completely with the external applied electrical field during poling. As a result, the macroscopic spontaneous polarization and strain values are smaller than for a single crystal.

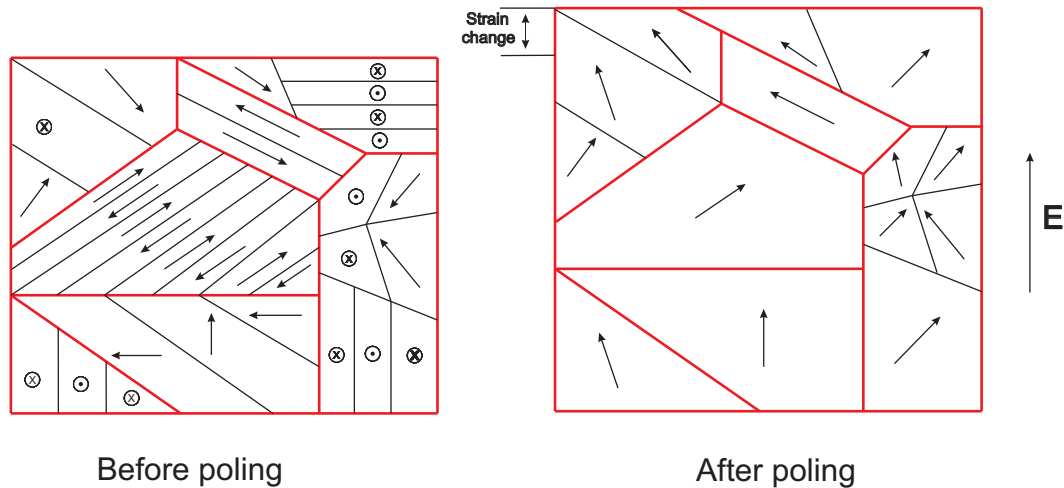


Figure 3.14: Grains and domains of polycrystalline ferroelectric materials before and after poling.

Domain wall motion is the mechanism for the phase change in grains of ferroelectric materials during poling. Figure 3.15 illustrates both 180° and 90° domain wall motions under the effect of pure electrical loading. Domain wall movements inside grains will result in a change of orientation of the polarization, which will be the same direction as the applied electric field. As it can be observed in figure 3.15 that 180° domain wall motion does not have any shape change in the grain. On the contrary, non- 180° domain wall motions which are 90° for tetragonal and 70.5° or 109.5° for rhombohedral structures give rise to strain changes in the grain of ferroelectric materials.

3.3.4 Domain switching

As explained above, the macroscopic behaviour of piezoelectric ceramics cannot be described by linear constitutive equations when they are under high electromechanical fields. Domain switching in microstructures is the main reason for the nonlinearity. There are six possible orientations for the polarization in the lattice structure for a perovskite type tetragonal microstructure. Therefore, only two types of domain switching are possible. These are 90° and 180° domain switching the names of which are related to the angle of rotation, which the position vector of the central atom undergoes during domain switching relative to its previous direction. (figure 3.16).

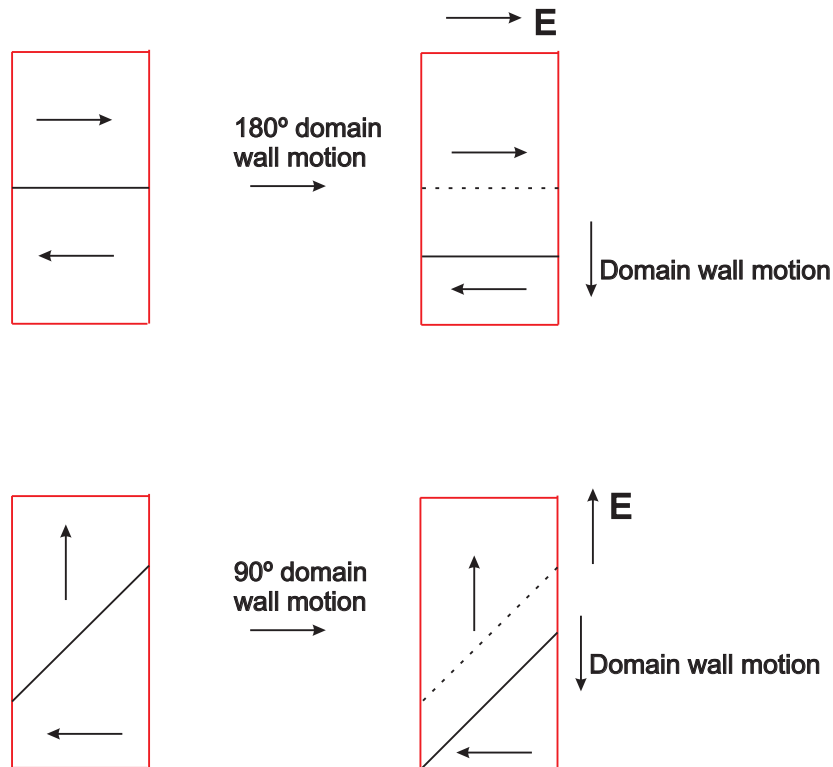


Figure 3.15: 180° and 90° domain wall motions during phase change of tetragonal ferroelectric structures [Cro93].

3.3.5 Rhombohedral structures

As explained before, phases of polycrystalline piezoelectric materials can change from cubic to rhombohedral according to the constitutional elements of the materials when their operating temperature is reduced below the Curie temperature (figure 3.17). Unlike perovskite type tetragonal elements, negative atoms are located at the corner of the lattice in rhombohedral structures. So the center of positive atoms can have the possibility to move inside the lattice diagonally. There are four possibilities for lines along which the center atom can be displaced in diagonal direction, which refer to eight different positions of the center atom. Therefore, it is expected to have elongation through the corner of the lattice structure, when the structure is under electromechanical loading. The angle between any of these diagonal vectors inside the rhombohedral element is 70.5° or 109.5° . There is no 90° domain switchings like in tetragonal structures. So, there are three different phase transformations with 180° switching in addition to 70.5° or 109.5° switchings.

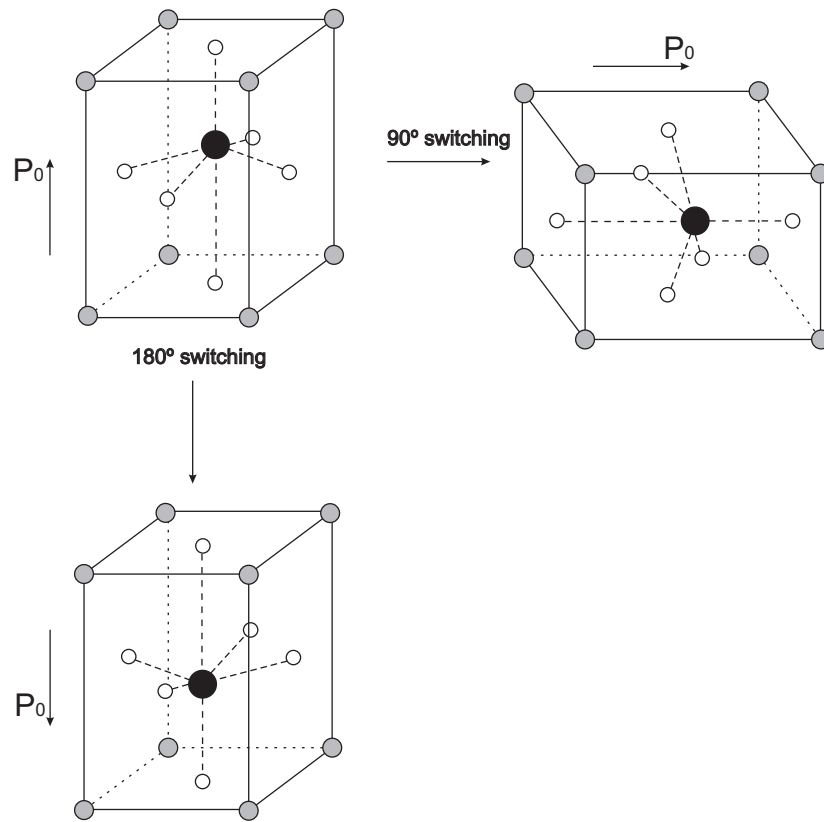


Figure 3.16: 90°-180° domain switching in the lattice structure of perovskite type tetragonal structure

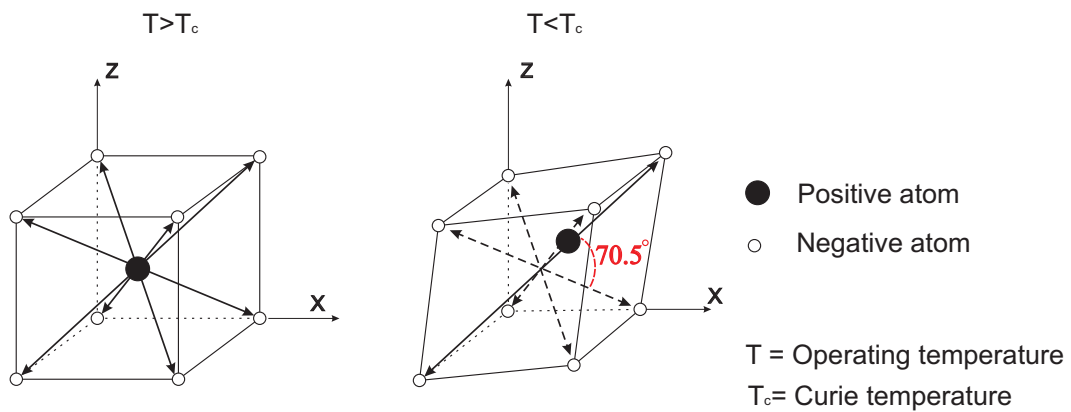


Figure 3.17: The lattice structure of cubic and rhombohedral structures above and below the Curie temperature

3.3.6 Ferroelectric domain switching

An externally applied electric field can cause a nonlinear domain switching with the change of the position of the central atom, which is a titanium atom for BaTiO_3

when the magnitude of the electric field is above the coercive field. Domain switching which can occur by a strong electric field is called ferroelectric domain switching. If the applied electric field is in the reverse direction of the spontaneous polarization of the microstructure, 180° ferroelectric domain switching will be produced. On the other hand, if the application of electric field is in the perpendicular direction of the spontaneous polarization, the central atom will orient in the same direction as the electric field that brings out 90° ferroelectric domain switching for tetragonal structures or 70.5° and 109.5° ferroelectric domain switchings for rhombohedral structures (figures 3.18, 3.19).

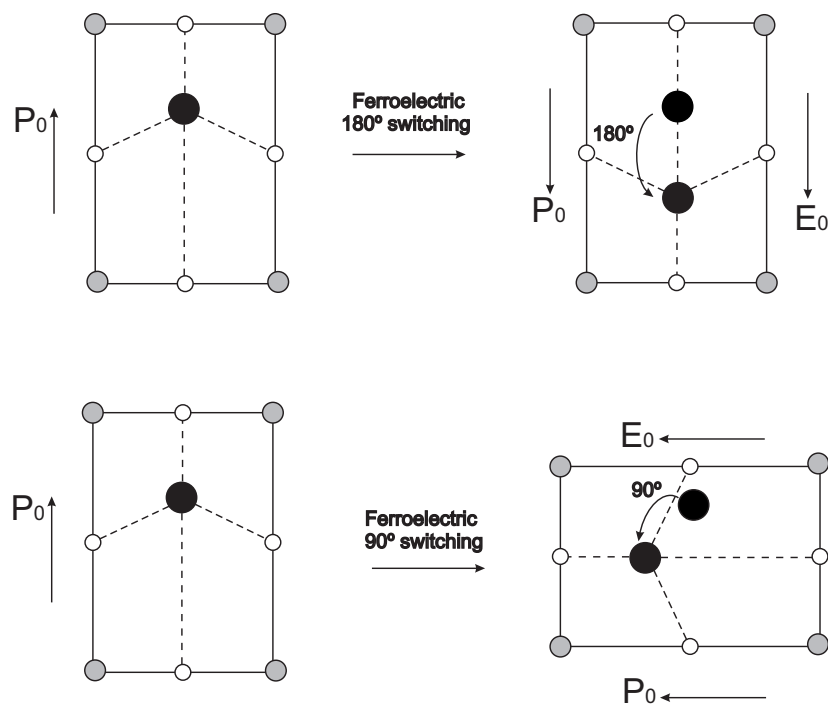


Figure 3.18: Ferroelectric domain switching (90° and 180°) in a perovskite type tetragonal element under the effect of an electric field

3.3.7 Ferroelastic domain switching

As it can be seen in figure 3.20 domain switching can also be induced by the application of mechanical stress. This is called ferroelastic domain switching. When the applied mechanical stress exceeds the coercive stress value, the central atom will reorient according to the magnitude and direction of the mechanical stresses. Unlike for ferroelectric domain switching, only non- 180° domain switchings can be possible in the case of ferroelastic domain switching which is 90° for tetragonal structures and 70.5°

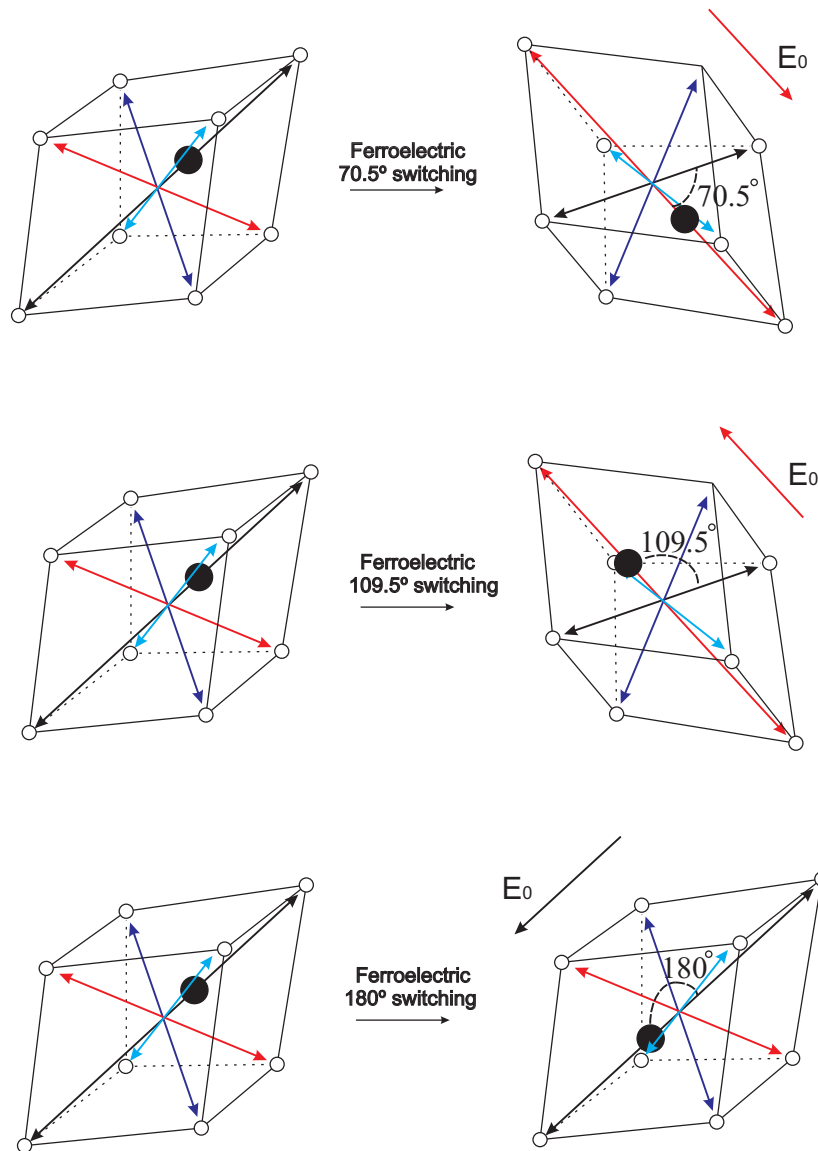


Figure 3.19: Ferroelectric domain switching (70.5° and 109.5°) in the lattice structure of a rhombohedral element under the effect of an electric field

or 109.5° for rhombohedral structures. Actually, there are four possible 90° domain switchings when the tetragonal microstructure is subjected to pure compressive stress. Reoriented direction of the spontaneous polarization will be definitely in a direction perpendicular to the applied compressive stress. The number of possible domain switchings is reduced to 2, if the applied mechanical stress is tensile. In this case the direction of domain switchings is the same as the direction of the applied tensile stress (figure 3.20).

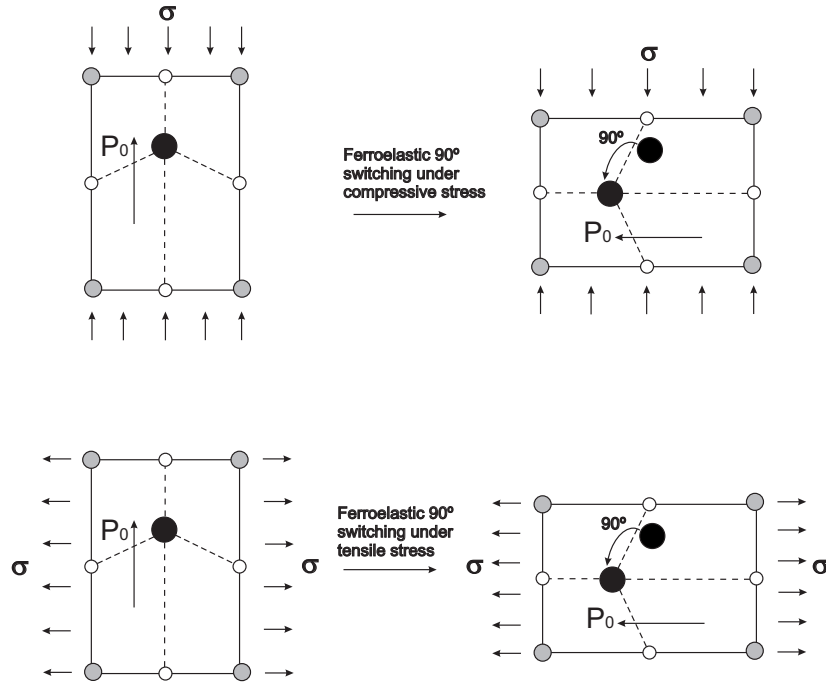


Figure 3.20: Ferroelastic domain switching (90°) in the lattice structure of perovskite type tetragonal structure under the effect of both compressive and tensile mechanical stresses

3.3.8 Macroscopic properties

Figure 3.22 shows a typical macroscopic electric displacement (D) versus electric field (E) hysteresis curve for a quasi-static, uni-axial electrical loading. The experiment starts with the initially unpoled ceramic (virgin state) with zero electric displacement. During the simulation a cyclic, uni-axial electric field is applied with a fixed amplitude. At the initial virgin state, the domains are distributed randomly. Orientations of spontaneous polarizations are stochastic. Therefore, the resulting macroscopic spontaneous polarization and spontaneous strain are zero. When the electric field is increased gradually from zero at point 1, there is a linear increase due to the dielectric response up to point 2. The linear constitutive equation (3.4) is valid in the region between 1 and 2 in which the electric field is not high enough for domain switching. After this point, there is a sudden nonlinear increase in the polarization. The electric field at point 2 is called the coercive electric field for a virgin state. At this region domain switchings occur, which is the main reason for the nonlinear behaviour of piezoelectric materials. Domains are beginning to be oriented to the loading direction during coercive electric field level. In this region, the linear constitutive equation is no longer valid. This nonlinear response to the electric field continues up to point 3, where the electric displacement saturates for a further loading, because there are no more domains for which

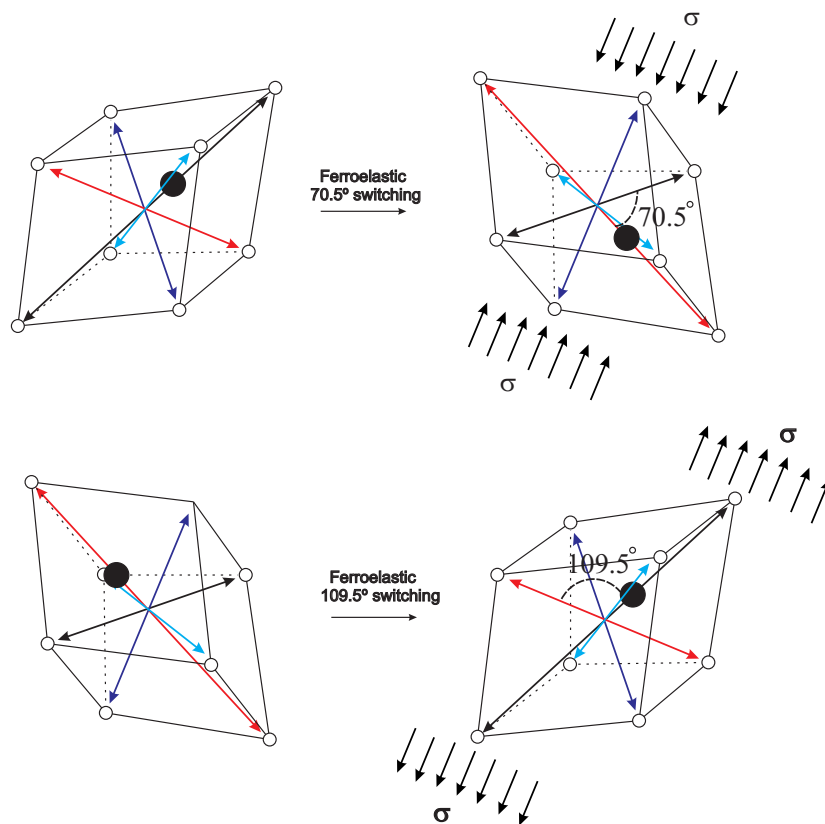


Figure 3.21: Ferroelastic domain switching (70.5° and 109.5°) in the lattice structure of a rhombohedral structure under the effect of both compressive and tensile mechanical stresses

a domain switching is possible. As a result, no more domain switching can be observed beyond this point. All the domains are aligned in loading direction. As a cyclic loading is applied also the electric field reduces quasi-statically. The electric displacement decreases linearly with the electric field until a zero electric loading is reached. This phase is called unloading. Although there are some back-switchings among domains occurring in this region, there is still a polarization, which is called the remnant polarization (P_r) at zero electric field after one complete loading. A linear response to the electric field, which is actually increasing its magnitude in negative direction, continues to point 4 which is the threshold point for the negative coercive field ($-E_c$). Actually, the coercive field is the electric field where polarization or strain equals zero. The polarization begins to decrease sharply again beyond this point up to point 5, where the piezoelectric material saturates again and the domains are fully aligned in the negative electric field direction. The electric field is then reduced in negative direction and increased in the positive direction to complete the cyclic electric displacement versus electric field hysteresis loop. A second time the remnant polarization ($-P_r$) is observed in the un-

loading from negative electric field, when the applied electric field is decreased to zero.

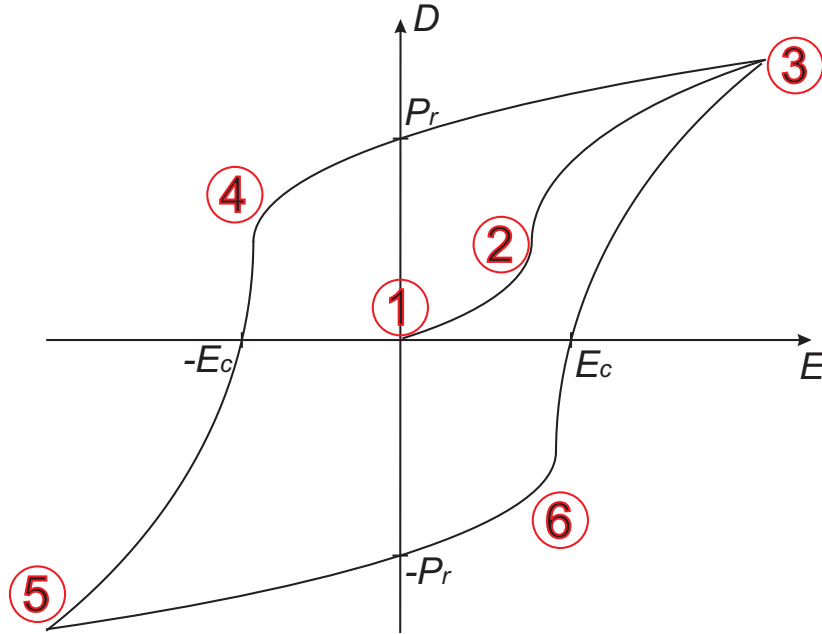


Figure 3.22: Hysteresis curve

The mechanical longitudinal strain (S) versus electric field (E) butterfly curve is illustrated in figure 3.23. The lettered points in figure 3.23 correspond to the same letters in figure 3.22. There are three basic effects for resembling these curves to butterfly shape. One of them is the converse piezoelectric effect and the other two are domain switching and domain wall motions [Dam98]. As the electric field is increased from zero, the microstructures expand according to equation (3.5). Beyond point 2, the expansion becomes nonlinear due to domain switching polarization characteristics. During unloading after point 3, a linear contraction occurs for the fully poled saturated microstructure. Reduction in strain continues up to point 4, where domain switching dominates again. In some cases, point 4 can have a negative strain value which is due to 90° domain switching. Effects of different types of domain switching on butterfly curves will be explained in chapter 6. Beyond point 4, increasing the electric field causes domains to stretch instead of a further contraction. Therefore, the strain is increasing in positive direction up to the saturated point 5, although the applied electric field is increased in negative direction. As the electric field is again reduced to zero, the curve intersects at the positive remnant polarization. The remnant polarization is negative for the hysteresis curve at the same location. Now, when a positive electric field is applied to complete the loop, microstructures undergo the same experience as for a loading in negative direction. Point 6 becomes a turning point for the curve to increase the strain.

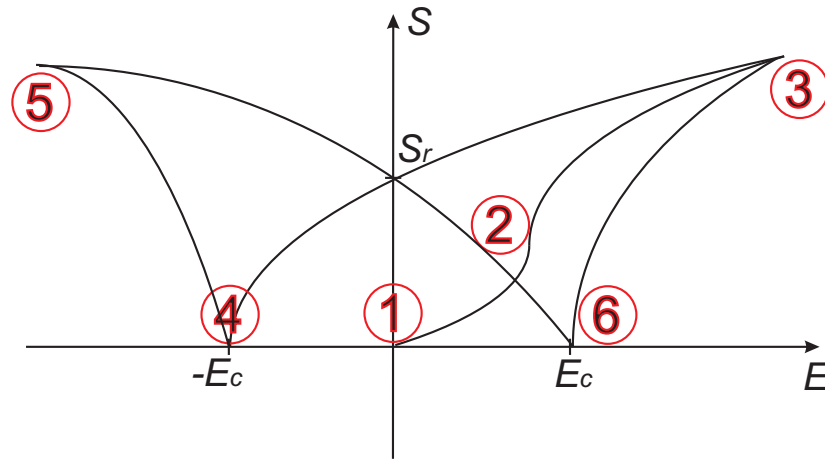


Figure 3.23: Butterfly curve

Typical mechanical longitudinal strain (S) versus applied compressive stress (σ) for piezoceramic materials is shown in figure 3.24. The lettered points in figures 3.24 are different from the letters in figures 3.22 and 3.23. The materials are initially at virgin state without any remnant values. When the mechanical stress is increased in negative direction (compressive stress) from stage 1, there is a quasi-linear reduction in strain value up to stage 2. As the compressive stress exceeds some critical value, the polarization begins to switch and the material again shows a nonlinear reduction in strain value points 2 and 3. Further applied compressive stress has quasi-linear reduction to a strain value due to saturation. After reaching point 4, the material is unloaded to zero stress. In this region, only small part of the domains switch back. Therefore, the reduction in negative strain is in a quasi-linear manner, which results in a negative remnant polarization at point 5.

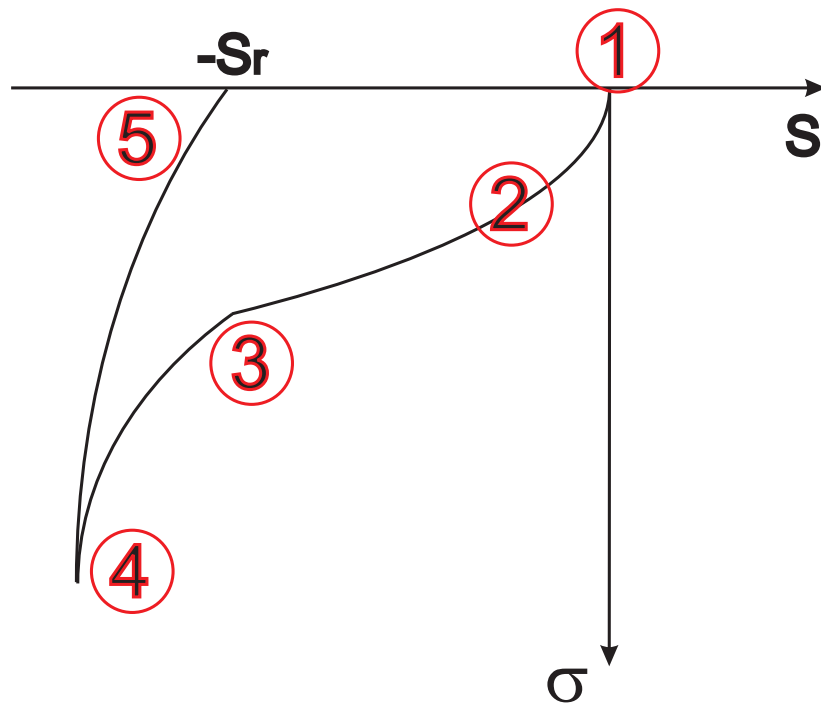


Figure 3.24: Typical stress strain curve

Chapter 4

Quasi-static Models

As explained before, domain switching is dependent on the loading rate. If a triangular voltage is applied, then the frequency of the cyclic loading affects the macroscopic characteristics of piezoelectric materials. Before explaining the details of rate dependency, which will be implemented in the following chapter, a rate independent model and the corresponding properties should be understood. In order to analyse rate independent macroscopic properties of piezoelectric materials, one should implement a quasi-static loading which means that load increments are applied such that the time between the increments are sufficiently large so that the time dependency can be neglected. Quasi-static loading for experimental and modelling of ferroelectric materials is defined in such a way that the application of loading does not have any rate or time dependent effect on the microstructure of materials. During quasi-static modelling, an adequate time is allowed for grains to complete the domain switching. In this chapter, a three-dimensional micromechanical model is presented with macroscopic simulations of piezoelectric materials which are subject to quasi-static, cyclic, uni-axial electro-mechanical loading.

4.1 Structure of the model

In this three-dimensional micromechanical model a bulk piezoelectric ceramic is considered, which consists of 1000 regularly shaped elements each of which is assumed to show the characteristics of an individual domain shown in figure 4.1. The crystal axes and therefore the polarization direction in each grain has random orientation. In the simulation these orientations of the grains are given statistically by using a random generator of the dynamic system simulation software program MATLAB. Randomness of orientations is given to every element by means of Euler angles (α, β, γ) which are chosen to be equally distributed between 0 and 2π . A global coordinate system for the bulk material and a local coordinate system for each element are introduced in order

to transform the values obtained by the calculations in the local coordinate systems to global coordinates and vice versa. Although it is clear that equally distributed Euler angles do not guaranty a uniform distribution of the polarization directions, it is common to use these equally distributed Euler angles for such simulations in micromechanical models. Polarization, strain and electric field given in local coordinates (x_l, y_l, z_l) in a domain can be transformed to global coordinates (x_g, y_g, z_g) or vice versa with the help of the corresponding transformations $R(\alpha, \beta, \gamma)$.

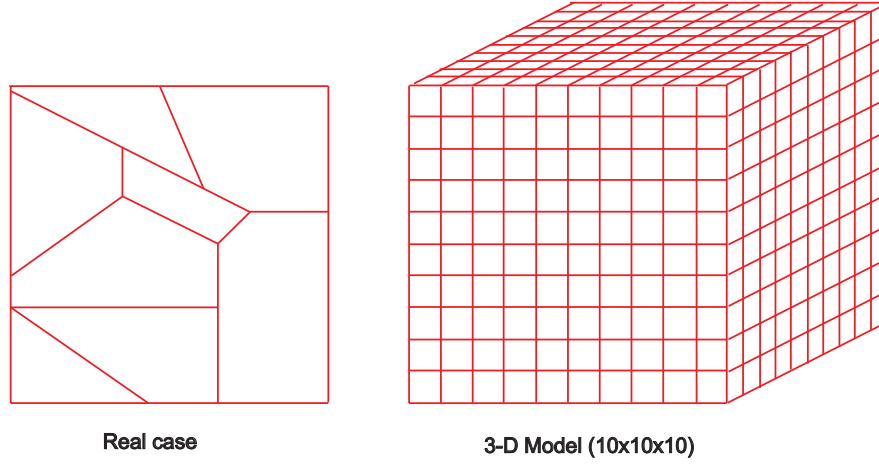


Figure 4.1: 3-D micromechanical model in form of 1000 cubic elements compared to the real microstructure

$$(x_l y_l z_l)^T = R(\alpha, \beta, \gamma)(x_g y_g z_g)^T \quad (4.1)$$

The transformation matrix $R(\alpha, \beta, \gamma)$ is calculated by multiplication of subsequent three rotation matrices ($R_z(\alpha), R_y(\beta), R_z(\gamma)$) the result of which is given by (4.2) and (4.3).

$$R_z(\alpha) = \begin{bmatrix} c(\alpha) & s(\alpha) & 0 \\ -s(\alpha) & c(\alpha) & 0 \\ 0 & 0 & 1 \end{bmatrix} \quad R_y(\beta) = \begin{bmatrix} c(\beta) & 0 & -s(\beta) \\ 0 & 1 & 0 \\ s(\beta) & 0 & c(\beta) \end{bmatrix} \quad R_z(\gamma) = \begin{bmatrix} c(\gamma) & s(\gamma) & 0 \\ -s(\gamma) & c(\gamma) & 0 \\ 0 & 0 & 1 \end{bmatrix} \quad (4.2)$$

$$R(\alpha, \beta, \gamma) = \begin{bmatrix} c(\alpha)c(\beta)c(\gamma) - s(\alpha)s(\gamma) & s(\alpha)c(\beta)c(\gamma) + c(\alpha)s(\beta) & -c(\gamma)s(\beta) \\ -c(\alpha)c(\beta)s(\gamma) - s(\alpha)c(\gamma) & s(\alpha)c(\beta)s(\gamma) + c(\alpha)s(\gamma) & s(\gamma)s(\beta) \\ c(\alpha)s(\beta) & s(\alpha)s(\beta) & c(\beta) \end{bmatrix} \quad (4.3)$$

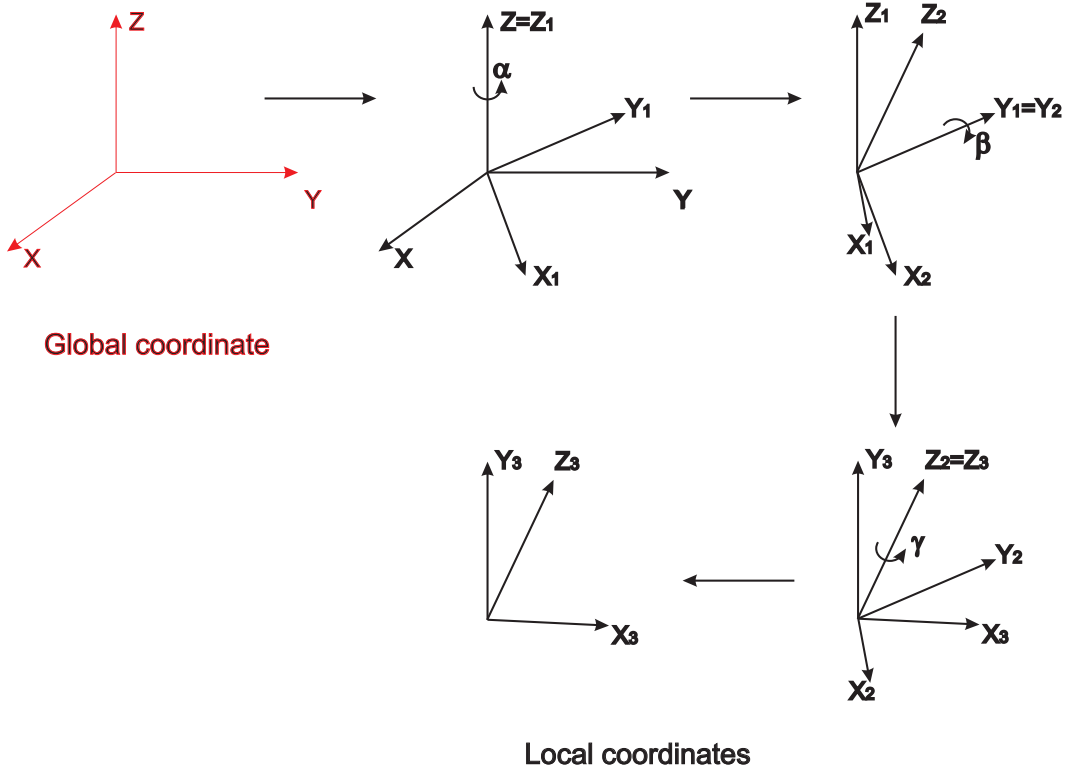


Figure 4.2: Coordinate transformation by using Euler angles ZYZ convention

where c and s mean cosine and sine functions of the corresponding arguments.

For the rotation angles and axes, the Euler ZYZ convention is considered, figure 4.2.

During the simulation, the external macroscopic load applied in the model is assumed to be equal to the load on each element of the bulk piezoelectric ceramic. Parameters of soft PZT-51 material is chosen for getting a better match of the electric displacement versus electric field curve to experimental results that are given in the literature [LFLH99]. The lattice constants of PZT-51 ceramic are given in table 4.1. In order to simplify the calculations, the dielectric permittivity is assumed to be isotropic and the same for all grains. The value for the dielectric permittivity (ϵ) is taken to be $6.0 \cdot 10^{-8}$ F/m, which is a typical value for PZT materials. The spontaneous polarization value is taken as 0.3 C/m². At each element, in addition to the piezoelectric linear constitutive equation, the non-linear domain switching model is also implemented. During the first simulations a cyclic, uni-axial, quasi-static electric field is applied with a maximum absolute value of 2 kV/mm amplitude without any mechanical loading. The starting point for the first cycle is at zero electric field for the unpoled virgin bulk piezoelectric ceramic. The domain switching at each element is determined by using the electromechanical energy

criterion that was presented before by Hwang et al. [HLM95].

$$\Delta P_i E_i + \Delta S_{ij} \sigma_{ij} \geq 2E_c P_c \quad (4.4)$$

In this relation, E_i and σ_{ij} are electric field and mechanical stress, E_c is the coercive electric field, P_c is the critical value of the spontaneous polarization. Both E_c and P_c are dependent on the piezoelectric material constants. ΔP_i and ΔS_{ij} are the polarization and mechanical strain change during domain switching, correspondingly. During the first part of the simulation only an external electric field is applied, the external mechanical stress is taken to be zero. Therefore, on the left side of the inequality, the mechanical stress term vanishes. According to this electromechanical energy criterion, domain switching occurs if the change of energy is higher than a certain critical threshold. During the simulation, the same energy levels are assumed for 90° and 180° domain switchings, which can be different from each other for the real case. In following chapters, this assumption will not be taken into account where energy levels for the threshold of domain switching will be assumed to be related to intergranular effects. Therefore, the electromechanical equation will be changed and not used anymore.

Lattice constants	Dimensions (<i>nm</i>)
a_0 (cubic)	0.4071
a (tetragonal)	0.4055
b_c (tetragonal)	0.4102

Table 4.1: Lattice constants of PZT-51 ceramics used in the simulations under quasi-static loading [LFLH99].

Another important nonlinearity of piezoceramic materials arises due to intergranular effects which is going to be explained deeply and micromechanically in the following chapter. Since the orientations of the spontaneous polarization of all grains are different from each other during both virgin and fully poled state, mechanical stresses are expected to occur at the grain boundaries. This is even more apparent in the domain switching range. Therefore, local values of the loading, which can be the electric field or the mechanical stress can be much different in neighbouring grains, so that a domain switching can occur even at levels of the macroscopic loading, which are well below the coercive field. Because of this reason the corresponding nonlinearities can be observed even in a small electromechanical loading range. In order to take into account intergranular effects phenomenologically, a certain probability for domain switching is introduced in the described model. In the present model, a probability for domain switching can be any function for which the probability is high near the coercive field strength and low far away from it. The function should contain parameters, which can

be adjusted in order to fit the simulation results to experimental results. The probability for domain switching is taken to be a polynomial function of some degree (n) of the ratio of the absolute values of the actual applied free energy and the critical energy equation (4.5) - (4.6).

$$p(E_i) = \left(\frac{E_i \Delta P_i}{2E_c P_c}\right)^n \quad |E_i| < |E_{ci}| \quad (4.5)$$

$$p(E_i) = 1 \quad |E_i| \geq |E_{ci}| \quad (4.6)$$

E_c and P_c values are assumed to be the same as the coercive electric field value and spontaneous polarization value correspondingly. The value of the probability (p) is varying between 0 and 1 according to the applied electric field (figure 4.3). When the applied electric field is greater than or equal to the coercive electric field, the probability value is taken as 1. In the described model n is an unknown parameter the value of which can be chosen arbitrarily in order to get optimum matching of the results to experimental data. When the value of n is increased, the probability for domain switching is decreased as seen in figure 4.3. Probability for domain switching is decreased more when higher n values are used and finally probability is reduced to zero under coercive field level for n towards infinity. In the simulations n has been chosen to be two, three, four or five. Other functions for the probability like exponential or hyperbolic functions may also be used in the simulations. However the present simulations are restricted to polynomials and other probability functions are not implemented in this paper.

According to the probabilistic approach, domain switching only depends on equation (4.5), if the applied free energy is smaller than the critical energy. So, with this polynomial function the probability for a domain to switch its polarization direction is more and more increasing, if the applied electric field is approaching the level of the coercive electric field. For a loading higher than the coercive field, equation (4.6) is automatically satisfied, which means that the domain switching occurs in any case. For example, if the applied electric field E_i is 0.4 kV/mm and the polarization change ΔP_i which is assumed to have the same magnitude as the critical value of the spontaneous polarization P_c is 0.3. When coercive field (E_c) is 0.676 kV/mm and n is chosen to be 3, then $P(0.4)$ equals 0.026. So we have 2.6 % of probability of domain switching. In the simulation code, random generators are implemented according to this result in order to give a corresponding percentage of domain switching. Therefore, 26 elements are estimated to have domain switching among 1000 elements with this relative loading when the applied electric field (E) is 0.4 kV/mm.

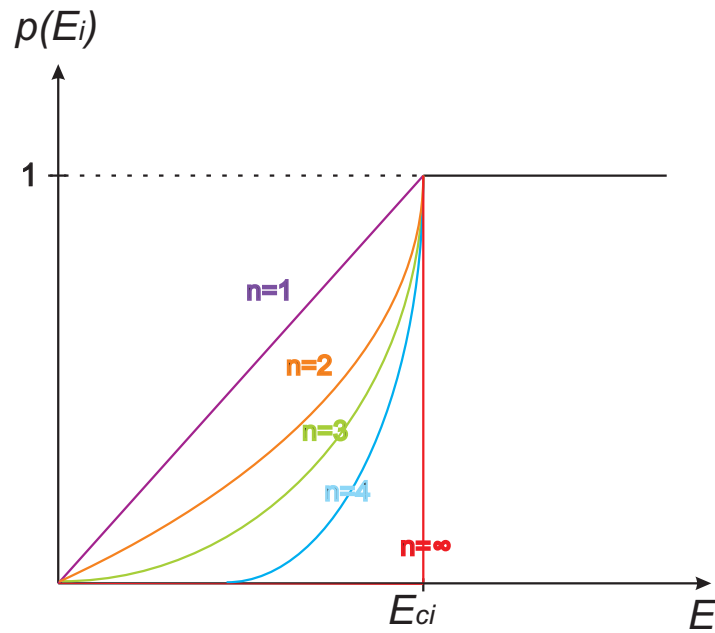


Figure 4.3: Probability of domain switching with respect to the electric field as a function of the polynomial function.

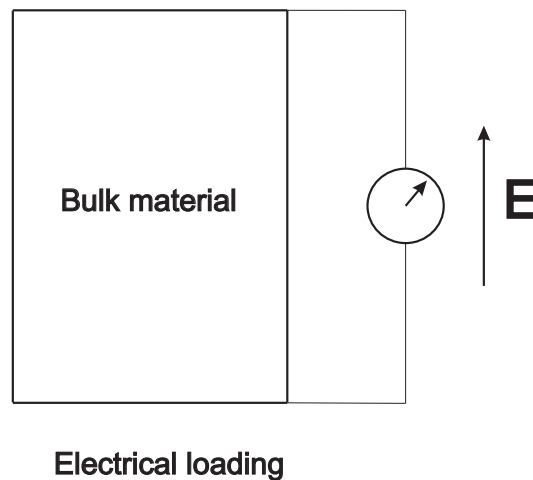


Figure 4.4: Electrical loading with a cyclic electric field.

4.2 Electrical loading

In this section, only electric loading without any mechanical stress is considered. During the simulation a cyclic, uni-axial electric field is applied with a maximum absolute amplitude value of 2 kV/mm. The electrical loading of the bulk material is illustrated in figure 4.4. Figure 4.5 shows a polarization (electric displacement) versus electric field

hysteresis curve without considering a probability function in the simulation for quasi-static loading. As can be seen in this figure the polarization curve has a sharp corner near the coercive electric field, which is the main difference of the model compared to experimental data. Figure 4.6 illustrates the hysteresis curve with a third order polynomial ($n = 3$) for the probability function. Figure 4.7 is the curve from the model in which a fourth order polynomial ($n = 4$) for the probability function is implemented. Smoothness of the curves near the coercive electric field levels can be observed easily from figures 4.6 and 4.7 compared to figure 4.5. A comparison of the simulation with experimental data which was measured by Lu et al. [LFLH99] is also given (figure 4.8). The simulated results obtained with a fifth order ($n = 5$) probability function fit better to experimental results than those curves, which were simulated without using the probabilistic approach.

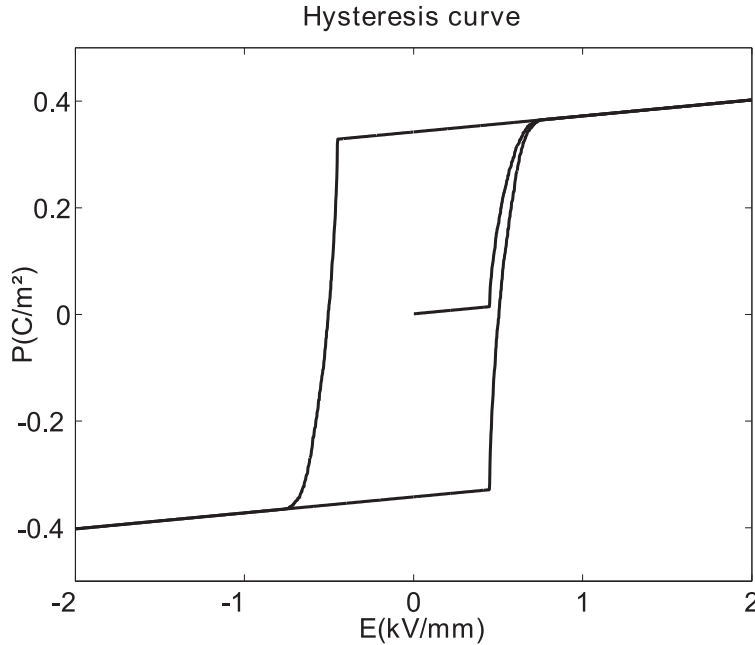


Figure 4.5: Hysteresis curve without probability function.

Figures 4.9 and 4.10 show the simulated macroscopic mechanical strain versus electric field butterfly curves. In order to get such butterfly curves, one should assume different energy levels for the threshold of domain switching, because nonlinear reduction during coercive electric field level can only be simulated with much more 90° domain switching than 180° domain switching for tetragonal ferroelectrics in micromechanical modelling. At this point, electromechanical energy requirement for 90° domain switching is assumed to be half of the one for 180° domain switching. Because, only 90° domain switching gives change in mechanical strain. The right hand side of inequality (4.4) is changed and reduced to only $P_c E_c$ instead of $2P_c E_c$ for the case of 90° domain

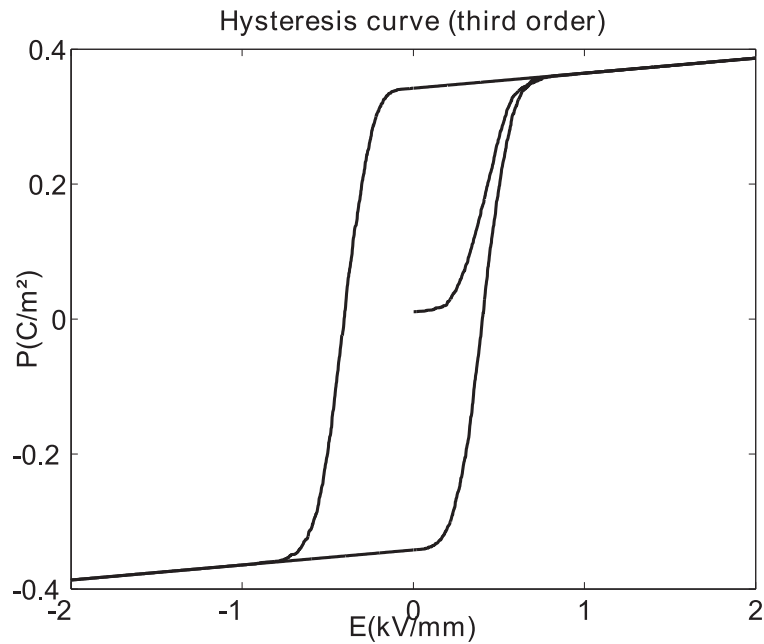


Figure 4.6: Hysteresis curve with third order polynomial for the probability function.

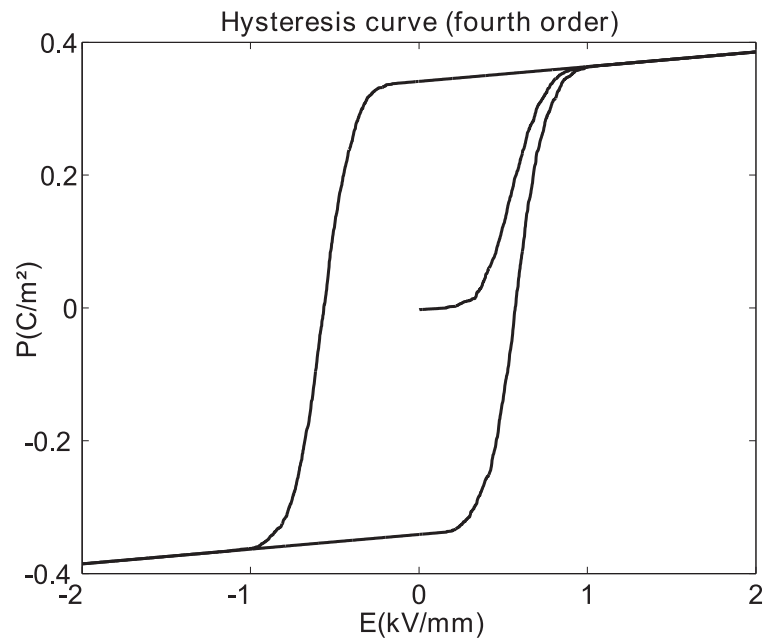


Figure 4.7: Hysteresis curve with fourth order polynomial for the probability function.

switching. This leads to the energy inequality given in equation (4.7). Equation (4.8) remains the same as equation (4.4) which is applied for 180° domain switching energy

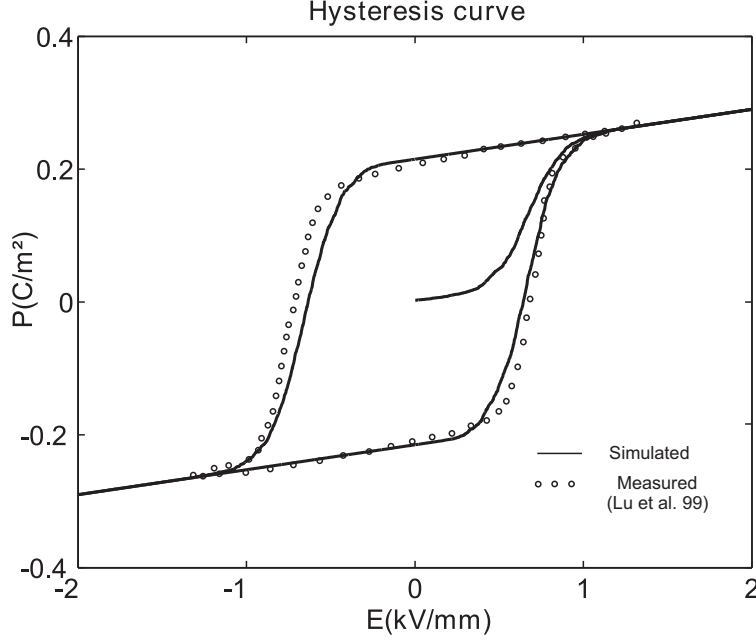


Figure 4.8: Comparison between simulation (fifth order polynomial for the probability function) and measured data [LFLH99].

level. Although such assumptions of energy levels for different domain switchings are very simple, it is just implemented for understanding the probabilistic characteristics of the model in butterfly curves. As explained before, this assumption will not be used anymore in the following chapters. Instead, a new method is introduced, which covers intergranular effects in electromechanical energy equations.

$$\Delta P_i E_i + \Delta S_{ij} \sigma_{ij} \geq E_c P_c, \quad \text{for } 90^\circ \text{ domain switching} \quad (4.7)$$

$$\Delta P_i E_i + \Delta S_{ij} \sigma_{ij} \geq 2E_c P_c, \quad \text{for } 180^\circ \text{ domain switching} \quad (4.8)$$

Figure 4.9 shows a butterfly curve without considering a probability function in the simulation. As can be seen in the figure the macroscopic mechanical strain is responding sharply like the polarisation curve in figure 4.5 near the coercive electric field. Figure 4.10 is the butterfly curve of the model with a probabilistic approach, in which a fifth order polynomial ($n = 5$) for the probability function is implemented. In addition to the spontaneous polarization, a value of 0.0012 (0.12%) is chosen as a spontaneous strain for each element [DAS04]. The smoothness of the curves in the range of the electric field in which domain switching occurs is similar to the smoothness of the polarization curves.

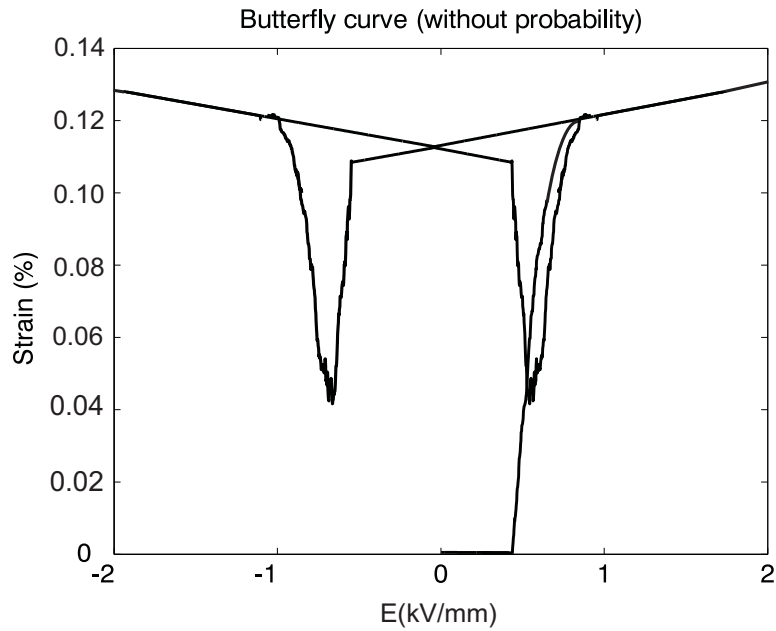


Figure 4.9: Butterfly curve without probability function.

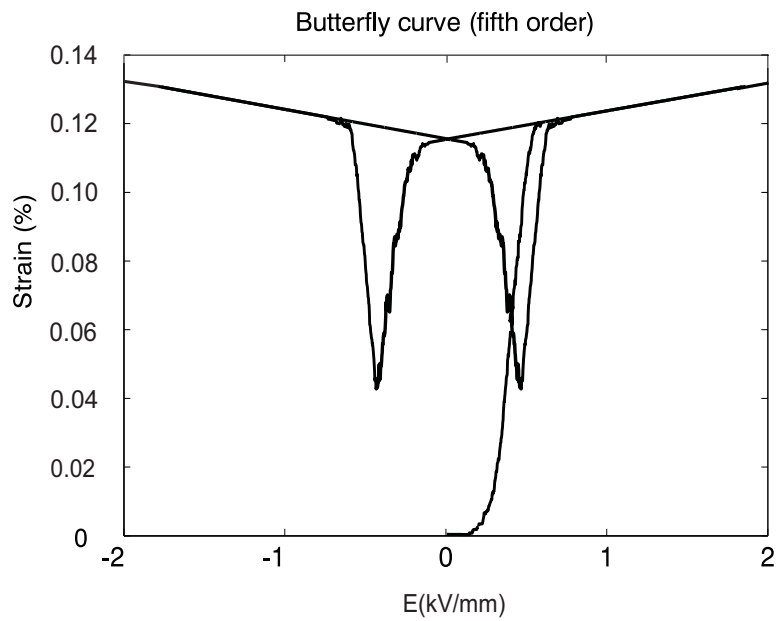


Figure 4.10: Butterfly curve with fifth order polynomial for the probability function.

The energy requirement for the threshold of different types of domain switching can change the behaviour of the butterfly curve drastically. Unlike the hysteresis curve, the characteristics of the butterfly curve is highly dependent on 90° domain switching,

which is the main cause of the tip properties of the curve. If the electromechanical energy level for 90° domain switching is chosen much lower than 180° domain switching, the domain switchings are mostly dominated by two 90° instead of one complete 180° domain switching. Therefore, tips of butterfly curve will even have negative strain values during the loading in both directions. In order to understand the effects of the type of domain switching, the electromechanical energy requirement for 180° domain switching, equation (4.9), is assumed to be 5 times higher than for a 90° domain switching, equation (4.10). The parameters of the equations (4.9)-(4.10) are taken to be the same as the ones in equations (4.7)-(4.8). In this simulation, the probabilistic approach is not implemented. Figure 4.11 shows this simulation of the butterfly curve. It can be easily observed that the beginning of the domain switching in figure 4.11 is sharper and the strain value is decreasing in a smaller electric field range around the coercive field level compared to figures 4.9 and 4.10. The reason is that such electromechanical energy equations favour 90° domain switching at the coercive electric field level in figure 4.11. Since the energy requirement for the threshold of a 180° domain switching is so high, the butterfly curve is smooth just after the curve is passing through the deepest strain value. Therefore, 180° domain switching will continue in a high electrical loading range and extend to the saturation value at the maximum amplitude of the loading which is 2 kV/mm.

$$\Delta P_i E_i + \Delta S_{ij} \sigma_{ij} \geq 5 E_c P_c, \quad \text{for } 180^\circ \text{ domain switching} \quad (4.9)$$

$$\Delta P_i E_i + \Delta S_{ij} \sigma_{ij} \geq E_c P_c, \quad \text{for } 90^\circ \text{ domain switching} \quad (4.10)$$

4.3 Stress-strain and stress-polarization relations

As explained before, there may be ferroelastic domain switchings, which are only possible as 90° switchings for a perovskite type tetragonal structure when they are subjected to a mechanical loading instead of an electrical one. Unlike ferroelectric domain switching, ferroelastic domain switching accompanies high strain output at the level of the coercive mechanical stress (σ_c).

In the following, the non-linear mechanical stress versus longitudinal strain curve for polycrystalline piezoelectric materials are simulated by the application of a mechanical stress, which is compressive, uni-axial and quasi-static (figure 4.11). In this part of the simulation, the electrical loading is kept constant and zero ($E = 0$). The compressive stress is applied starting from zero to a maximum of 100 MPa. The stress-strain curve is simulated only for the case of a fully poled piezoceramic material. Therefore, the mechanical loading is not bipolar and cyclic like in the hysteresis and butterfly simulations. The simulations are performed both with and without a probabilistic approach,

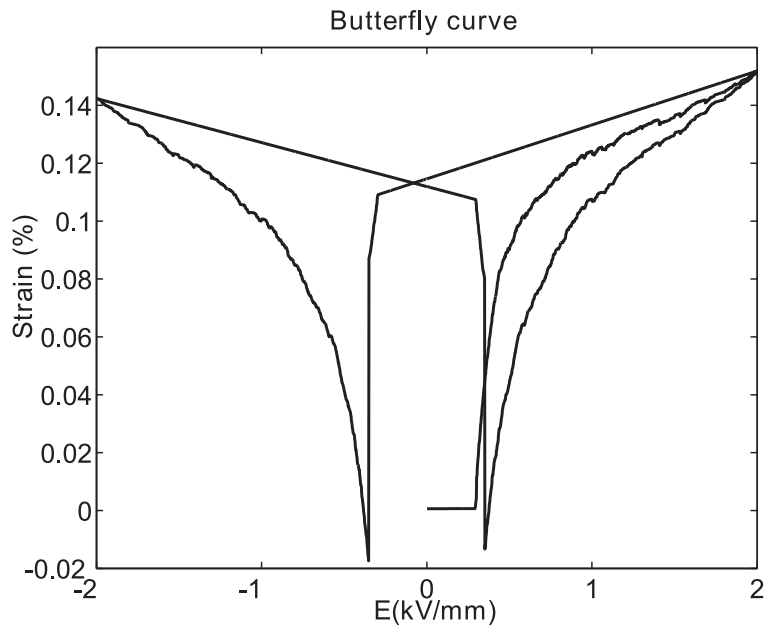


Figure 4.11: Butterfly curve assuming an energy requirement for a 180° domain switching which is five times higher than for a 90° domain switching

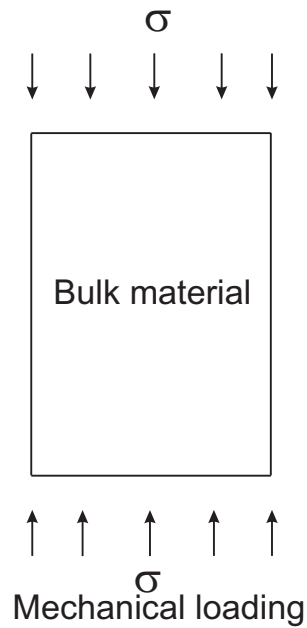


Figure 4.12: Mechanical loading with a constant compressive stress.

equations (4.11) and (4.12). Figure 4.13 shows functions of the probability of domain switching with respect to the applied mechanical stress by using various n values for

the case of a probabilistic approach in the simulation.

$$p(\sigma_{ij}) = \left(\frac{\sigma_{ij}\Delta S_{ij}}{2\sigma_c S_c}\right)^n \quad |\sigma_{ij}| < |\sigma_c| \quad (4.11)$$

$$p(\sigma_{ij}) = 1 \quad |\sigma_{ij}| \geq |\sigma_c| \quad (4.12)$$

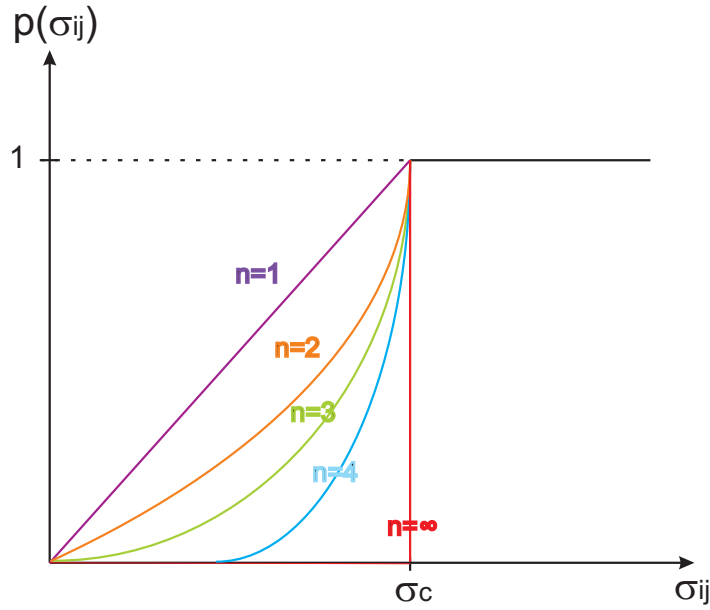


Figure 4.13: Probability of domain switching with respect to the mechanical stress as a function of the exponential.

The material parameters which are used in the simulations are identical to the ones used for hysteresis and butterfly simulations. The coercive mechanical stress is assumed to be 20 MPa. The spontaneous strain is taken as 0.2 %.

Figure 4.14 shows the corresponding stress-strain curve, in which a probabilistic approach is not implemented. As expected the stress-strain curve near the coercive mechanical stress range has a sharp edge, which is not the case in the experimental stress-strain curve. Simulations with third ($n = 3$) and fourth ($n = 4$) order probability functions are plotted in figures 4.15 and 4.16. These curves are smoother than figure 4.16.

Figure 4.17 illustrates the best matching of the stress-strain curve with a seventh order ($n = 7$) probabilistic approach with the experimental curve which are taken from Lu et al. [LFLH99].

Similarly, the electrical displacement or macroscopic polarization of piezoceramic materials are influenced by the application of a compressive stress. Figures 4.18, 4.19, 4.20

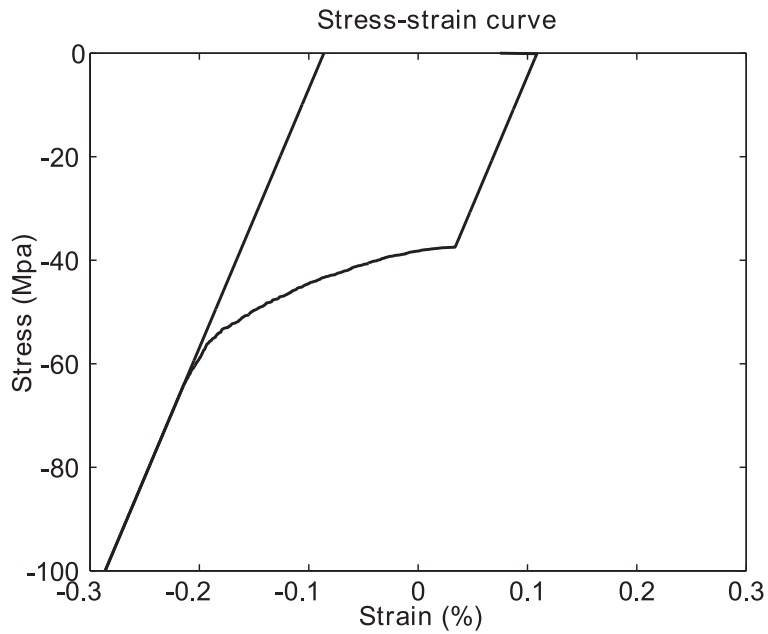


Figure 4.14: Stress strain curve without probabilistic approach.

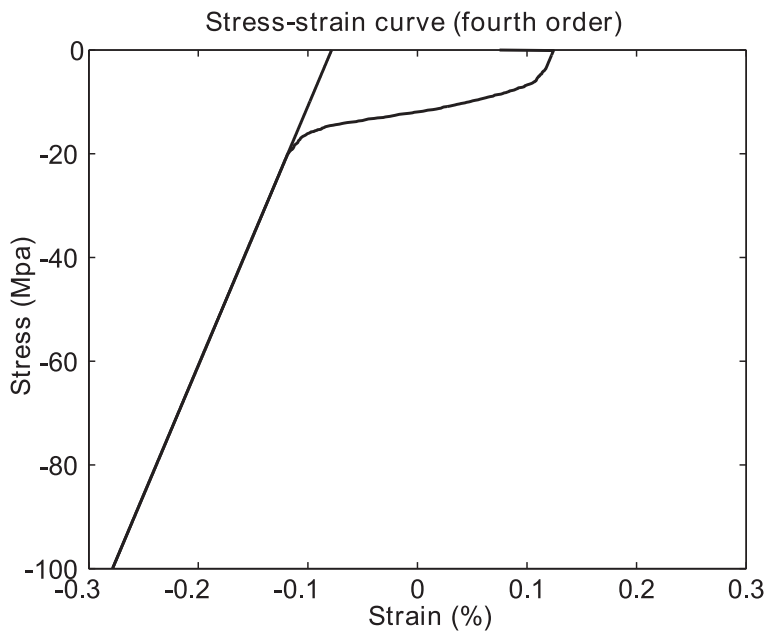


Figure 4.15: Stress strain curve with third order polynomial for the probability function.

and 4.21 show the compressive stress versus electric displacement curves at zero electric field for initially fully poled materials. At the beginning of the loading from zero

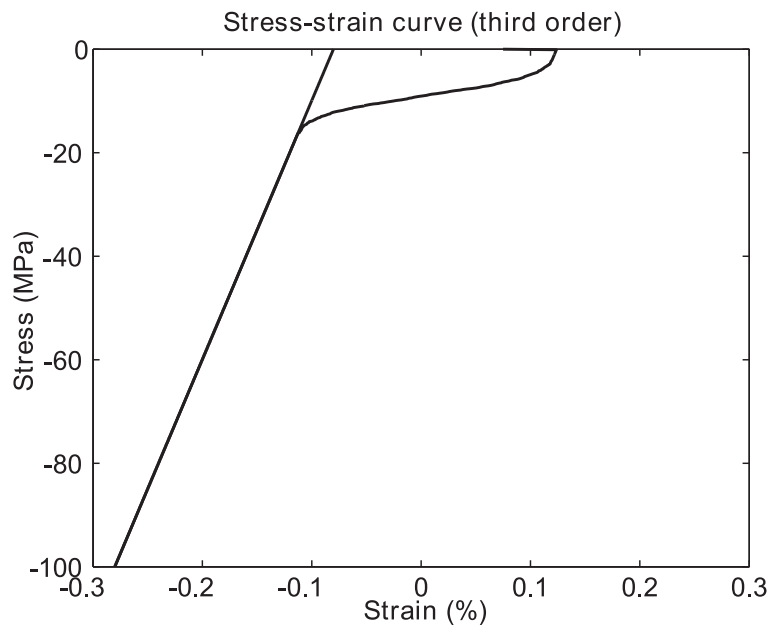


Figure 4.16: Stress strain curve with fourth order polynomial for the probability function.

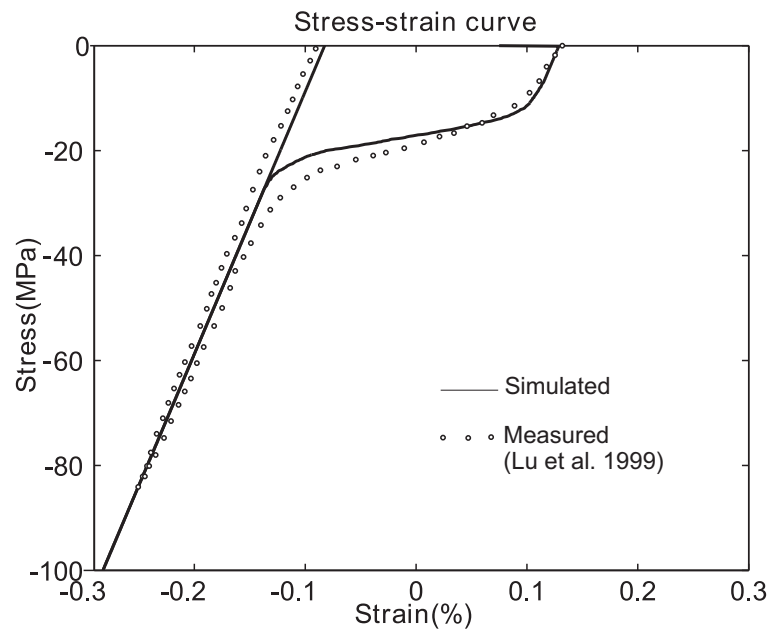


Figure 4.17: Comparison between simulation (seventh order polynomial for the probability function) and measured data [LFLH99].

to the coercive mechanical stress, it is observed that there is a linear decrease in the electric displacement. This is due to the linear piezoelectric effect, which is macroscopically positive in the fully poled case. Therefore, when the loading is increased up to the coercive mechanical stress, there is a linear decrement in the electric displacement value (refer to direct piezoelectric effect, $D = d\sigma$). As soon as the coercive mechanical field is achieved, the ferroelastic domain switching occurs. These switchings are mainly 90° domain switchings for perovskite type tetragonal structures. During 90° domain switching, there are two possible switching directions, which can produce either positive or negative polarization, but the same strain values. Thereby, the directions of the spontaneous polarization of grains or domains become random when the saturation level of the stress is reached. When the applied compressive stress is released from the fully depolarised state, the electric displacement response is nearly independent of the compressive stress, because depolarised domains or randomly oriented domains are macroscopically leading to a piezoelectric constant of zero value. Therefore, it is expected that the material does not have a direct linear piezoelectric effect.

Figure 4.18 shows the curve of the compressive stress versus electric displacement in loading direction without implementation of a probabilistic approach. Figures 4.19 and 4.20 show the same curves with third ($n = 3$) and fourth ($n = 4$) order probability functions correspondingly. Finally, figure 4.21 illustrates the comparison of simulation and experimental curves [LFLH99] of the compressive stress as a function of the electric displacement. In this simulation a sixth ($n = 6$) order probability function is implemented for the comparison.

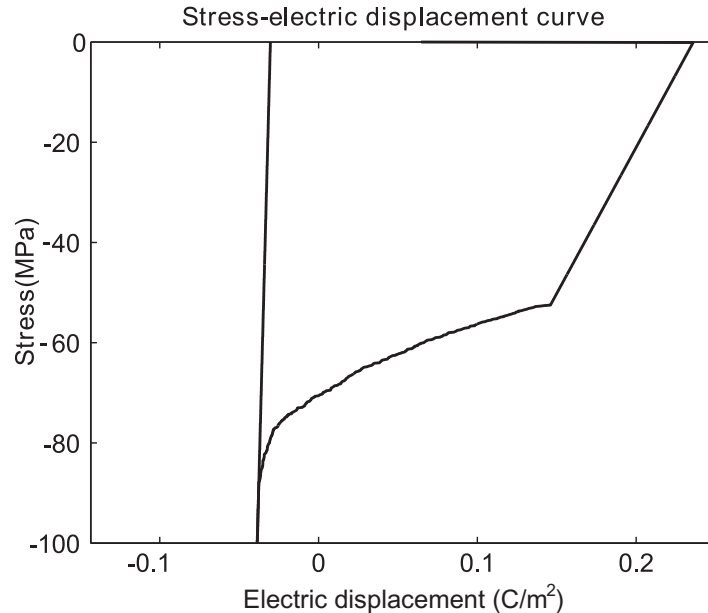


Figure 4.18: Stress-electric displacement curve without probabilistic approach

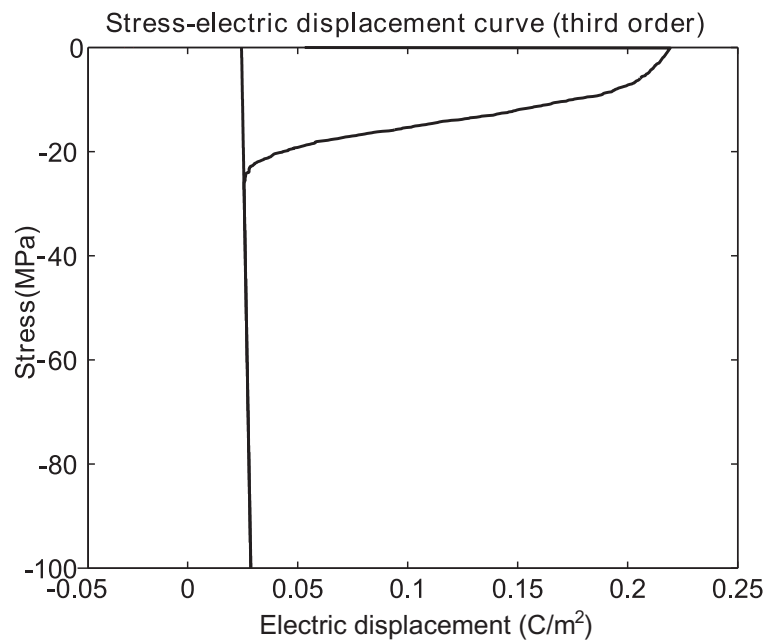


Figure 4.19: Stress-electric displacement curve with third order polynomial for the probability function

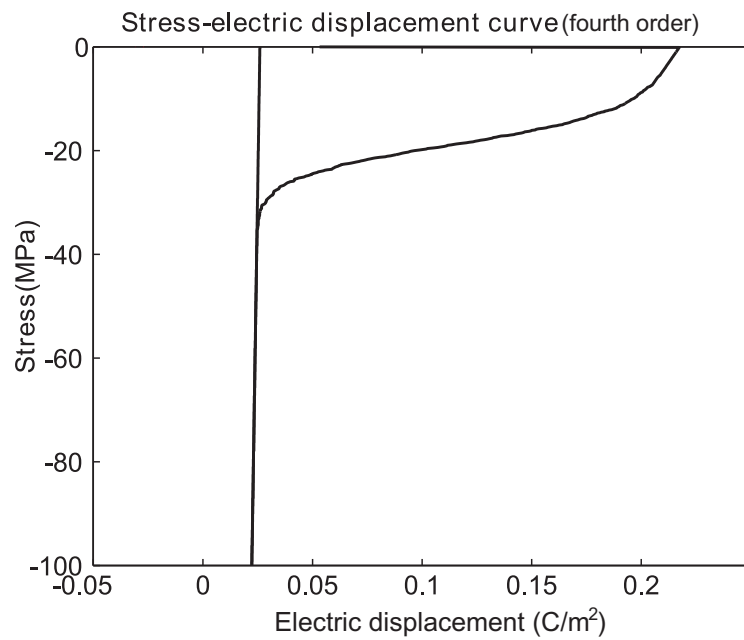


Figure 4.20: Stress-electric displacement curve with fourth order polynomial for the probability function

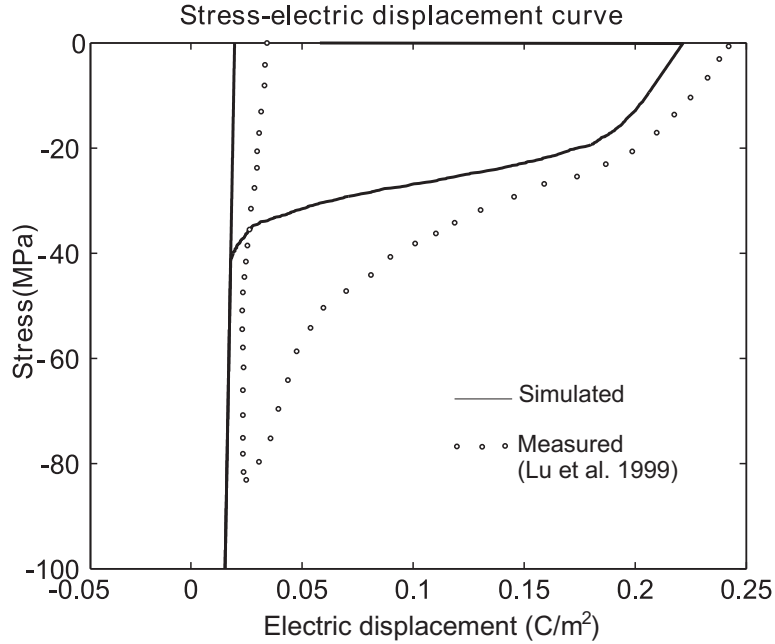


Figure 4.21: Comparison between simulation (sixth order polynomial for the probability function) and measured data [LFLH99].

4.4 Electric field and constant compressive stress

Most commercial piezoelectric actuators which are used in industrial applications are operated under high mechanical loading conditions. Therefore, it is required to analyse the effects of a mechanical stress on the loading of piezoelectric materials. In this section, the macroscopic properties of piezoelectric ceramics are analysed when a constant compressive stress is applied in the same direction as the electric field, figure 4.22. The experimental results, which are given in literature show that if a fixed high compressive stress is applied during a cyclic electrical loading of piezoelectric ceramics, there are three basic differences, which are observed in the electric displacement versus electric field hysteresis curve. The first observation is the decreasing of the coercive electric field value, which is the threshold for domain switching. The reason for this behaviour is explained by the types of domain switchings (90° and 180°) under the loading of a compressive stress. It is experimentally proofed that there occur much more 90° domain switchings under a mechanical loading than without any mechanical loading. The basic reason for the decreasing of the coercive electric field level is the reduction of energy required for domain switching for the first 90° domain switching due to the stress distribution inside the microstructure of the material. On the other hand, this stress distribution in the same microstructure of the piezoelectric ceramic increases the energy required for the second 90° domain switching (figure 4.23). Thereby, the

total range of the electric field in which domain switching occurs is enlarged for the case of a compressive stress compared to the no stress case. The domain switching range is linearly increasing with the magnitude of the applied compressive stress. For a better explanation one lattice structure of a piezoelectric ceramic after applying a fixed compressive stress and a cyclic electric field is considered. The mechanical stresses ($\sigma_1 > \sigma_2 > \sigma_3$) and electric fields ($E_1 > E_2 > E_3$) are assumed to be like in local coordinates (x_1, x_2, x_3) of the lattice structure in figure 4.22. For some microstructures the internal mechanical stresses can be tensile, because of the orientations of local directions of the microstructures. Therefore, the second term of the left side of the energy relation in equation (4.4) can become positive for the first 90° domain switching of the piezoelectric ceramic material. Then three energy relations for domain switchings in corresponding three local directions of the lattice structure can be ordered for a low electric field as $E_3\Delta P + \sigma_3\Delta S \geq E_2\Delta P + \sigma_2\Delta S \geq E_1\Delta P + \sigma_1\Delta S$. When the critical energy is achieved for the third local direction of the lattice structure, a 90° domain switching occurs. After the first domain switching, with increasing electric field the inequality energy relation for the second 90° domain switching is expected to exceed the energy threshold value. When the electric field is increased, the energy inequality relation reverses due to the dominance of the electric field in local directions $E_1\Delta P + \sigma_1\Delta S \geq E_2\Delta P + \sigma_2\Delta S \geq E_3\Delta P + \sigma_3\Delta S$. For the second 90° domain switching, a higher electric field is required to overcome the negative effect of the compressive stress in the energy equation in local direction 1. Therefore, the mechanical stress in direction 1 discourages the second 90° domain switching.

The second major influence of the constant compressive stress is the reduction of the remnant and saturation polarization values of the macroscopic electric displacement versus electric field curve. This phenomenon is explained by the negative effect of the mechanical stress term in the linear constitutive equation (3.4). As it can be seen from this equation, the magnitude of remnant and saturation polarization is decreasing proportionally when the magnitude of the applied compressive stress is increased.

A nonlinear changing of the piezoelectric coefficient is the third important effect when a compressive stress is applied. According to experiments [Lyn96], there is no linear correlation between the applied mechanical stress and the piezoelectric coefficient (d_{ijk}), which is assumed to be related to the macroscopic spontaneous polarization value shown in equation (4.13) during the simulations. The piezoelectric constant is assumed to behave transversely isotropic as mentioned before. The value of the piezoelectric constant (d) in the loading direction is taken to be $3.0 \cdot 10^{-9}(\text{m/V})$.

In this model, it is also tried to simulate the macroscopic electric displacement versus electric field curve under a constant compressive stress. In the simulations the constant compressive stress values are chosen as 20 MPa and 40 MPa.

Figures 4.24, 4.25 and 4.26 show the electric displacement versus electric field hysteresis curves with and without probability functions for piezoelectric ceramics that have

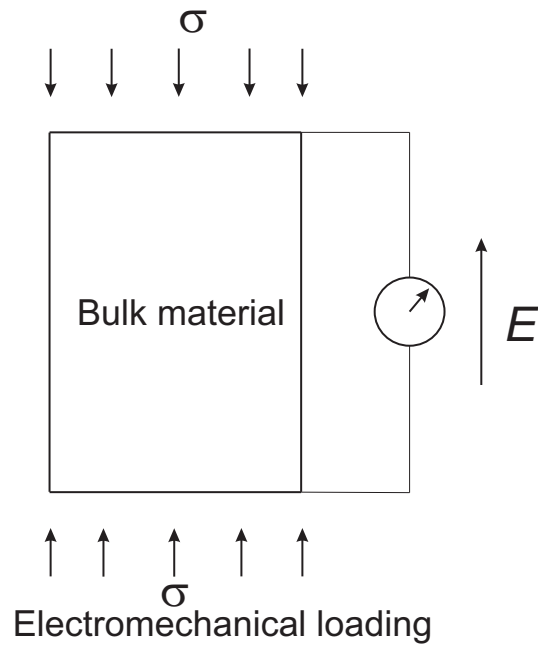


Figure 4.22: Electromechanical loading, cyclic electric field with constant compressive stress.

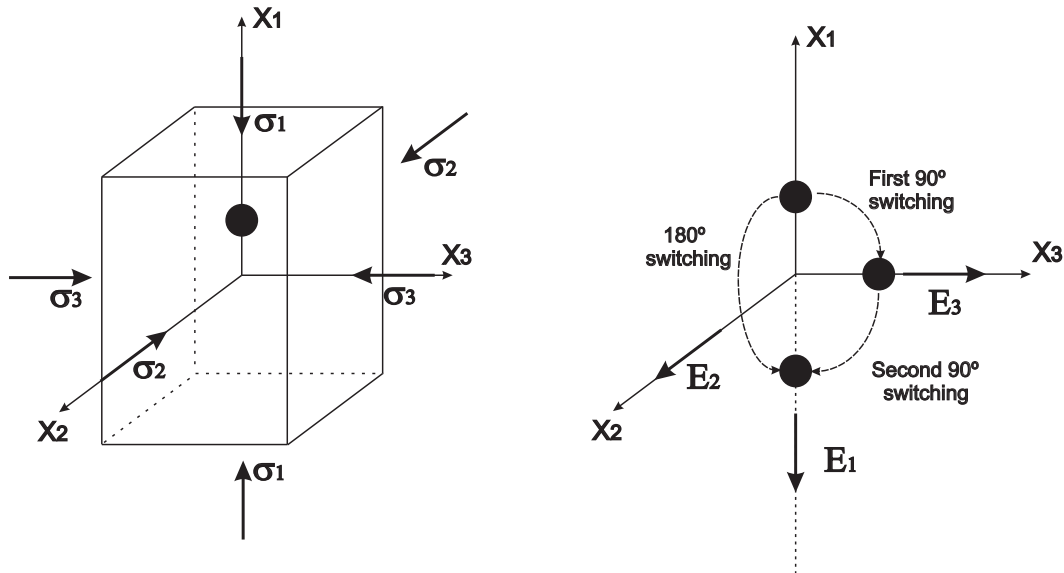


Figure 4.23: Lattice structure under constant compressive stress with electric field and domain switching possibilities.

a tetragonal perovskite type microstructure subject to 20 MPa constant compressive stress with cyclic uni-axial quasi-static electric field. Figure 4.24 demonstrates a hys-

teresis curve, which was simulated without taking into consideration the probability function. It can be seen easily that there are two stepwise changes of the electric displacement near both the loading and the unloading coercive electric field levels. This behaviour is explained by the different types of domain switchings (90° and 180°) due to the effect of the compressive stress. The first step during the domain switching range is dominated by a first 90° domain switching, which is encouraged by the compressive stress in the microstructures due to the electromechanical energy equation. In a real experimental case, such a stepwise increasing is not so apparent. Therefore, the author has once more used probability functions in the simulations in order to have a better matching with the experimental curve. Figures 4.25 and 4.26 have been obtained by using third and fourth order polynomials for the probability functions. Especially figure 4.25 matches the corresponding experimental curve. An increased switching period range and decreased macroscopic remnant and saturation polarization values are well approximated in these simulations [DAS05].

$$d_{ijk} = d \frac{P_i}{P_{si}} \quad (4.13)$$

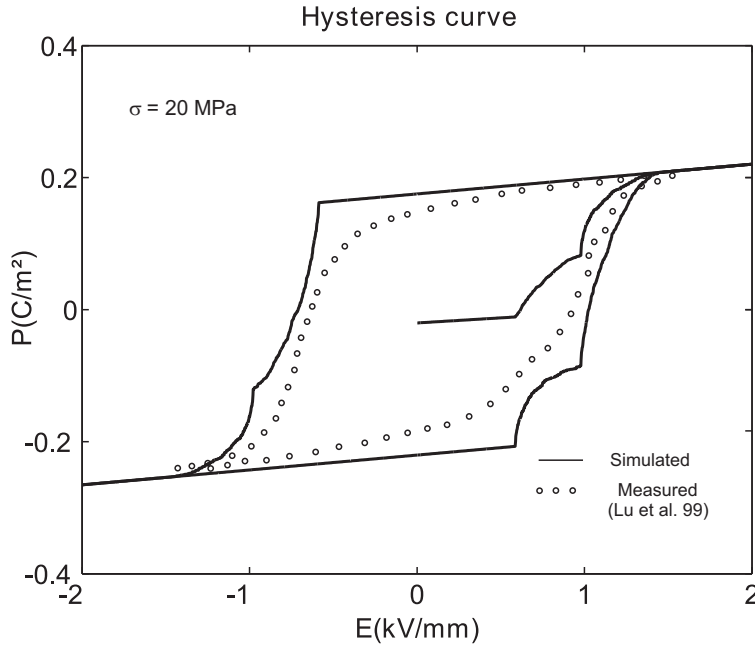


Figure 4.24: Comparison between simulation (without probability function) and measured data.

A higher mechanical loading case has been also simulated and compared with experimental data. Figure 4.27 shows the hysteresis curve with 40 MPa constant compressive stress using a third order polynomial for the probability function with corresponding

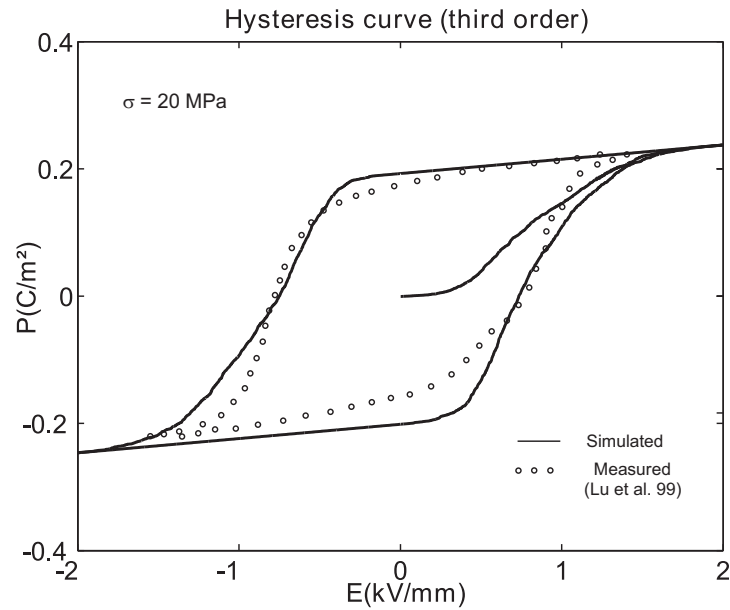


Figure 4.25: Comparison between simulation (third order polynomial for the probability function) and measured data.

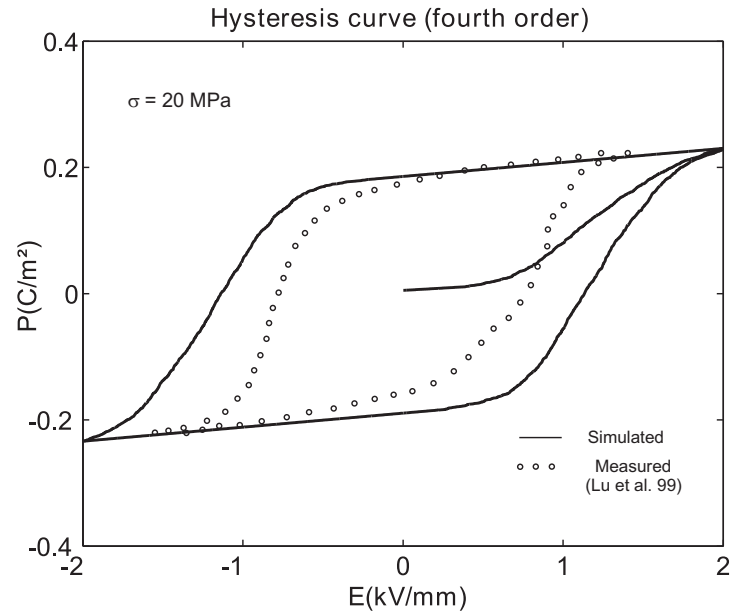


Figure 4.26: Comparison between simulation (fourth order polynomial for the probability function) and measured data.

experimental data. As the constant compressive stress is increased, the period of domain switching is enlarged, which is approximated well in the simulation. However, the magnitude of the change of macroscopic electric displacement or remnant polarization has been overestimated.

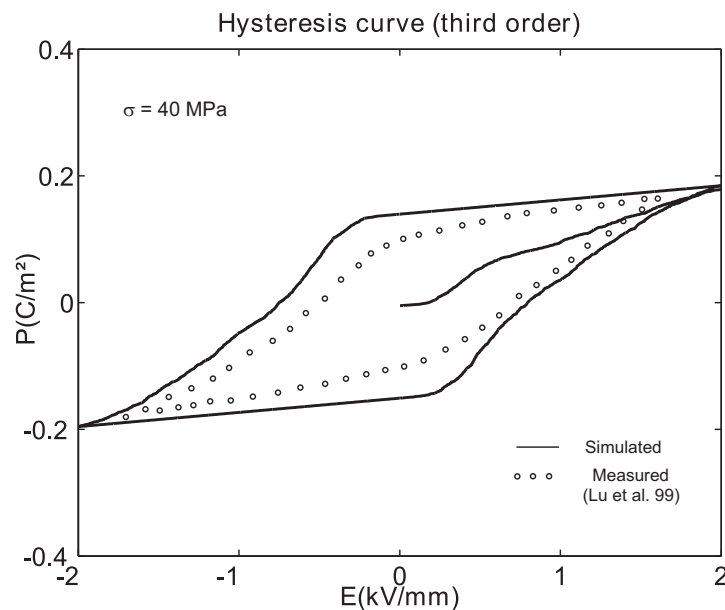


Figure 4.27: Comparison between simulation (third order polynomial for the probability function) and measured data.

4.5 Concluding remarks

Characteristics of perovskite type tetragonal polycrystalline piezoelectric ceramics have been simulated by using a three dimensional micromechanical model under uni-axial quasi-static high electric cyclic loading and constant compressive stress. A piezoelectric linear constitutive model and nonlinear domain switching with probability functions have been implemented in the model. By using this probability function, the influence of intergranular stress can be assumed to be taken into account phenomenologically. The electric displacement versus electric field curves, using probability functions do better match to the experimental hysteresis curves than simulation results in which probability functions have not been used. Piezoelectric ceramics under fixed compressive stress have been deeply investigated in this chapter. Hysteresis curves under different constant compressive stress values are also simulated. In the next chapter, the model will be implemented to get rate dependent properties of such materials with various alternating loading conditions.

Chapter 5

Rate dependent model

5.1 Relaxation time and frequency

In experiments it can be found that the response of ferroelectric materials to applied electromechanical loading is not rate independent. The time required for dipole reversal or domain switching in ferroelectric materials is called relaxation time and its reciprocal is the relaxation frequency [RCW76]. Experiments and models for the quasi-static loading case cannot explain the rate dependent characteristic of such materials. Therefore, quasi-static relations will not be valid for high dynamic loadings with fast changing electric fields. Figure 5.1 illustrates an experimental observation of polarizability of a typical dielectric material with respect to the frequency of the loading. In these experiments a triangular electric field is applied. It can be seen from figure 5.1 that the total polarizability of the material reduces with increasing frequency of the applied field if the frequency exceeds the relaxation frequency of the material [RCW76],[MM37].

5.2 Rate dependent model

Early experiments to determine the dependence of the electric field and the temperature on the switching time and the switching current were performed by Merz [Mer54] for BaTiO₃ single crystals. In addition he explained the switching mechanism as the nucleation of new domains and a growth process with domain wall motion. For an applied constant electric field, a reduction of the switching time and thus an increasing switching current is observed for increasing temperatures at which the experiments were performed. This means that the nucleation of domains and the growth process are faster at higher temperatures. Likewise, the dependence of the switching time and the current on the applied electric field and the coercive field at a fixed temperature is observed. As can be seen in figure 5.2 the switching time is dependent on the applied

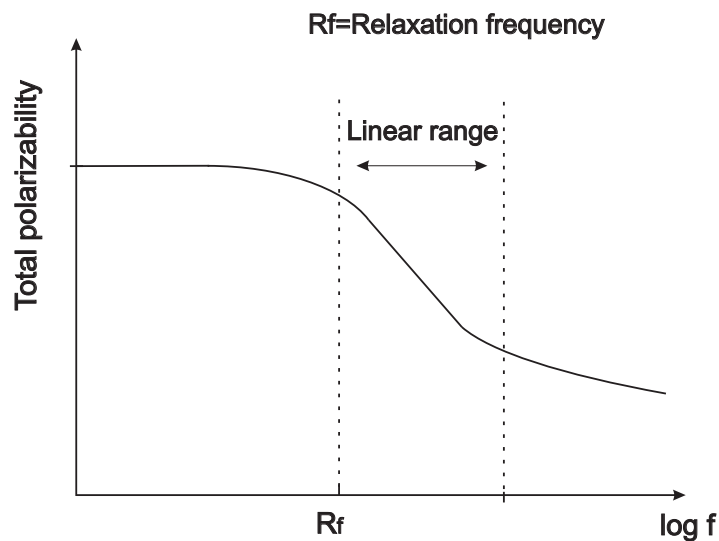


Figure 5.1: Polarizability of typical dielectric material as a function of the frequency of the applied electric field.

electric field hyperbolically. The time necessary for domain switching is decreasing with respect to the electric field. It can also be concluded from these experiments that the reciprocal of the switching time increases when the applied electric field is increased [Mer54]. One of the first publications on the simulation of the rate dependency of polarization curves for BaTiO_3 was given by Landauer et al. [LYD56]. They used the observations of Merz [Mer54], in which the rate of switching was basically expressed as an exponential function of the applied electric field. Although the switching process was not determined clearly as a nucleation with further domain expansion, they managed to illustrate the change of the coercive field due to different loading rates. The minimum coercive electric field was found for the lowest loading rate.

It is known from literature that domain switching starts inside a domain of the piezoelectric material at a critical level of either the applied electrical field or the mechanical stress. The generation of the new phase during the domain switching process can be separated into two parts: nucleation and kinetics of the new phase [AKK94]. The beginning of the nucleation of the new phase is assumed to take place at the threshold of the critical energy. The propagation of the new phase is dominated by the motion of the phase boundary between the old and the new nucleated phases [Arl96S], [Arl96A], [Arl97]. The propagation of the new phase is determined by a so called kinetics relation. The completion of domain switching inside the domain requires a certain time period. The simulation of piezoelectric materials for quasi-static loading uses the assumption of complete domain switching inside the domains during each incremental loading step. When the loading is faster, the time between two successive loading steps is not adequate for a complete domain switching. Therefore, the overall electric dis-

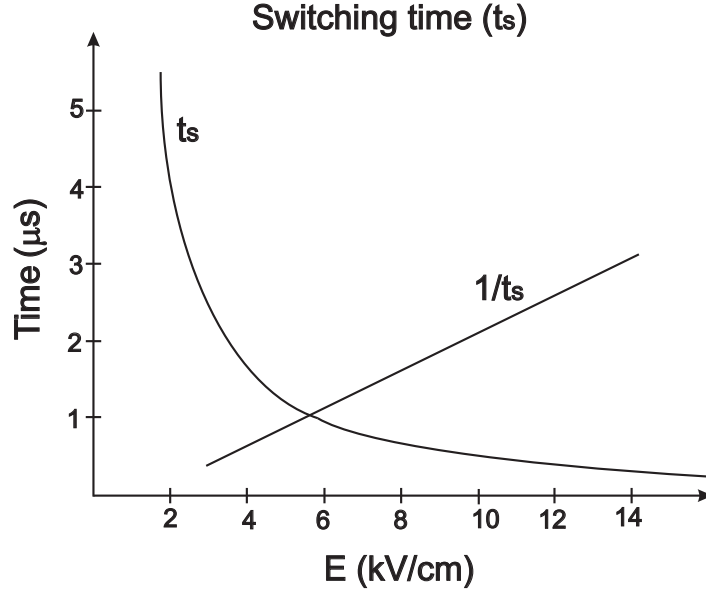


Figure 5.2: Switching time and reciprocal of it with respect to applied electric field.

placement and strain versus electric field curves will change for cyclic loadings with increasing frequencies. For the propagation of the new phase, linear kinetics theory is used in this thesis. Due to linear kinetics theory, there is a critical time step (Δt_l) during the simulation. This limit time is the time, which the phase boundary needs to propagate completely through the domain whenever nucleation has been initiated. It is a material, temperature and field dependent parameter. If the time interval between two subsequent incremental steps is larger than this critical time period, the phase boundary can completely propagate through the domain, i.e. the switching process can be completed. If the time between two simulation steps is smaller than the limit time (Δt_l), then the switching process in the grain is not finished after one simulation step. For a simulation of the quasi-static case the time step in the simulation should be greater than the limit time (Δt_l)

5.3 Rate dependent cyclic electric loading

The limit time (Δt_l) can be expressed with respect to the electric field, eqn. (5.1), which is bipolar, cyclic, uni-axial and triangular in a shape shown in figure 5.3.

$$\Delta t_l = \frac{C}{E - E_c} \quad (5.1)$$

In equation 5.1, C is a material constant, which depends on temperature [Mer54]. Its

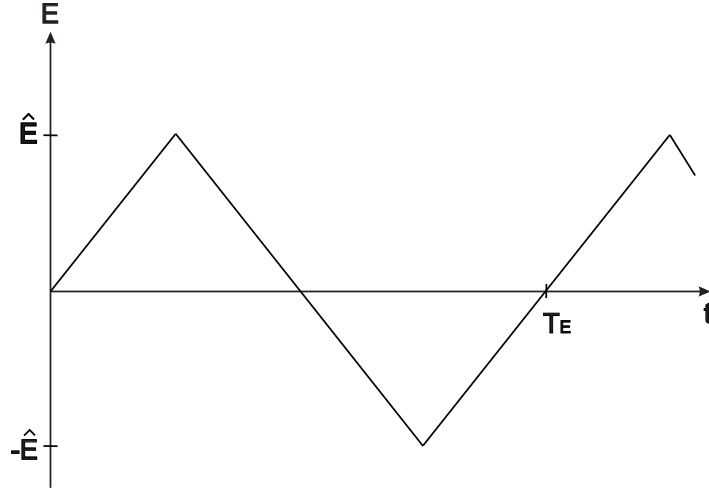


Figure 5.3: Cyclic triangular electric field.

values with respect to various temperature levels for piezoelectric ceramics with 10 mm thickness are tabulated in table 5.1.

Parameter, C(kV/mm)	Temperature (°C)
0.0036	23
0.0027	50
0.0018	75
0.0008	100

Table 5.1: Material parameter values (C) under various temperature levels [Mer54].

In the simulation the frequency of the applied electric field is given by

$$f_E = \frac{1}{T_E} \quad (5.2)$$

where T_E is the period according to Figure 5.3. The rate of change of the electric field (\dot{E}) is given in figure 5.3 with the amplitude \hat{E} of the electric field according to

$$\dot{E} = \pm \frac{2\hat{E}}{T_E/2} = \pm \frac{4\hat{E}}{T_E} = \pm 4\hat{E}f_E \quad (5.3)$$

During the simulation the increments of the electric field ΔE between different loading steps are given explicitly. In Figure 5.4 it can be seen that such an increment

corresponds to a time step Δt_s for which

$$\Delta t_s = \frac{\Delta E}{\dot{E}} = \frac{\Delta E}{(4\hat{E}f_E)} \quad (5.4)$$

holds. This is the simulation time step.

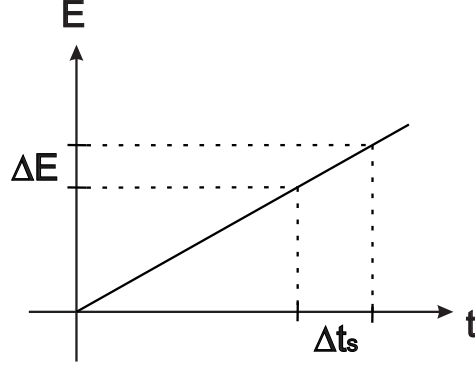


Figure 5.4: Loading steps $(\Delta E, \Delta t_s)$

Equation (5.4) shows that the time step Δt_s is decreasing for increasing frequencies of the electric field. It has to be mentioned that ΔE and \hat{E} is kept constant for the simulations. If Δt_s is smaller than Δt_l a domain, which begins to change the direction of polarization, does not change the phase in the whole domain during one simulation step Δt_s . Instead, due to linear kinetics theory only a fraction $(\frac{\Delta t_s}{\Delta t_l})$ will have the new polarization direction. Especially, if Δt_s is very small compared to Δt_l due to a high frequency f_E , the domain switching process may take several simulation steps until the whole domain is switched. In order to determine the volume fraction ΔV of the switched part of the total volume V of the domain, the time Δt_p has to be determined, which has elapsed since the nucleation process begins.

$$\Delta V = V \frac{\Delta t_p}{\Delta t_l} \rightarrow \frac{\Delta V}{V} = \frac{\Delta t_p}{\Delta t_l} \quad (5.5)$$

Note that Δt_p may be a multiple of Δt_s . If P_{0b} and P_{0a} denote the polarization together with the polarization direction of the whole domain before and after the switching process, then the polarization P_0 during the switching process after inserting the volume fractions is

$$P_0 = (1 - \frac{\Delta V}{V})P_{0b} + \frac{\Delta V}{V}P_{0a} = (1 - \frac{\Delta t_p}{\Delta t_l})P_{0b} + \frac{\Delta t_p}{\Delta t_l}P_{0a} \quad (5.6)$$

As discretized the time axis, the polarization at one loading step after the beginning of the nucleation is

$$P_{01} = (1 - \frac{\Delta t_s}{\Delta t_l})P_{0b} + \frac{\Delta t_s}{\Delta t_l}P_{0a} \quad (5.7)$$

As explained before, if the value of Δt_s is much lower than the value of Δt_l , the domain switching process may take many incremental steps to be completed. Due to this fact a number n is introduced for each domain, which has already started the switching process. This number denotes the number of time steps, which have already passed after the beginning of the switching process in the corresponding domain. For the n_{th} time step after nucleation the polarization during domain switching is obtained

$$P_{0(n)} = \left(1 - \frac{(n-1)\Delta t_s}{\Delta t_l} - \frac{\Delta t_s}{\Delta t_l}\right)P_{0b} + \frac{(n-1)\Delta t_s}{\Delta t_l}P_{0a} + \frac{\Delta t_s}{\Delta t_l}P_{0a} \quad (5.8)$$

$$P_{0(n)} = \left(1 - \frac{(n-1)\Delta t_s}{\Delta t_l}\right)P_{0b} - \frac{(n-1)\Delta t_s}{\Delta t_l}P_{0a} + \frac{\Delta t_s}{\Delta t_l}(P_{0a} - P_{0b}) \quad (5.9)$$

$$P_{0(n)} = P_{0(n-1)} + \frac{\Delta t_s}{\Delta t_l}(P_{0a} - P_{0b}) \quad (5.10)$$

This is repeated until

$$n\Delta t_s = \Delta t_l \quad (5.11)$$

where at the end of the switching $P_0=P_{0a}$ is assumed. Equations (5.5) to (5.11) are derived in order to get a discretized linear kinetics model for the computer simulation program.

5.3.1 Simulations

Simulations are performed for electric displacement versus electric field curves with different frequencies (0.01 Hz, 0.1 Hz, and 1 Hz) and amplitudes of the electric field (2 kV/mm, 1.5 kV/mm, and 1 kV/mm). These values are chosen in order to be able to compare the simulation results with experiments that were performed for the same values. Although equation (5.1) shows that limit time (Δt_l) is highly dependent on the electric field, the limit time is considered to be constant. For the simplicity of calculations in the simulation it is taken to be 0.07 seconds for the assumption of a piezoelectric ceramic under the condition of room temperature (23 °C). This means that 0.0018 Hz will be the maximum frequency for a quasi-static loading at an amplitude of 2 kV/mm for the electric field and increments of $\Delta E=1$ V/mm. PIC 151 is taken as a sample piezoelectric material, which was also used in the experiments [Zho03]. Therefore, the dielectric permittivity (ϵ) is taken to be $2.124 \cdot 10^{-8}$ F/m and for simplicity it is assumed to be isotropic. The spontaneous polarization P_0 and the critical value of the spontaneous polarization (P_c) are chosen to be 0.4 C/m². A value of 1 kV/mm is assumed for the coercive electric field level. The piezoelectric constant is considered to behave transversely isotropic. The value of the piezoelectric constant

in loading direction is taken as $0.45 \cdot 10^{-9}$ m/V. The elastic constant (s_{33}) is $1.9 \cdot 10^{-11}$ N/m². For a better explanation of the model, one additional example are also inserted for the case of $\Delta t_s < \Delta t_l$. If the domain switching criterion, equation (4.4) is fulfilled, a new element nucleates and begins to propagate with respect to linear kinetics model. According to the applied electric field with a frequency of 1 Hz, Δt_s is 0.00125 second. Therefore, n equals $\frac{\Delta t_l}{\Delta t_s} = 0.07/0.00125=56$. This means that 56 steps are required for the corresponding element to finish its domain switching. So, the polarization change for each step for this particular element is actually the polarization change for a quasi-static loading divided by 56. For every step, in order to have a simple calculation, equation (5.10) is used. The domain switching continues during the range of 56 V/mm electric field loading range since each electrical loading step (ΔE) is 1 V/mm.

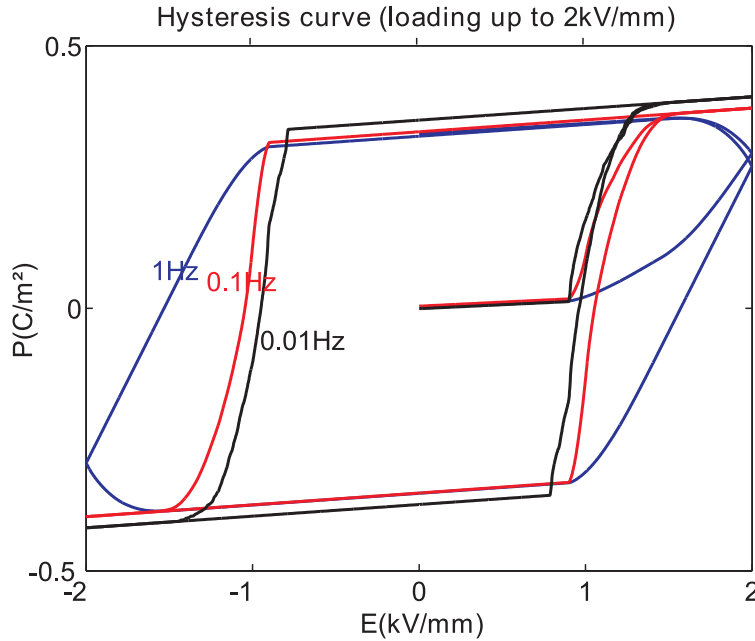


Figure 5.5: Hysteresis curves without probabilistic approach, $\hat{E} = 2$ kV/mm

Simulations without probabilistic approach

Simulation results are shown in figures 5.5, 5.6 and 5.7 for the case in which a probability for domain switching is not taken into account [CFH97]. It is experimentally found that the coercive electric field is dependent on the frequency of the loading which apparently can also be seen in the simulated curves. The coercive electric field is increasing when the frequency is increased from 0.01 Hz to 1 Hz. This can even be seen in figure 5.7 for an amplitude of electric field of 1 kV/mm, which corresponds to the coercive electric field level chosen above. Another important observation for these curves under cyclic

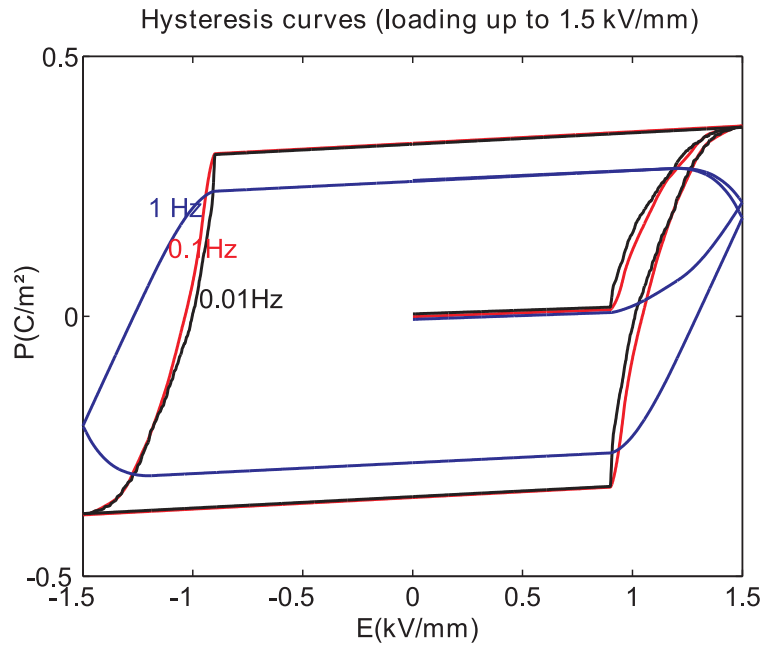


Figure 5.6: Hysteresis curves without probabilistic approach, $\hat{E} = 1.5$ kV/mm

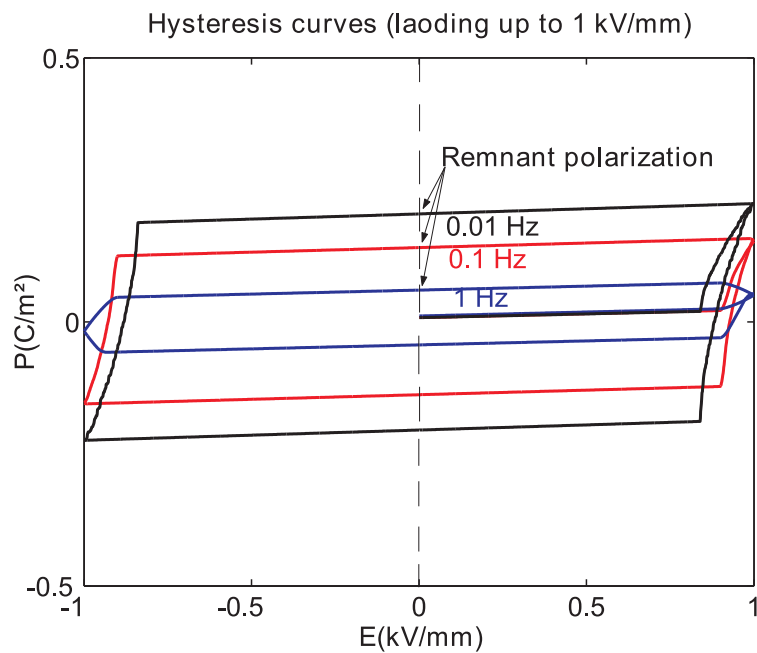


Figure 5.7: Hysteresis curves without probabilistic approach, $\hat{E} = 1$ kV/mm, leading to different remnant polarizations for different loading frequencies

loading with a high frequency is that the electric displacement is increasing even for a decreasing electric field during unloading provided that the actual electric field is larger than the coercive field. For a cyclic loading with a frequency of 1 Hz and an amplitude of the electric field of 2 and 1.5 kV/mm, the electric displacement cannot reach the saturation level which corresponds to a quasi-static loading. Instead, in a certain range the electric displacement is increasing for a decreasing electric field as far as the applied electric field is larger than the coercive field. The remnant polarization, which is the polarization at zero electric field, is not changing too much for frequencies of 0.01 Hz and 0.1 Hz and amplitudes of the electric field of 2 and 1.5 kV/mm, because all possible domain switchings are approximately completed at the point where the maximum electric field is reached for such amplitudes and frequencies of the applied loading. On the other hand, as shown in figure 5.7 the saturation polarization cannot be reached and the frequency of the loading has a strong influence on the remnant polarization, if the amplitude of the applied electric field is near the coercive field. The remnant polarization is decreasing if the frequency of the cyclic loading is increasing, see figure 5.10.

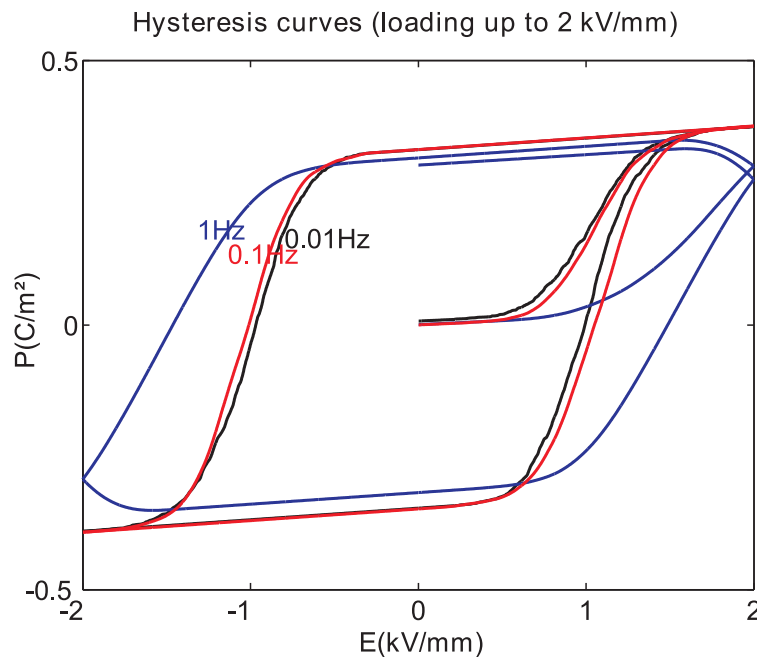


Figure 5.8: Hysteresis curves with fourth order polynomial for the probability function, $\hat{E} = 2$ kV/mm

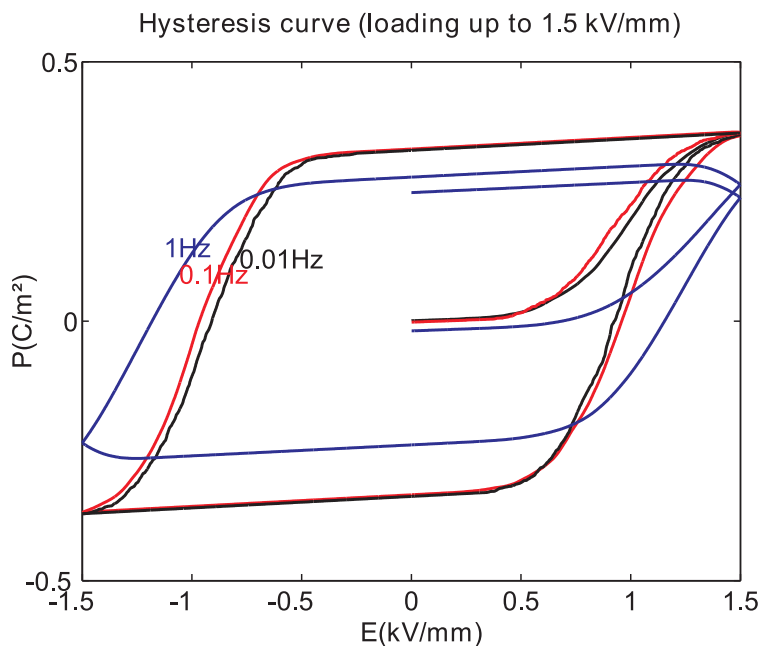


Figure 5.9: Hysteresis curves with fourth order polynomial for the probability function, $\hat{E} = 1.5$ kV/mm

Simulations with probabilistic approach

As explained before, in piezoceramic materials it is observed that there occur some domain switchings below the coercive field. In previous publications this was modeled by a probability criterion, which is explained in the previous chapter and can be found for example in [DAS04]. Such a probability is also implemented for the simulation of the rate dependent characteristics of PIC 151 using a micromechanical model, for which the nucleation starts with a certain probability depending on the energy difference between actual and switched state during switching. Figures 5.8) to 5.10 show electric displacement versus electric field curves again for a cyclic loading with different amplitudes and frequencies. For the simulations a fourth order probability function is implemented. As it can be seen in the figures, the curves are smoother, especially in the range near the coercive field level compared to the ones that were simulated without adding the probability criterion. Therefore, these curves correspond better to the experimental results for electric field values near the coercive field. All other important properties already explained for the simulation without probability criterion are observed as well: decreasing of the electric field level for zero overall polarization with decreasing frequency of loading. Other phenomena are the increase of the remnant polarization for smaller amplitudes of the loading and decreasing frequencies or continuing further domain switchings during the early unloading stage as far as the

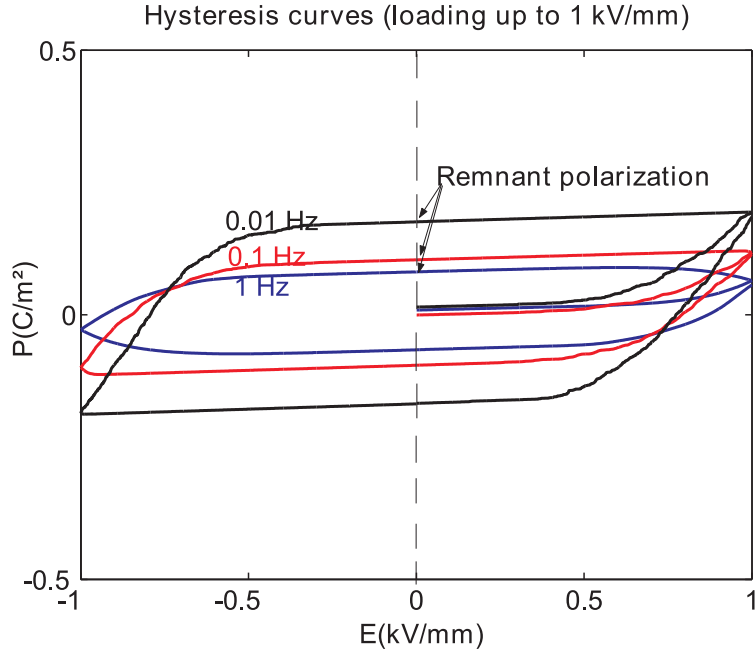


Figure 5.10: Hysteresis curves with fourth order polynomial for the probability function, $\hat{E} = 1$ kV/mm

cyclic electric field is above the coercive field [DAS1].

5.4 Rate dependent mechanical loading

If instead of a cyclic electric field, a cyclic mechanical stress is applied then it can be estimated that the occurring polarization switchings are also time dependent. Similar to an electric field a limit time (Δt_l) can be formulated

$$\Delta t_l = \frac{C_\sigma}{\sigma - \sigma_c} \quad (5.12)$$

in which σ_c denotes the coercive stress, σ is actual mechanical loading and C_σ is a constant. There is no adequate data for the value and dependence of C_σ in literature. In order to be compatible with the results of the rate dependency of the electrical loading in the previous section, C_σ is assumed to be constant and to have a value of 0.0036 MPa.

During the simulation the frequency of the applied compressive stress is given by

$$f_\sigma = \frac{1}{T_\sigma} \quad (5.13)$$

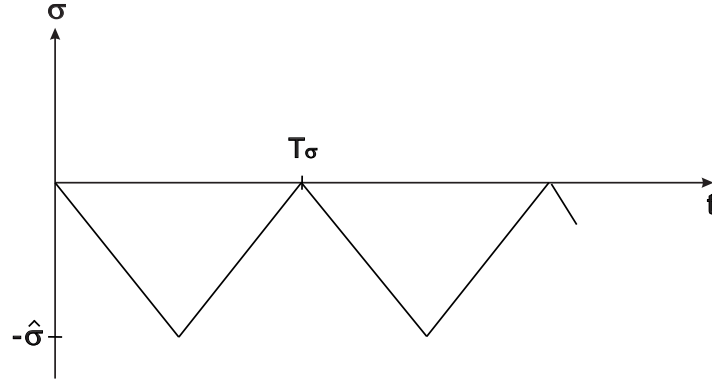


Figure 5.11: Applied triangular compressive stress

where T_σ is the period according to Figure 5.11. The rate of change of the compressive stress ($\dot{\sigma}$) can be derived by equation (5.14). $\hat{\sigma}$ is the amplitude of the compressive stress.

$$\dot{\sigma} = \pm \frac{\hat{\sigma}}{T_\sigma/2} = \pm \frac{2\hat{\sigma}}{T_\sigma} = \pm 2\hat{\sigma}f_\sigma \quad (5.14)$$

In the simulation the increments of the compressive stress $\Delta\sigma$ between different loading steps are given by.

$$\Delta t_s = \frac{\Delta\sigma}{\dot{\sigma}} = \frac{\Delta\sigma}{(2\hat{\sigma}f_\sigma)} \quad (5.15)$$

Δt_s is the simulation time step for the rate dependent compressive loading. The same procedure as for an electrical loading in the previous section is followed to find out numerical kinetic relations due to the mechanical loading. Equations (5.5) to (5.11) which are independent of loading types are implemented for getting a discretized linear kinetics model for a computer simulation program for an applied compressive stress.

5.4.1 Simulations

Simulations are performed for mechanical strain versus mechanical stress and electric displacement versus mechanical stress curves with various loading frequencies (0.01 Hz, 0.1 Hz, and 1 Hz) and amplitudes of the compressive stress (-100 MPa, -75 MPa, -50 MPa). The limit time (Δt_l) is assumed to be independent of equation (5.12) and constant C_σ during the application of the unipolar stress and to be 0.07 seconds. Therefore 0.0018 Hz is the maximum frequency for a quasi-static loading for an amplitude of 100 MPa of the compressive stress and increments of $\Delta t_s=0.05$ MPa. Material parameter are already given in the section in which the electrical loading for PIC 151 is piezoelectric material.

Simulation results (mechanical strain versus compressive stress) are presented in figures 5.12 to 5.14 for the case, in which probability functions are not considered. It is apparently seen in the simulations that the coercive mechanical stress is dependent on the frequency of the loading like for an electrical loading. One of the basic important observations for these curves is that the mechanical strain is further decreasing even during the releasing of compressive stress provided that the actual compressive stress is larger than the coercive mechanical stress. For a mechanical loading with an amplitude of 100 MPa and a frequency of 1 Hz, the strain is observed to arrive saturation level during unloading. The negative remnant strain is not changing much for frequencies between 0.1 Hz and 1 Hz, but the absolute value of remnant strains for 0.1 Hz and 1 Hz are lower than the one in a 0.01 Hz loading.

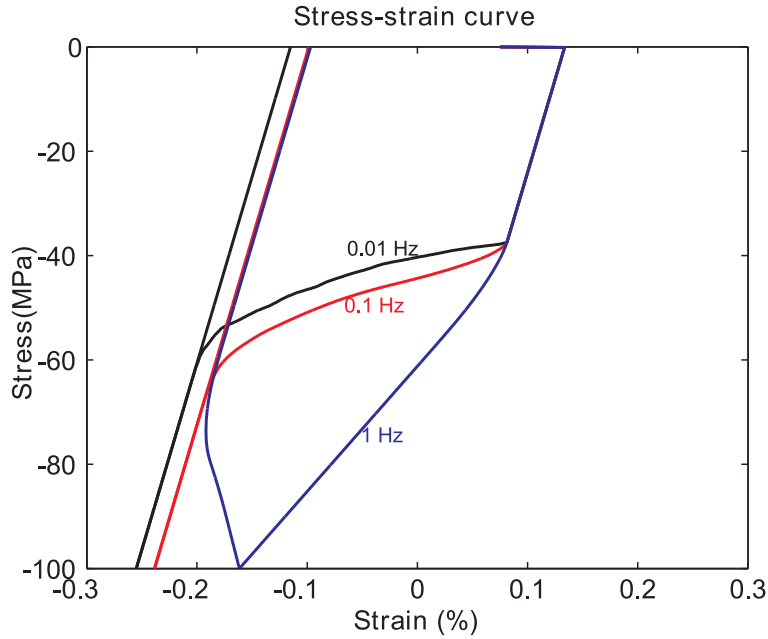


Figure 5.12: Stress-strain curves without probabilistic approach, $\sigma_{max} = 100$ MPa

Finally, if the frequency of loading is further increased to an amplitude of 100 MPa, it is observed that such increment during unloading for catching saturation value is not visible anymore. Figure 5.15 shows this behaviour in the stress-strain curve with 100 MPa amplitude alternating compressive stress with a frequency of 2 Hz. Unlike for the case of 1 Hz in figure 5.12, the mechanical strain is not increasing for 2 Hz loading in figure 5.15, when the loading is reduced from 100 MPa. This observation can be explained as follows; the response of domain switching is not as fast as the response of linear characteristics of piezoelectrics, which is assumed to be independent of kinetics relations. Additionally, the saturation strain and remnant strain value decreases considerably.

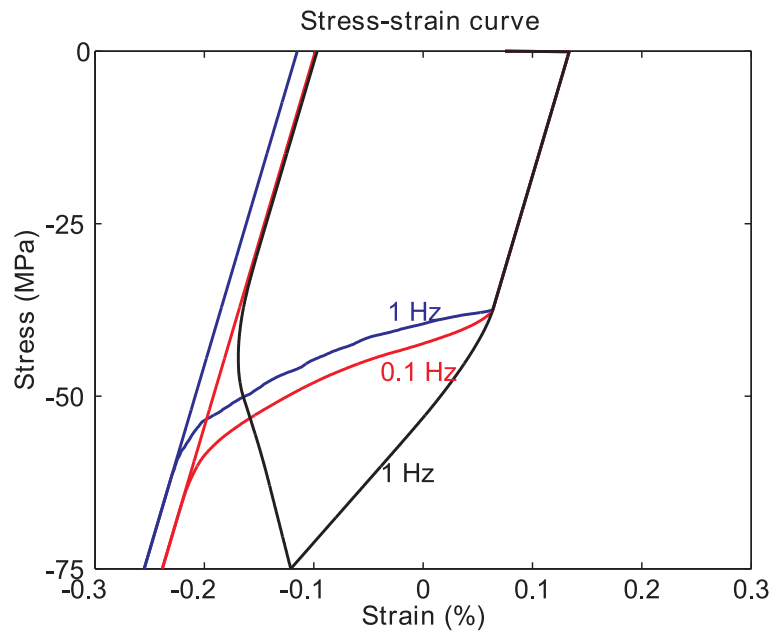


Figure 5.13: Stress-strain curves without probabilistic approach, $\sigma_{max} = 75$ MPa

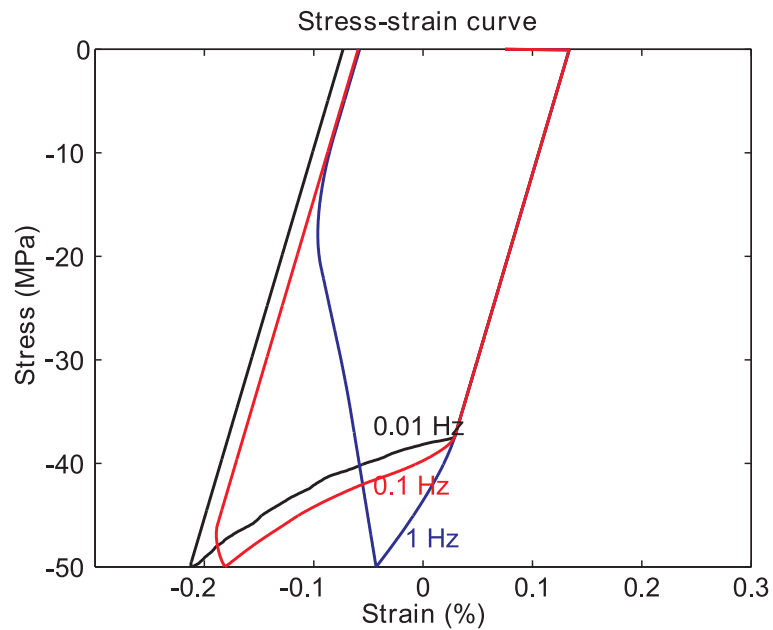


Figure 5.14: Stress-strain curves without probabilistic approach, $\sigma_{max} = 50$ MPa

Mechanical stress versus electric displacement or macroscopic polarization curves under the same compressive loading amplitudes (100 MPa, 75 MPa, 50 MPa) and frequencies

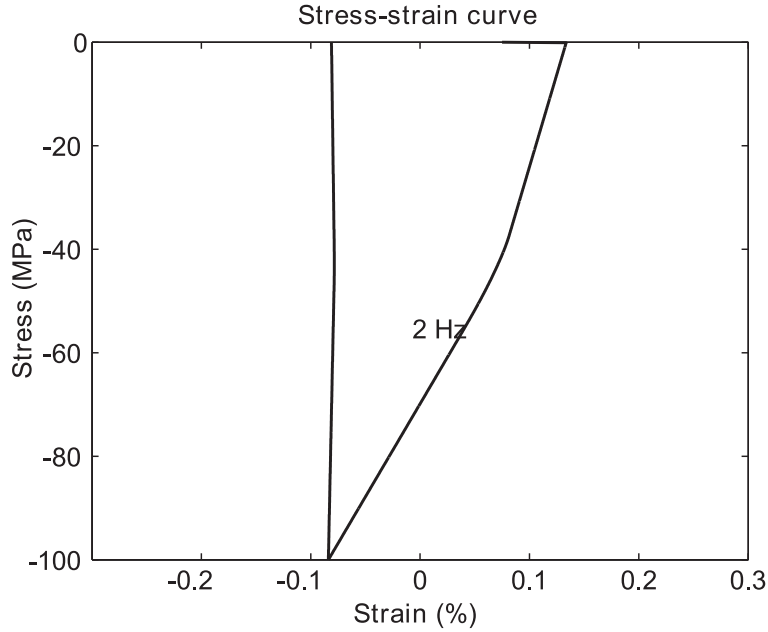


Figure 5.15: Stress-strain curves without probability approach (2 Hz), $\sigma_{max} = 100$ MPa

(0.01 Hz, 0.1 Hz, and 1 Hz) without using a probabilistic approach are shown in figures 5.16 to 5.18. Adoption of 60 MPa as a coercive mechanical stress during the simulation is the only significant difference of assumption unlike stress versus strain curves in which 20 MPa coercive mechanical stress is applied. This assumption leads to a different domain switching level in the electromechanical energy equation. Therefore, the simulation results are expected to have considerable change when they are compared with stress versus strain curves. But the fact that domain switching level is increased when the rate of loading is faster is still valid irrespective of the assumed value of the coercive mechanical stress level unless the amplitude of the applied mechanical stress is lower than this coercive stress level (figures 5.16 and 5.17). The results in figure 5.18 show only linear straight lines in which there are no domain switchings for all three different frequency ranges of loading. The simulations stay under the level of the domain switching range below which only linear constitutive relations are implemented. From the saturation or remnant electric displacement point of view, one can easily observe that the absolute value of the remnant polarization is reduced steadily if the frequency of loading is becoming higher at a loading level of 100 MPa amplitude, which is strong enough to force grains to have domain switching (figure 5.16). Such an observation cannot be apparently seen in the simulations like in figure 5.17 when the amplitude of the applied compressive stress is close to the coercive mechanical stress level. But still, the remnant polarization in the 1 Hz curve is much lower than one for 0.1 and 0.01 Hz curves. The characteristics of curves during unloading are also interesting for

various loading conditions. The response of the curve of 0.01 Hz is nearly constant and independent on the mechanical stress during unloading from 100 MPa to a zero level like the same behaviour in a quasi-static unloading (figure 4.18). As it is already explained, all grains are depoled due to non-180° domain switching (90° for tetragonal, 70.5° and 109.5° for rhombohedral) and becoming again randomly distributed like in the virgin state, when the applied compressive stress is high enough to let grains depole. Responses are related to compressive stress during unloading for the case of loading with 0.1 Hz and 1 Hz of 100 MPa amplitude of compressive stress. Electric displacement is decreasing linearly in absolute value (increasing in real value) as the compressive stress is released. However, there is a nonlinear increment in the absolute value of polarization in the case of unloading of the curve with 1 Hz loading up to a mechanical coercive stress level below which the response again becomes linear like in 0.01 Hz. The cause of such increment during unloading can be explained by continuing of the domain switching in the early unloading case which are also observable in hysteresis curves with electrical loading and stress versus strain curves in mechanical loading. The slope of the responses during unloading, which is nothing but the macroscopic piezoelectric constant, is going to increase as the amplitude of the compressive stress is decreased provided that amplitude will not be lower than the coercive stress level, figure 5.17. It can easily be concluded that a small amount of grains are depoled with 75 MPa amplitude stress compared to the ones with an amplitude of 100 MPa.

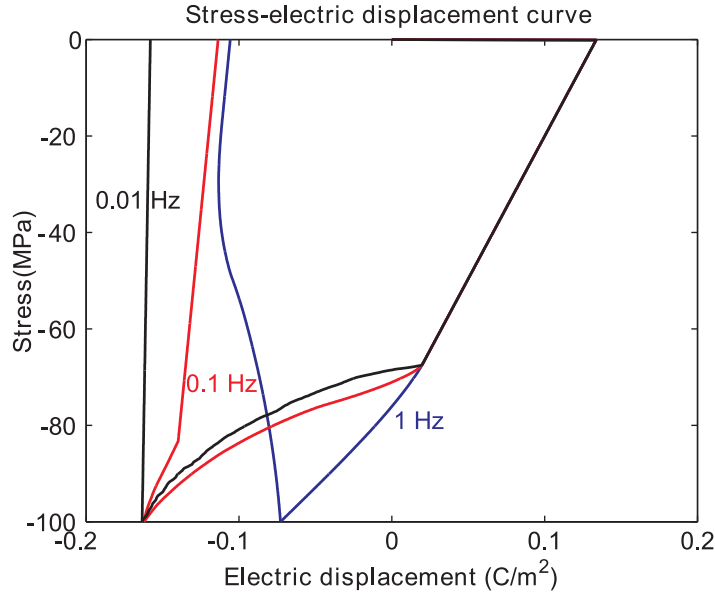


Figure 5.16: Stress-electric displacement curves without probabilistic approach, $\sigma_{max} = 100$ MPa

As explained before, for polycrystalline piezoelectric materials it is observed that do-

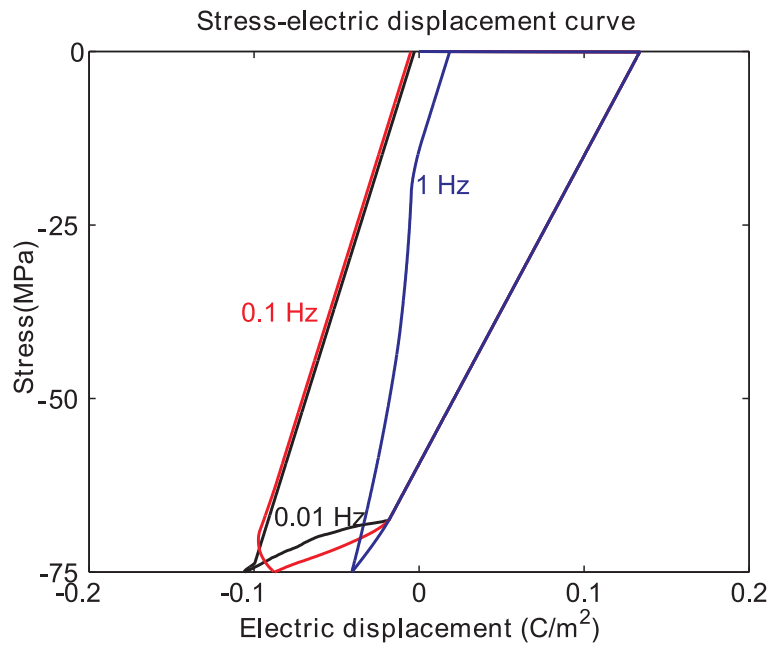


Figure 5.17: Stress-electric displacement curves without probabilistic approach, $\sigma_{max} = 75$ MPa

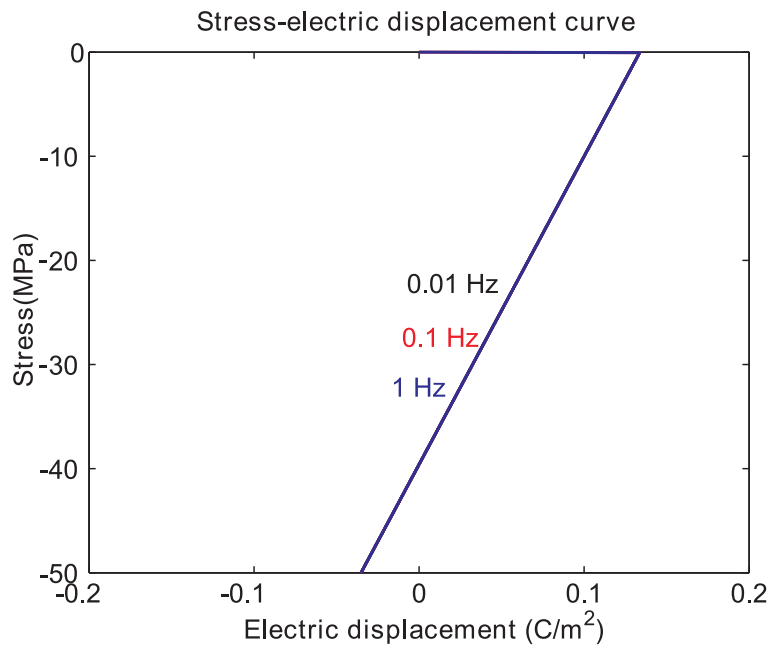


Figure 5.18: Stress-electric displacement curves without probabilistic approach, $\sigma_{max} = 50$ MPa

main switching can occur below the coercive field. This was modeled by probability functions in previous sections. Such a probability for domain switching below the coercive level is also implemented in the simulation of the rate dependent characteristics of PIC 151 by using a micromechanical model of piezoelectric materials which are subject to compressive stress. Figures 5.19 to 5.21 show compressive stress versus mechanical strain curves with an implementation of fourth order ($n=4$) probability function for loading with the same amplitudes and frequencies as in the non probabilistic approach. As it can be seen in the figures, the curves become smoother especially in the region near the coercive mechanical stress level compared with the ones that were simulated without implementing the probability criterion. So, the curves have a better correspondence to the experimental ones, especially for mechanical stress values in the region of the coercive field. The facts that decreasing of the coercive mechanical stress level with decreasing frequency of loading and further domain switching at the early unloading stage up to the coercive mechanical stress field for a compressive stress of higher frequencies are also noticeable in these curves.

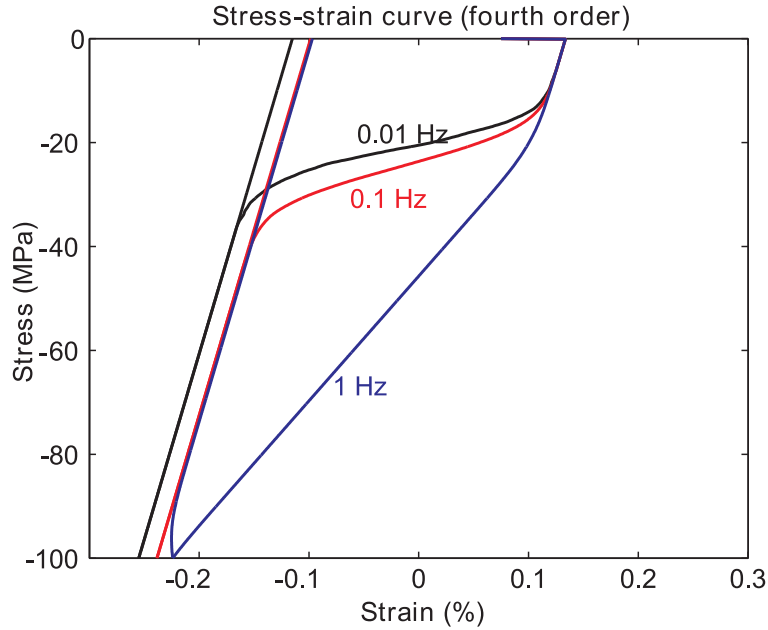


Figure 5.19: Stress-strain curves with fourth order polynomial for the probability function, $\sigma_{max} = 100$ MPa

Similarly, probabilistic approaches of fourth order ($n=4$) are also implemented to get a comparison of mechanical stress versus electric displacement curves in figures 5.22 to 5.24. All three figures illustrate the same characteristics and behaviours since the coercive mechanical stress level is considerably reduced when the probabilistic approach is used. Even curves for a 50 MPa amplitude value all possible domain switchings are

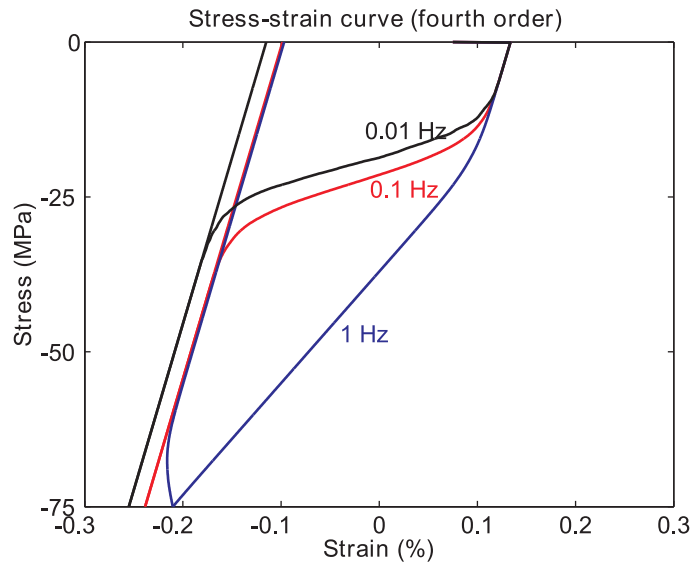


Figure 5.20: Stress-strain curves with fourth order polynomial for the probability function, $\sigma_{max} = 75$ MPa

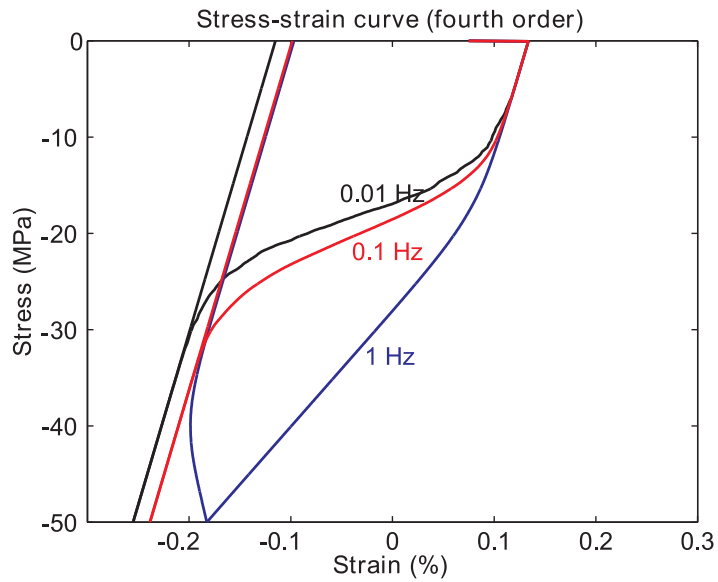


Figure 5.21: Stress-strain curves with fourth order polynomial for the probability function, $\sigma_{max} = 50$ MPa

accomplished and the electric displacement is saturated in lower rate loadings (0.1 Hz, 0.01 Hz). Therefore, responses become linear and independent of the applied stress

during unloading. Only the curve with 1 Hz frequency loading is not obeying such a behaviour due to the unfinished domain switching range to have complete depoled grains before unloading begins, so that there is a linearly inclined curve after the domain switching range ends as the compressive stress is released from its highest amplitude level.

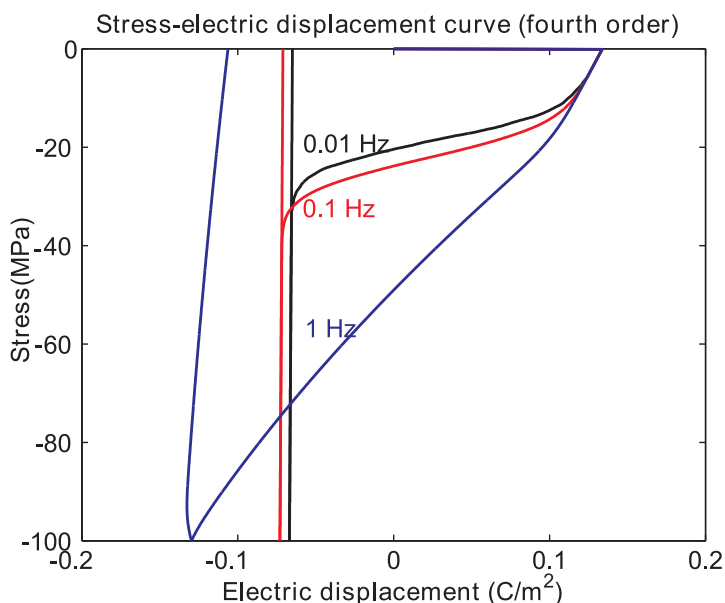


Figure 5.22: Stress-electric displacement curves with fourth order polynomial for the probability function, $\sigma_{max} = 100$ MPa

5.5 Concluding remarks

Nonlinear properties of perovskite type tetragonal ferroelectric and piezoelectric materials under uni-axial, high, cyclic, bipolar electric loading and uni-axial, unipolar compressive stress with various loading frequencies and amplitudes are simulated by using a micromechanical model. For the simulation material parameters of PIC 151 PZT ceramics are used. A piezoelectric linear constitutive model and a nonlinear domain switching with probability functions have been applied in the model. A linear kinetics model is used for the propagation of the new phase during the domain switching process. The simulated curves with a probabilistic approach do match better to the experimental curves than simulation results, in which probability functions have not been used. The model follows the basic characteristics of polycrystalline piezoelectric materials for different loading rates and amplitudes such as the change of the coercive mechanical and electric field and the change of the remnant polarization and strain.

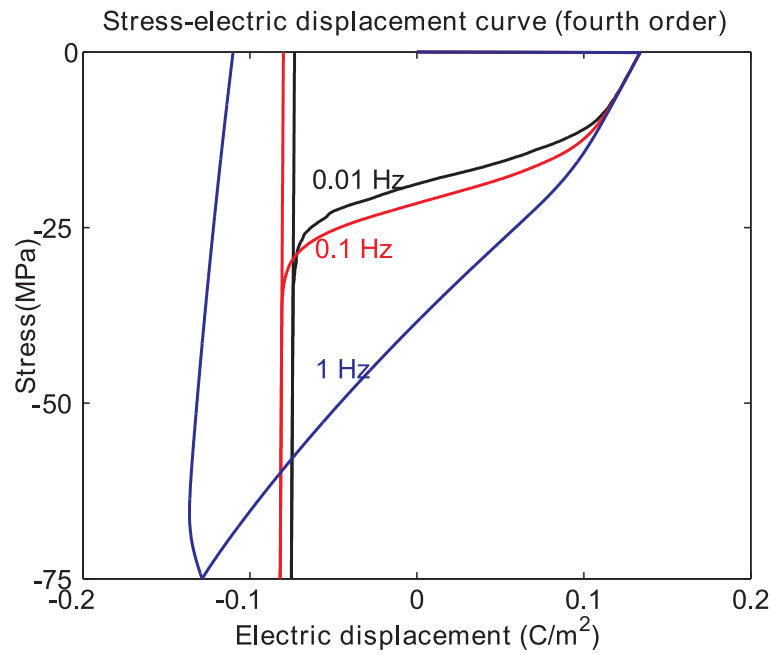


Figure 5.23: Stress-electric displacement curves with fourth order polynomial for the probability function, $\sigma_{max} = 75$ MPa

The simulations are presented in electric displacement versus electrical field hysteresis curves for electrical loading and mechanical stress versus mechanical strain, mechanical stress versus electric displacement curves for mechanical loading both during loading and unloading conditions explicitly.

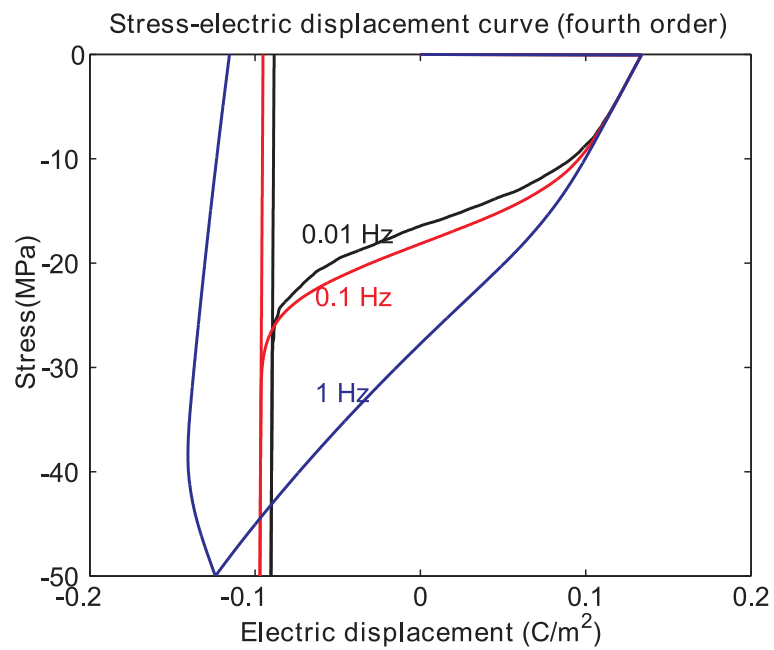


Figure 5.24: Stress-electric displacement curves with fourth order polynomial for the probability function, $\sigma_{max} = 50$ MPa

Chapter 6

Intergranular effects

6.1 Concepts

As it was mentioned in previous chapters, intergranular effects are significant factors for the nonlinearities in the characteristics of polycrystalline ferroelectric materials. Since domains and their polarization vectors are random in orientation and are connected by domain boundaries, they cannot behave independently from each other. Therefore, it is expected that they depend on polarization and strain characteristics of neighbouring domains. Figure 6.1 illustrates the effects of neighbouring microstructures to the domain switching behaviour of a particular lattice. Due to continuum theory, lattices which did not yet undergo a domain switching are sharing boundaries of high stress with neighbouring lattices which have no domain switching.

In chapter 4 intergranular effects are considered and simulated phenomenologically by using a probabilistic approach. In the present chapter, electrical and mechanical field effects are micromechanically taken into account for the consideration of intergranular effects in the simulations. Since all domains have a so-called spontaneous polarization in their microstructures, they can serve as an electrical source in addition to the macroscopic electric field for neighbouring elements (Refer to $D = \epsilon E$). Thus the electromechanical energy equation for the threshold of domain switching is extended to have such an electrical source term for neighbouring elements. Likewise, different displacement behaviours of domains lead to mechanical fields for neighbouring domains (Refer to $S = s\sigma$). Thereby, the electromechanical energy equation should contain such mechanical field terms of neighbouring domains. In this sense, it is now proposed to have a new electromechanical equation, which considers both mechanical and electrical field characteristics of neighbouring elements.

$$E_n P_n + C_{pe} \sum_i^{N_n} P_i E_i T_i + \sigma_n S_n + C_{pm} \sum_i^{N_n} S_i \sigma_i T_i \geq 0. \quad (6.1)$$

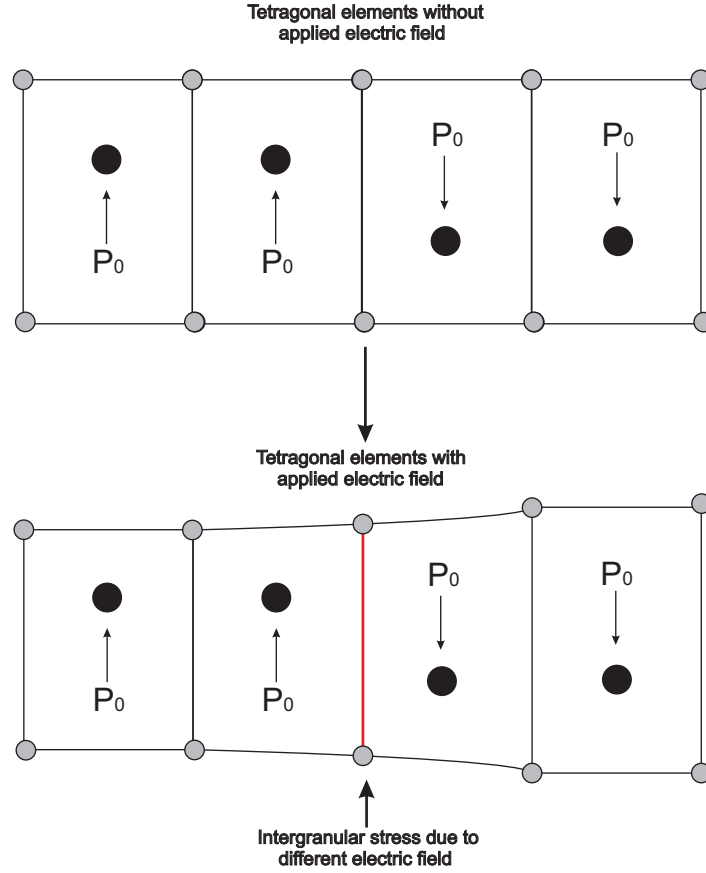


Figure 6.1: Intergranular effects between microstructures

where, C_{pe} and C_{pm} are assumed to be material dependent parameters regarding the electrical and mechanical fields of neighbouring elements. These material parameters will be investigated during simulations by using various different numerical values to understand their effects to the macroscopic curves. N_n is the number of neighbouring elements. T_i is the transformation matrix between elements.

Unlike Hwang's approach [HLM95] for the energy equation, this relation does not contain any critical and coercive electric field level at the right hand side of equation (6.1). The terms beginning with C_{pe} and C_{pm} are internally generated electrical and mechanical fields. Therefore, they do not have to be zero even though the externally applied electrical or mechanical fields are zero.

For the simplicity and in order to save time, simulations are performed for a two dimensional model with 30×30 elements. Therefore, there are 4 neighbours for each element to take intergranular calculations into consideration in the energy equation. This means that N_n is 4. A particular element, whose energy equation is calculated, is denoted with subscript n . Neighbours of this particular element are represented with

Grains with neighbouring elements

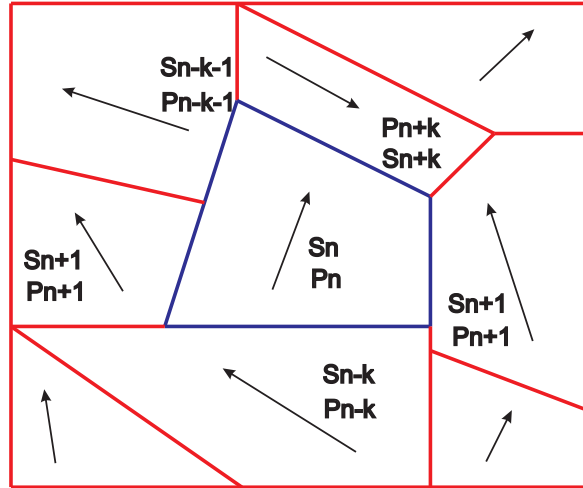


Figure 6.2: Particular element and neighbouring ones with corresponding strain and polarization assignments for energy equation

subscripts $n + 1$ or $n - 1$. Figure 6.3 illustrates the two dimensional elements with subscripts. Therefore, equation (6.1) takes the form

$$E_n P_n + \sum_{i=1}^4 C_{pe}(P_{n+i} E_{n+i} T_{n+i}) + \sigma_n S_n + \sum_{i=1}^4 C_{pm}(S_{n+i} \sigma_{n+i} T_{n+i}) \geq 0 \quad (6.2)$$

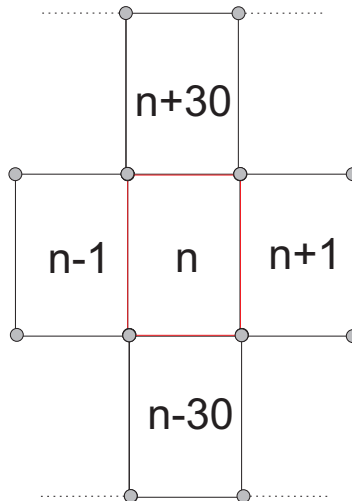


Figure 6.3: Element n and the corresponding neighbours in a 2-D assignment

6.2 Simulations

Simulations are carried out under the loading conditions of an alternating, uni-axial, bipolar electrical field with an amplitude of 1 kV/mm. So, except the magnitude of the amplitude of the electric field, the pure electrical loading has the same characteristics as the loading in the previous chapters. Despite the externally applied mechanical stress is zero, the mechanical stress terms of neighbouring elements in the electromechanical energy equation are not zero, since internal stresses are generated due to the nonlinear phase transformation. These internal stresses are calculated and inserted in the electromechanical energy equation by using linear elasticity theory. Simulation results are presented only in mechanical strain versus electric field butterfly curves, because parameters in the electromechanical energy relations can significantly effect mechanical strain versus electric field butterfly curves much more than electric displacement versus electric field hysteresis curves. Since the shape of the butterfly curves are strongly dependent on the types of domain switching, it is much more logical to evaluate the electromechanical energy relation which is mainly based on intergranular effects with different types of domain switchings (90° and 180°) in perovskite type tetragonal piezoelectric materials. The simulation curves presented here have the information about how many percent of domain switchings are 90° or 180° type.

Figure 6.4 shows mechanical strain versus electric field butterfly curves, in which 0.65 and 0.35 are assumed for the parameters C_{pe} and C_{pm} in the electromechanical energy equation. These parameters are chosen arbitrarily. During the simulation, 66 % of elements are performing 90° domain switching whereas the rest are 180° domain switchings. Figure 6.5 illustrates another butterfly curve with the same C_{pe} value but a different C_{pm} value with a magnitude of 0.7, namely two times the one used in figure 6.4. It is found that the percentage of 90° domain switching is reduced to 59 % by an amount of 6 % compared to figure 6.5. As it is known that the main cause of negative strain and tips of the butterfly curve at coercive electric field level is 90° switching. One can easily observe the difference between these two curves by comparing their tip or minimum strain values, which can go below zero values for figure 6.4. On the other hand, the tip values could not reduce to negative strain values in figure 6.5. According to this observation one can conclude that the strain value can go down to negative values as the value of C_{pm} is decreased in the model. Another significant difference between these two curves is the coercive electric field value, which can be defined as the electric field where the strain reaches its tip magnitude. As it was explained before, there is no constant coercive electric field value defined in our electromechanical energy relation. Therefore, the coercive electric field value can change according to the parameters (C_{pe} and C_{pm}) chosen in this relation. In figure 6.4, the coercive electric field is found to be 0.28 kV/mm which is smaller than the coercive field (0.33 kV/mm) found in 6.5. If the material dependent C_{pm} value is further increased more as in figure 6.6, the coercive field increases to 0.44 kV/mm. The C_{pm} value is changed to 1.05

while C_{pe} is kept constant during the simulation. 55 % of domains are observed to have 90° domain switchings in figure 6.6. Another important parameter of butterfly curves is that the remnant or saturation strain does not change remarkably with respect to different material dependent C_{pm} values used to simulate these curves.

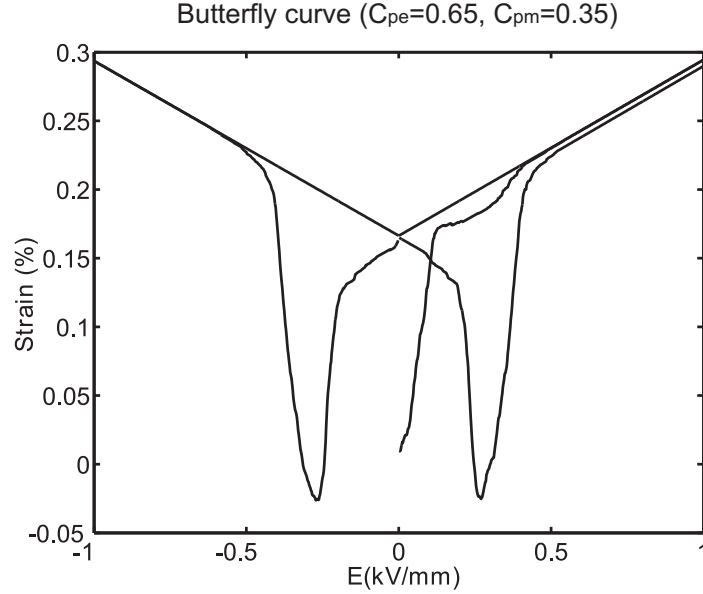


Figure 6.4: Butterfly curve ($C_{pe} = 0.65$, $C_{pm} = 0.35$)

Figures 6.7 and 6.8 show mechanical strain versus electric field curves for the same C_{pm} value, which is 0.7. This time the C_{pe} values are varied during the simulations. In figure 6.7 C_{pe} is chosen to be 0.45 which is two times the value used in the simulation in figure 6.8. In the former butterfly curve, tips are smooth and enlarged, whereas in the latter butterfly curve tips are much sharper. Unlike figure 6.7, the minimum strain value does not go below zero in figure 6.8. So we can claim that reduction of the C_{pe} value will decrease the magnitude of the strain tips in the butterfly curves. This statement can be proven by another observation from these simulations that more domains are undergoing 90° domain switching in figure 6.7 than in figure 6.8. 59 % of elements are found to have 90° domain switching in the simulation of figure 6.7, whereas this percentage is reduced drastically in figure 6.8 to 38 %. There is also a slight increment in remnant strain in figure 6.8 compared to figure 6.7. But this difference is not high enough to argue that the electrical material constant C_{pe} has a strong influence on the remnant or saturation value of the butterfly curves. Still, there are some domain switchings occurring in the early stage of the loading below the coercive level for figure 6.7. That is why, there are discontinuities at zero electric field in figure 6.8. Also it cannot be concluded that the domain switching level is affected by this C_{pe} parameter. The reason is that the macroscopic coercive electric field levels are approximately the

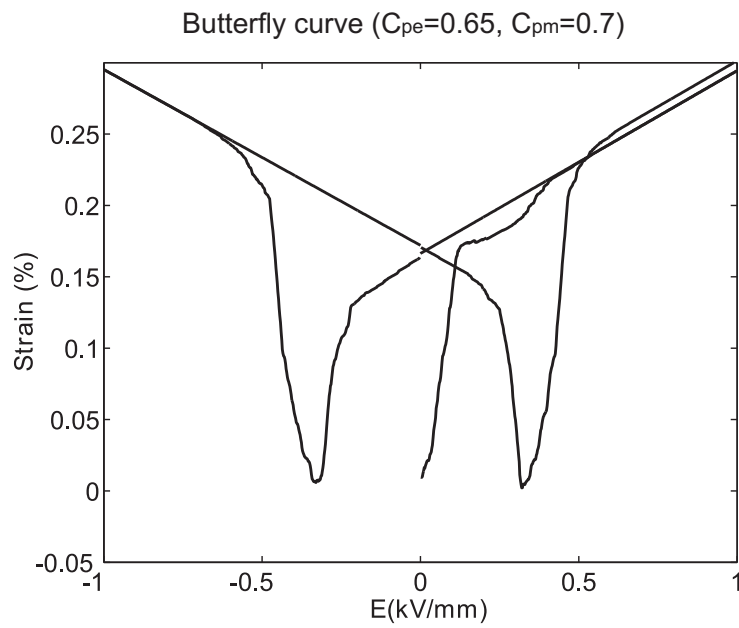


Figure 6.5: Butterfly curve ($C_{pe} = 0.65, C_{pm} = 0.7$)

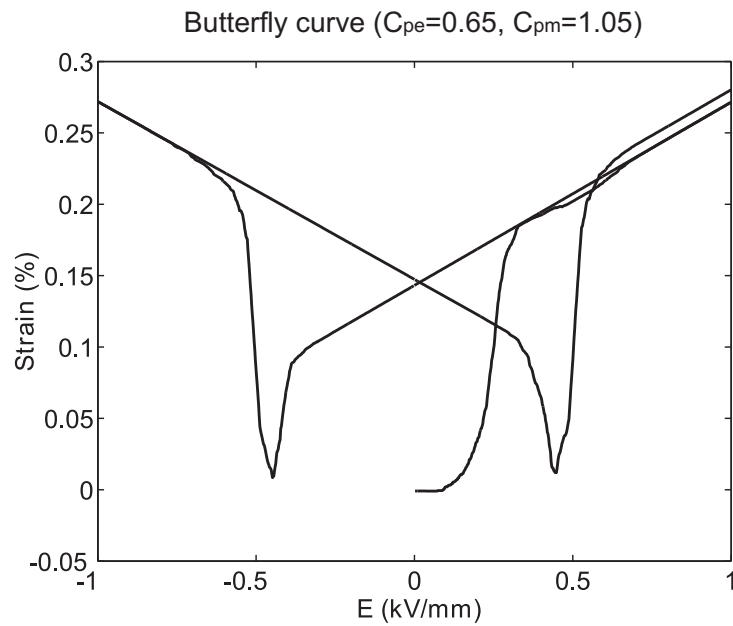
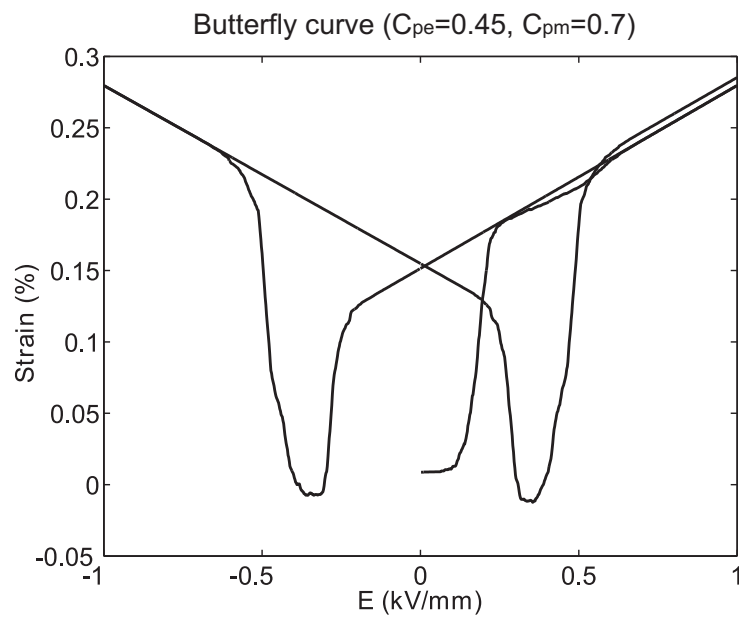
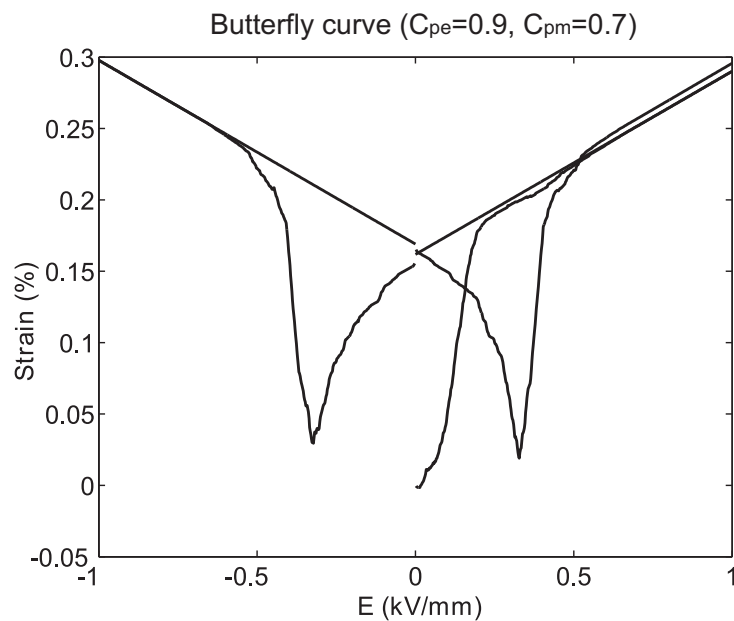


Figure 6.6: Butterfly curve ($C_{pe} = 0.65, C_{pm} = 1.05$)

same for both of the simulations. In figure 6.4, the coercive electric field value is found to be 0.34 kV/mm which is just 0.02 kV/mm higher than the coercive field shown in figure 6.8.

Figure 6.7: Butterfly curve ($C_{pe}=0.45, C_{pm}=0.7$)Figure 6.8: Butterfly curve ($C_{pe}=0.9, C_{pm}=0.7$)

As earlier explained commercial piezoelectric motors or sensors show nonlinearities when they are operated with an electrical loading, which is much lower than the coercive electric field level. The reason for such nonlinearities or small hysteresis loops

is also domain switching, which occurs due to intergranular effects between grains. Such small hysteresis loops can be a problem for the applications of these piezoelectric actuators and sensors. Recently, there are some control units which are developed for the compensation of these nonlinearities to have linear characteristics during small electromechanical operations by using a Preisach model [Pre38]. In previous chapters such small hysteresis loops in butterfly curves are modeled by using a phenomenologically based probabilistic approach. In this chapter additional terms are introduced in the electromechanical energy equation to consider intergranular effects and to explain these small nonlinear behaviours. In order to reproduce nonlinearities for a low electromechanical loading uni-axial, quasi-static, bipolar electrical loading is applied with 0.1 kV/mm or 0.2 kV/mm amplitude, which is one tenth or one fifth of the amplitude of the value of the loading which is implemented for the butterfly curves in figures 6.9 to 6.11. This alternating loading is applied to a fully poled perovskite type tetragonal piezoelectric material. Figure 6.9 illustrates the mechanical strain versus electric field curve with a cyclic loading of 0.1 kV/mm amplitude with the addition of the first poling of PIC 151 piezoelectric material up to 1 kV/mm. In this simulation, C_{pe} and C_{pm} values are assumed to be 0.65 and 0.7, respectively. After the fully poled case and releasing of the loading from 1 kV/mm to zero, the material is subjected to a cyclic electric field starting with a negative electric field with an amplitude of 0.1 kV/mm. In this phase, there occur some domain switchings despite the amplitude is lower than the coercive field. 6.3 % of the elements are undergoing a domain switching in which all of them are 90° switching leading to strain changes and a hysteresis loop. But still the amplitude of the loading is not strong enough to let all domains to have domain switching. Therefore, the tips of the butterfly curves cannot be seen in this simulation. Figure 6.10 illustrates also the mechanical strain versus electric field butterfly curve with the same loading conditions but with a different amplitude, which is 0.2 kV/mm. The same C_{pe} and C_{pm} values are chosen as in figure 6.9. Although the amplitude of loading is still under the level of the coercive electric field, 35 % of the elements have domain switching 95 % of which undergo a 90° domain switching during the first loading in negative direction. Like in figure 6.9 the loading amplitude in figure 6.10 is still not strong enough to let the strain go to the deepest value. As it can be expected the area of the hysteresis loop is enlarged due to the increased number of 90° domain switchings. If the amplitude of the applied alternating electric field is increased, domain switching will dominate and the butterfly curve will occur again. Figure 6.11 shows a mechanical strain versus electric field curve with an amplitude of 0.4 kV/mm uni-axial, quasi-static electric field for piezoelectric material, which is initially fully poled up to 1 kV/mm electric field. The loading is not complete cyclic. The same C_{pe} and C_{pm} values are again chosen as in figures 6.9 and 6.10. It is found that 83 % of the elements experience a domain switching and among them 54 % are 90° switchings. Especially, just after the loading passes through an electric field of -0.2 kV/mm, the strain is decreasing with a high slope. Most of the 90° domain switchings are occurring in this

region. Having reduced the minimum tip value, the strain is going to increase by the second 90° switchings which give rise to a positive strain in loading direction. Although the amplitude of the electric field is high enough to reach the minimum strain value, it is still not strong enough to have saturation. The reason is that 17 % of elements have not experienced any domain switching. Therefore, the mechanical strain stays below 0.15 % which is under the level of the remnant polarization, as the maximum electric field is achieved. One of the basic drawbacks of this simulation is the lack of symmetry. There occur some 180° domain switchings before 90° switchings at the positive loading range, which cannot be explained physically. Still the same minimum strain value with negative loading is also achieved in the positive loading range.

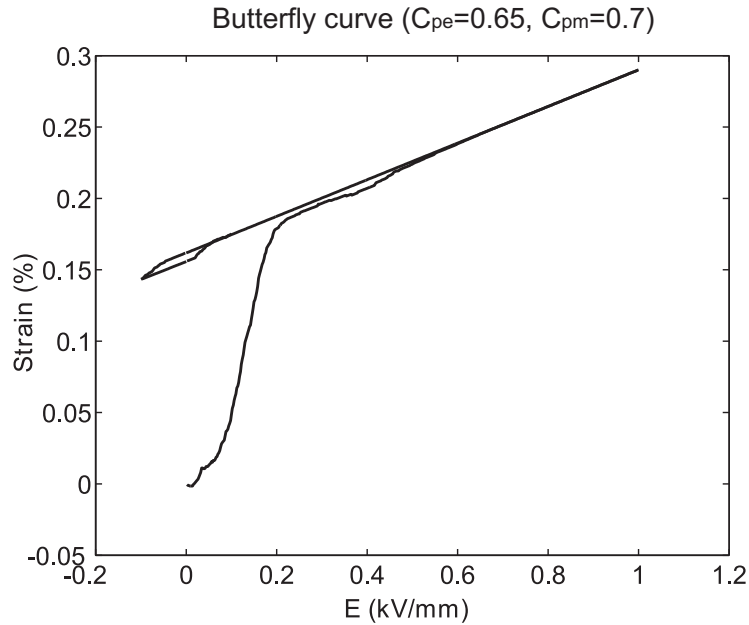


Figure 6.9: Hysteresis loop in the butterfly curve with 0.1 kV/mm amplitude of the cyclic electric field ($C_{pe}=0.65$, $C_{pm}=0.7$)

Rate or frequency dependent characteristics of mechanical strain versus electric field butterfly curves are also investigated with the new electromechanical energy relation by using a linear kinetics model, which has been formulated and explained in previous chapters in detail. Simulations are performed for the electric loading with different frequencies (0.01 Hz, 0.1 Hz, and 1 Hz) and an amplitude of the electric field of 1 kV/mm, which corresponds to the electric field level far above the coercive field. The simulation results are presented in figure 6.12, in which C_{pe} and C_{pm} values are assumed to be 0.65 and 0.7. The coercive electric field is increasing when the frequency is increased from 0.01 Hz to 1 Hz in analogy to the observations in chapter 5. Another important property of these curves with alternating loading with a high frequency

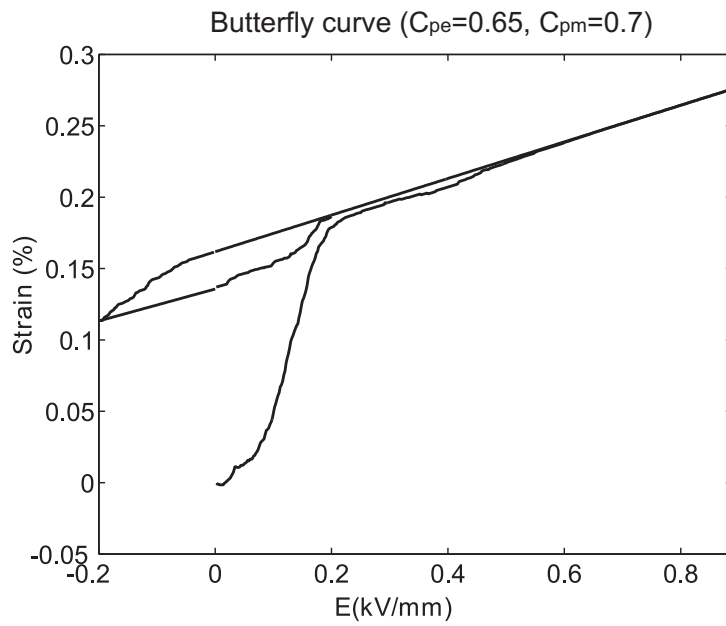


Figure 6.10: Hysteresis loop in the butterfly curve with 0.2 kV/mm amplitude of the cyclic electric field ($C_{pe}=0.65, C_{pm}=0.7$)

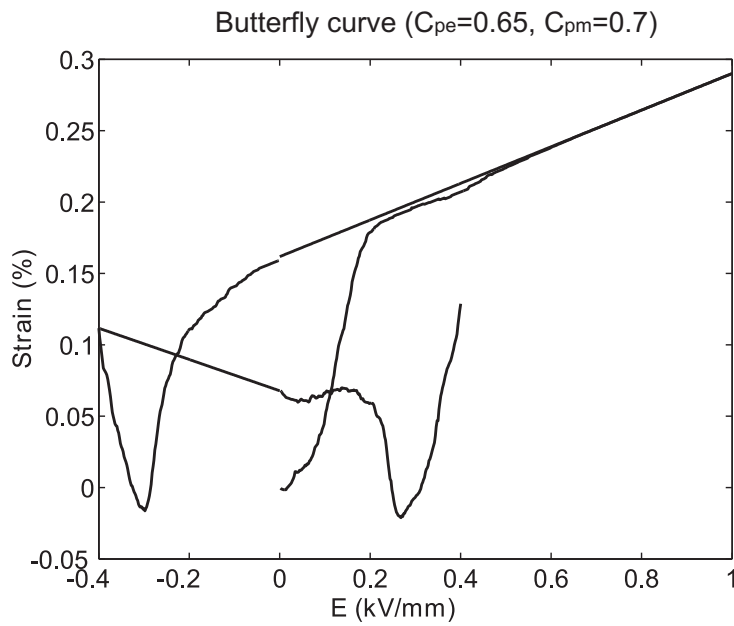


Figure 6.11: Butterfly curve with 0.4 kV/mm amplitude of electric field ($C_{pe}=0.65, C_{pm}=0.7$)

is that the mechanical strain is increasing even for a decreasing electric field during unloading provided that the actual electric field is larger than the coercive field. For a cyclic loading with a frequency of 1 Hz the strain value cannot reach the saturation level. Yet, the strain is increasing for a decreasing electric field as far as the applied electric field is larger than the coercive field. The remnant or saturation polarization is approximately constant for all frequency levels. The amplitude of the electric field is so strong that all elements finish their domain switching processes. On the other hand, the minimum mechanical strain value is slightly increasing (tips are going up) when the loading frequency is increased from 0.1 Hz to 1 Hz, but this statement cannot be generalized, since there is no difference of strain between the loading of 0.1 Hz and 0.01 Hz. Finally, it should be added that the percentage of 90° or 180° domain switchings is nearly constant when the frequency of the loading is changing.

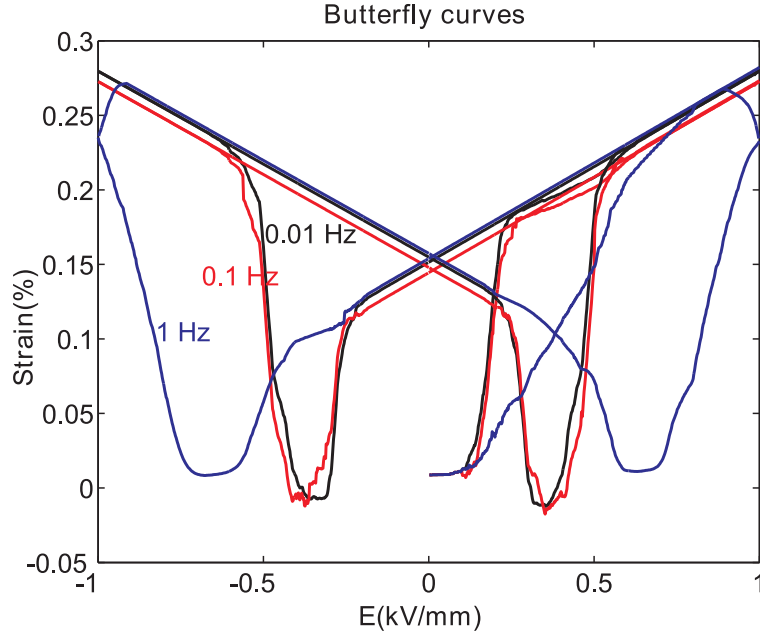


Figure 6.12: Butterfly curves with 1 kV/mm amplitude of the cyclic electric field ($C_{pe}=0.65$, $C_{pm}=0.7$)

6.3 Concluding remarks

In this chapter nonlinear properties of tetragonal ferroelectric and piezoelectric materials under uni-axial, cyclic and quasi-static electrical loading are simulated by using a micromechanical model based on intergranular effects. A piezoelectric linear constitutive model and a nonlinear domain switching with electromechanical energy relation

with various material parameters have been used in the model. Material parameters are varied in order to understand their influence to mechanical strain versus electric field butterfly curves. Butterfly curves are also investigated with different amplitude values for the electric field, which are lower than the coercive field for getting small hysteresis loops. Lastly, this electromechanical energy relation is combined with a linear kinetics model to get rate dependent characteristics of butterfly curves with different frequency conditions.

Chapter 7

Summary

Nonlinear properties of piezoelectric materials are one of the significant problems for actuators and sensors, which are commonly used in scientific and engineering applications. The nonlinearities even increase and become complicated, when piezoelectric materials are operated in a high performance usage. Piezoelectric linear constitutive relations are approximations and cannot explain these nonlinear behaviours.

In this study, properties of tetragonal perovskite type piezoceramic materials have been simulated by using a new micromechanical model for PIC 151 PZT ceramics. In the first part of the study the model is presented with simulations of these materials under uni-axial, high, quasi-static, cyclic bipolar electric loading and compressive stress separately. A piezoelectric linear constitutive model, and nonlinear domain switching with probability functions have been used in the model. A probabilistic approach is implemented for the explanation of intergranular effects in a phenomenological manner. The maximum of the applied electrical field and mechanical stress are 2 kV/mm and 100 MPa, correspondingly. Simulation results are presented in macroscopic electric displacement versus electric field hysteresis and mechanical strain versus electric field butterfly curves for electrical loading and electric displacement versus mechanical stress and mechanical strain versus mechanical stress curves for a compressive loading. It is found that the hysteresis curves using probability functions do better match the experimental hysteresis curves than simulation results in which probability functions have not been used. Moreover, piezoelectric materials under various constant compressive stress (20 MPa, 40 MPa) with alternating electric field have been deeply investigated by the extension of the micromechanical model. Significant characteristics of piezoelectric materials under electromechanical loading are captured during the simulation according to the experiments.

The micromechanical model is further improved in order to simulate rate dependent properties under a cyclic loading by means of linear kinetics theory. The simulations are performed for moderate frequency levels (0.01 Hz - 1 Hz). Maximum applied electro-

mechanical loadings are varied (1 kV/mm - 2 kV/mm) for a better understanding of the characteristics of nonlinearities near and above the coercive electric levels where nonlinear phase transformations or domain switchings dominate. Amplitudes of the applied compressive stress are chosen in the range of 50 Mpa - 100 MPa. Increasing of the coercive field values and remnant or saturation polarization and mechanical strain for smaller amplitudes of the loading and continuing further domain switchings during the early unloading stage as far as the cyclic electric field or mechanical stress is above the coercive field are the common findings of these simulations. Interesting results about the effect of the coupling coefficient in the mechanical loading case especially in the depoling region for mechanical strain and electric displacement versus mechanical stress curves are shown for various critical amplitude values.

Simulation of the influence of intergranular effects to macroscopic properties of piezoelectric materials by a micromechanical approach has been one of the basic aims of this work. Electrical and mechanical characteristics of neighbouring grains have been successfully implemented in the calculation of electromechanical energy equation for the onset of phase transformation. By the application of intergranular effects of neighbouring elements nonlinear domain switchings have been simulated even in low electromechanical conditions. Therefore, the model can explain nonlinearities of polycrystalline piezoelectric materials, which are subjected to an electrical loading in a wide range of amplitude values (0.1 kV/mm - 1 kV/mm). The model becomes robust enough to explain nonlinearities both for low (below coercive electric field) and for strong loading conditions. In addition to this, the model is further extended to simulate a frequency dependent electrical loading with the help of linear kinetics theory.

In the future, the idea of intergranular effects can be improved more for the implementation of micromechanical models. In this research, there are only two parameters involved for intergranular mechanical and electrical effects. More material parameters are necessary regarding to the types of possible phase transformations. Further studies on these material parameters can lead to better simulation results and matching with corresponding experimental data. The model applied in this study can be used for a mechanical loading also.

Frequency dependent properties have been modelled by using linear kinetics, which has the same principle as given by Merz [Mer54]. Instead of using such an old model, nonlinear kinetics theory and movement of domain wall concepts can be implemented better for the simulation of electromechanical loading with moderate frequencies. Applied frequency and amplitude levels can also be varied in a wide range, especially for piezoelectric actuators and sensors in future works.

Bibliography

- [AKK94] Abeyaratne, R., Kim, S.J., Knowles J.K., "One dimensional model for shape memory alloys", *International Journal of Solids and Structures* 31, 2229-2249, 1994.
- [AH70] Allik, H., Hughes, T.J.R., "Finite element method for piezoelectric vibration", *International Journal for numerical methods in engineering.*, Vol. 2, pp. 151-157, 1970.
- [Arl97] Arlt, G., "A model for switching and hysteresis in ferroelectric ceramics," *Integrated Ferroelectrics*, Vol. 16, pp. 229-236, 1997.
- [Arl96A] Arlt, G., "A physical model for hysteresis curves of ferroelectric ceramics," *Ferroelectrics*, Vol. 189, pp. 103-119, 1996.
- [Arl96S] Arlt, G., "Switching and dielectric nonlinearity of ferroelectric ceramics," *Ferroelectrics*, Vol. 189, pp. 91-101, 1996.
- [AN88] Arlt, G. and Neumann, H., "Internal bias in ferroelectric ceramics: origin and time dependence," *Ferroelectrics*, Vol. 87, pp. 109-120, 1988.
- [ADMS1] Arockiarajan, A., Delibas, B., Menzel, A., Seemann, W., "Studies on rate-dependent switching effects of piezoelectric materials using a finite element model," *Computational material science*, (In press).
- [ADS04] Arockiarajan, A., Delibas, B., Seemann, W., "Nonlinear simulation of piezoelectric materials by micromechanical approach with probability function," *Computational modelling and simulation of materials*, (2004).
- [ADSM04] Arockiarajan, A., Delibas, B., Seemann, W., Menzel A, "Simulation of nonlinear behaviour of piezoceramic materials using probability functions," *3rd European conference on structural control*, (2004).
- [Aul90] Auld, B.A., "Acoustic fields and waves in solids", Robert E. Krieger, Florida, 1990.

- [Av39] Avrami, M., "Kinetics of phase change . I General Theory", *Journal of Chemical Physics*, Vol. 7, pp. 1103-1112, 1939.
- [Av40] Avrami, M., "Kinetics of phase change . II Transformation-time relations for random distribution of nuclei ", *Journal of Chemical Physics*, Vol. 8, pp. 212-224, 1940.
- [Av41] Avrami, M., "Kinetics of phase change . III Granulation, Phase Change, and Microstructure", *Journal of Chemical Physics*, Vol. 9, pp. 177-184, 1941.
- [BSKS05] Ball, B.L., Smith, R.C., Kim, S.-J., Seelecke, S., "A ferroelectric switching model for Lead Zirconate-Titanate (PZT)", *Center for Research in Scientific Computation-North Carolina State University*, Report-crsc-tr05-16, 2005.
- [BGM881] Bassiouny, E., Ghaleb, A.F., Maugin, G.A., "Thermodynamical formulation for coupled electromechanical hysteresis effects-I. Basic equations", *Int. J. Engng Sci.*, Vol. 26, No. 12, pp. 1279-1295, 1988.
- [BGM882] Bassiouny, E., Ghaleb, A.F., Maugin, G.A., "Thermodynamical formulation for coupled electromechanical hysteresis effects-II. Poling of ceramics", *Int. J. Engng Sci.* Vol., 26, No. 12, pp. 1297-1306, 1988.
- [BM891] Bassiouny, E., Maugin, G.A., "Thermodynamical formulation for coupled electromechanical hysteresis effects-III. Parameter identifications", *Int. J. Engng Sci.*, Vol. 27, No. 8, pp. 975-987, 1989.
- [BM892] Bassiouny, E., Maugin, G.A., "Thermodynamical formulation for coupled electromechanical hysteresis effects-IV. Combined electromechanical loading", *Int. J. Engng Sci.*, Vol. 27, No. 8, pp. 989-1000, 1989.
- [BW89] Bast, U., Wersing W., "The influence of internal voids with 3-1 connectivity on the properties of piezoelectric ceramics prepared by a new planar process", *Ferroelectrics*, 94, pp. 229-242, 1989.
- [BHY98] Beldica, E.C., Hilton, H.H., Yi, S., "Viscoelastic damping and piezo-electric control of structures subjected to aerodynamic noise", *Proc. 4th AIAA/CEAS Aeroacoustics Conf.*, pp. 805-815, 1998.
- [Bos87] Boser, O., "Statistical theory of hysteresis in ferroelectric materials", *Journal of Applied Physics*, Vol. 62(4), pp. 1344-1348, 1987.
- [BRB01] Burcu, E., Ravichandran, G., Bhattacharya, K., "Electro-mechanical behaviour of 90-degree domain motion in Barium Titanate single crystals", *Proceeding of SPIE* Vol. 4333, pp. 121-130, 2001.

- [BRB02] Burcesu, E., Ravichandran, G., Bhattacharya, K., "Observation of domain motion in single-crystal Barium Titanate under combined electromechanical loading conditions", IUTAM Sym. on Mechanics of Martensitic Phase Transformations in Solids, pp. 63-70, 2002.
- [Cad46] Caddy, W.G., Piezoelectricity, McGraw-Hill, New York, 1946.
- [CBKHSB02] Cao, S., Brand, U., Kleine-Besten, T., Hoffmann, W., Schwenke, H., Bütetisch, S., Büttgenbach, S., "Recent developments in dimensional metrology for microsystem components", *Microsystem technologies*, Vol. 8, pp. 3-6, 2002.
- [CE93] Cao, H., Evans, A.G., "Nonlinear deformation of ferroelectric ceramics," *Journal of Am. Ceram. Soc.*, 76, pp. 890-896, 1993.
- [CG01] Cao, X., Gabbert, U., "Nonlinear finite element modelling and analysis of piezoelectric materials and structures", *Innovationskollegs Adaptive mechanische Systeme*, Otto-von-Guericke-Universität Magdeburg, pp. 65-74, 2001.
- [CTX99] Cao, W., Tavener, S., Xie, S., "Simulation of boundary condition influence in a second order ferroelectric phase transition", *Journal of Applied Physics*, Vol. 86(10), pp. 5739-5746, 1999.
- [Cer] CeramTec. AG., www.ceramtec.com
- [CC01] Chaplya, P.M., Carman, G.P., "Dielectric and piezoelectric response of lead zirconate-lead titanate at high electric and mechanical loads in terms of non-180° domain wall motion", *Journal of applied Physics*, Vol. 90 (10), pp. 5278-5286, 2001.
- [CFH97] Chen, X., Fang, D.N., Hwang, K.C., "Micromechanics simulation of ferroelectric polarization switching," *Acta mater.*, Vol. 45, No. 8, pp. 3181-3189, 1997.
- [CL98] Chen, W., Lynch, C.S., "A micro-electro-mechanical model for polarization switching of ferroelectric materials," *Acta Mater.*, 46, No. 15, pp. 5303-5311, 1998.
- [CM80] Chen, P.J., Montgomery, S.T., "A macroscopic theory for the existence of the hysteresis and butterfly loops in ferroelectricity", *Ferroelectrics*, Vol. 23, pp. 199-208, 1980.
- [CW98] Chen, I-W., Wang, Y., "A domain wall model for relaxor ferroelectrics", *Ferroelectrics*, Vols. 206-207, pp. 245-263, 1998.
- [Chr88] Christensen, D.A., "Ultrasonic Bioinstrumentation", John Wiley, New York, 1988.

- [Cro93] Cross, L.E., "Ferroelectric ceramics: tailoring properties for specific applications," *Ferroelectric ceramics*, Basel: Birkhäuser, 1993.
- [CM99] Cocks, A.C.F., McMeeking, R.M., "A phenomenological constitutive law for the behaviour of ferroelectric ceramics", *Ferroelectrics*, Vol. 228, pp. 219-228, 1999.
- [Dam98] Damjanovic, D., "Ferroelectric, dielectric and piezoelectric properties of ferroelectric thin films and ceramics", *Rep. Prog. Phys.*, Vol. 61, pp. 1267-1324, 1998.
- [Dam97] Damjanovic, D., "Stress and frequency dependence of the direct piezoelectric effect in ferroelectric ceramics", *Journal of Applied Physics*, Vol. 82(4), pp. 1788-1797, 1997.
- [DSFF00] Dapino, M.J., Smith, R.C., Faidley, L.E., Flatau, A.B., "A coupled structural-magnetic strain and stress model for magnetostrictive transducer", *Journal of intelligent material systems and structures*, 11(2), pp. 134-152, 2000.
- [Dap02] Dapino, M.J., "Magnetostrictive materials", *Encyclopaedia of smart materials*, M. Schwartz, Ed., John Wiley and sons, New York, pp. 600-620, 2002.
- [Del02] Delibas, B., "Precision cutting in CNC turning machines", Master Thesis, Sabanci University, Graduate School of Engineering and Natural Sciences, 2002.
- [DAS04] Delibas, B., Arockiarajan, A., Seemann, W., "Nonlinear simulation of piezoceramic materials using micromechanical approach", 45th AIAA /ASME /ASCE /AHS /ASC structures, structural dynamics, and materials conference, 2004.
- [DAS05] Delibas, B., Arockiarajan, A., Seemann, W., "A nonlinear model to piezoelectric polycrystalline ceramics under quasi-static electromechanical loading", *Journal of material science: materials in electronics*, Vol. 16(8), pp.507-515, 2005.
- [DAS1] Delibas, B., Arockiarajan, A., Seemann, W., "Rate dependent properties of perovskite type tetragonal piezoelectric materials using micromechanical model", *International journal of solids and structures*, (In press).
- [Dro60] Drougard, M.E., "Detailed study of switching current in Barium Titanate", *Journal of Applied Physics*, Vol. 31(2), pp. 352-355, 1960.
- [Dun95] Dunn, M.L., "Effects of grain shape anisotropy, porosity, and microcracks on the elastic and dielectric constants of polycrystalline piezoelectric ceramics", *J. Appl. Phys.*, pp. 1533-1541, 1995.
- [EZP05] Elhadrouz, M., Zineb, T.B., Patoor, E., "Constitutive law for ferroelectric and ferroelastic single crystals: a micromechanical approach", *Computational materials science.*, 32, pp. 355-359, 2005.

- [FC00S] Fotinich, Y., Carman, G.P., "Nonlinear behaviour of polycrystalline piezoceramics," *Smart Structures and Materials*, Proceeding of SPIE Vol. 3992, pp. 319-330, 2000.
- [FC00J] Fotinich, Y., Carman, G.P., "Stresses in piezoceramics undergoing polarization switchings", *Journal of Applied Physics*, Vol. 88(11), pp. 6715-6725, 2000.
- [FC02] Fotinich, Y., Carman, G.P., "Modeling polycrystalline behaviour of piezoceramics ", *Ferroelectrics*, Vol. 274, pp. 101-119, 2002.
- [FBW00] Fröhlich, A., Bröckner-Foit, D., Weyer, S., "Effective properties of piezoelectric polycrystal," *Smart structures and materials*, Proceeding of SPIE Vol. 3992, pp. 279-287, 2000.
- [GH97] Ghandi, K., Hagood, N.W., "A hybrid finite element model for phase transitions in nonlinear electro-mechanically coupled material", *Proceeding of SPIE Vol. 3039*, pp. 97-112, 1997.
- [GK76] Gerthsen, P., Krüger, G., "Coercive field in fine grained PLZT ceramics", *Ferroelectrics*, Vol. 11, pp. 489-492, 1976.
- [Har04] Harsimar, S., "Simulation of butterfly loops in ferroelectric materials", *Continuum Mechanics and Thermodynamics*, Vol. 16, Issue 1-2, pp. 163-175, 2004.
- [HOG05] Haug, A., Onck, P.R. Giessen E.V., "Internal stress generation during switching of ferroelectrics", *Coupled nonlinear phenomena-modelling and simulation for smart, ferroic, and multiferroic materials*, *MRS Proc.*, Vol. 881E, CC4.4, 2005.
- [HF04] Huber, J.E., Fleck, N.A., "Ferroelectric switching: a micromechanical model versus measured behaviour", *European Journal of Mechanics A/Solids*, 23, pp. 203-217, 2004.
- [HF01] Huber, J.E., Fleck, N.A., "Multi-axial electrical switching of a ferroelectric theory versus experiment", *Journal of the mechanics and physics of solids*, 49, pp. 785-811, 2001.
- [HFLM99] Huber, J.E., Fleck, N.A., Landis, C.M., McMeeking, R.M., "A constitutive model for ferroelectric polycrystals," *Journal of the mechanics and physics of solids*, 47, pp. 1663-1697, 1999.
- [HA00] Hwang, S.C., Arlt, G., "Switching in ferroelectric polycrystals", *Journal of Applied Physics*, Vol. 87(2), pp. 869-875, 2000.
- [HHMF98] Hwang, S.C., Huber, J.E., McMeeking, R.M., Fleck, N.A., "The simulation of switching in polycrystalline ferroelectric ceramics", *Journal of Applied Physics*, Vol. 84 (3), pp. 1530-1540, 1998.

- [HLM95] Hwang, S.C., Lynch, C.S., McMeeking, R.M., "Ferroelectric/Ferroelastic interactions and a polarization switching model," *Acta Metal. Mater.*, Vol. 43, No. 5, pp. 465-495, 1995.
- [HM98] Hwang, S.C., McMeeking, R.M., "The prediction of switching in polycrystalline ferroelectric ceramics," *Ferroelectrics*, Vol. 207, pp.465-495, 1998.
- [HW00] Hwang, S.C., Waser, R., "Study of electrical and mechanical contribution to switching in ferroelectric/ferroelastic polycrystals", *Acta Mater.*, Vol. 48, pp. 3271-3282, 2000.
- [JCJ71] Jaffe, B., Cook, W.R. and Jaffe, H., "Piezoelectric Ceramics", Academic Press, London and New York, 1971.
- [Jos92] Joshi, S.P., "Non-linear constitutive relations for piezoelectric materials", *Smart Mater. Struct.*,1, pp. 80-83, 1992.
- [Kah85] Kahn, M, "Acoustic and elastic properties of PZT ceramics and anisotropic pores", *J. Am. Ceram. Soc.*, 68, pp. 623-628, 1985.
- [Kam01] Kamlah, M., "Ferroelectric and ferroelastic piezoceramics-modeling of electromechanical hysteresis phenomena," *Continuum mech. thermodyn.*, 13, pp. 219-268, 2001.
- [KBMT97] Kamlah, M., Böhle, U., Munz, D., Tsakmakis, C., "Macroscopic description of the non-linear electro-mechanical coupling in ferroelectrics," *Smart structures and materials*, *Proceeding of SPIE Vol. 3039*, pp. 144-155, 1997.
- [KJ97] Kamlah, M., Jiang, Q., "A model for PZT ceramics under uni-axial loading," *Wissenschaftliche berichte, Forschungszentrum Karlsruhe, Institut für Materialforschung*, 1997.
- [KT99] Kamlah, M., Tsakmakis, C., "Phenomenological modeling of non-linear electro-mechanical coupling in ferroelectrics," *International journal of solids and structures*, 36, pp. 666-695, 1999.
- [Kkaj] Keiji Kusumoto of AIST, Japan: www.geocities.jp/kusumotokeiji/yougoeng.htm
- [KB01] Kessler, H., Balke, H., "On the local and average energy release in polarization switching phenomena", *Journal of the mechanics and physics of solids.*, 49, pp. 953-978, 2001.
- [KJ02] Kim, S.-J., Jiang, Q., "A finite element model for rate-dependent behaviour of ferroelectric ceramics," *International journal of solids and structures*, 39, pp. 1015-1030, 2002.

- [KR98] Kreher, W.S., Rödel, J., "Ferroelectric ceramics and composites: Statistical models for effective piezoelectric and pyroelectric properties," International symposium on applications of ferroelectrics, pp. 455-458, 1998.
- [Kr76] Krüger, G., "Domain wall motion concept to describe ferroelectric rhombohedral PLZT ceramics", *Ferroelectrics*, Vol. 11, pp. 417-422, 1976.
- [KO02] Kukushkin, S.A., Osipov, A.V., "Theory of switching in Ferroelectrics", *Ferroelectrics*, Vol. 280, pp. 169-199, 2002.
- [LYD56] Landauer, R., Young, D.R. and Drougard, M.E., "Polarization reversal in the barium titanate hysteresis loop," *Journal of Applied Physics*, Vol. 27(7), pp. 752-758, 1956.
- [Lan02] Landis, C.M., "A new finite-element formulation for electromechanical boundary value problems", *International journal for numerical methods in engineering*, Vol. 55, pp. 613-628, 2002.
- [Lan02] Landis, C.M., "Fully coupled, multi-axial, symmetric constitutive laws for polycrystalline ferroelectric ceramics," *Journal of the mechanics and physics of solids*., 50, pp. 127-152, 2002.
- [Lan01] Landis, C.M., "Symmetric constitutive laws for polycrystalline ferroelectric ceramics", *Smart structures and materials*, Newport Beach, CA, 2001.
- [LM99] Landis, C.M., McMeeking, R.M., "A self consistent model for switching in polycrystalline ferroelectrics electrical polarization only", *Proceeding of SPIE* Vol. 3667, pp. 172-180, 1999.
- [LF04] Li, F., Fang, D., "Simulation of domain switching in ferroelectrics by a three dimensional finite element," *Mechanics of Materials* 36, pp. 959-973, 2004.
- [LW02] Li, W.F., Weng, G.J., "A theory of ferroelectric hysteresis with superimposed stress", *Journal of Applied Physics*, Vol. 91(6), pp. 3806-3815, 2002.
- [LS96] Loge, R.E., Suo, Z., "Nonequilibrium thermodynamics of ferroelectric domain evolution", *Acta mater.*, Vol. 44, No.8, pp. 3429-3438, 1996.
- [LFLH99] Lu, W., Fang, D.-N., Li, C.Q., Hwang, K.-C., "Nonlinear electric-mechanical behaviour and micromechanics modelling of ferroelectric domain evolution," *Acta Mater.*, 47, No. 10, pp. 2913-2926, 1999.
- [Lyn96] Lynch, C.S. "The effect of uniaxial stress on the electro-mechanical response of 8/65/35 PLZT," *Acta Mater.*, 44, No. 10, pp. 4137-4148, 1996.

- [LM94] Lynch, C.S., McMeeking, R.M., "Finite strain ferroelectric constitutive laws", *Ferroelectrics*, Vol. 160, pp. 177-184, 1994.
- [MH97] McMeeking, R.M., Hwang, S.C., "On the potential energy of a piezoelectric inclusion and the criterion for ferroelectric switching", *Ferroelectrics*, Vol. 200, pp. 151-173, 1997.
- [ML02] McMeeking, R.M., Landis, C.M., "A phenomenological multi-axial constitutive law for switching in polycrystalline ferroelectric ceramics," *Journal of engineering science.*, 40, pp. 1553-1577, 2002.
- [Mer54] Merz, W.J., "Domain formation and domain wall motions in ferroelectric BaTiO₃ single crystals," *Physical review*, Vol. 95(3), pp. 690-698, 1954.
- [MV02] Meyer, B., Vanderbilt, D., "Ab initio study of ferroelectric domain walls in PbTiO₃", *Physical Review B*, Vol. 65, pp. 104111/1-104111/10, 2002.
- [MK98] Michelitsch, T., Kreher, W.S., "A simple model for the nonlinear material behaviour of ferroelectrics," *Acta mater.*, Vol. 46, No. 14, pp. 5085-5094, 1998.
- [MRLMY01] Mukherjee, B.K., Ren, W., Liu, S.-F., Masys, A.J., Yang, G., "Non-linear properties of piezoelectric ceramics", *Proceeding of SPIE* Vol. 4333, pp. 41-54, 2001.
- [Mur] Murata Manufacturing Co., www.murata.com
- [MM37] Murphy, E.J., Morgen, S.O., *Bell system tech. J.*, 16, 493, 1937.
- [NIOB80] Nagata, K, Igarashi, H., Okazaki, K., and Bradt, R.C., "Properties of an interconnected porous Pb(Zr,Ti)O₃ ceramics", *Jpn. J. Appl. Phys.*, Vol. 19, L37-L40, 1980.
- [NXKC90] Newnham, R.E., Xu, Q.C., Kumar, S., Cross, L.E., "Smart Ceramics", *Ferroelectrics*, Vol. 102, pp. 259-266, 1990.
- [Nye85] Nye, J.F., *Physical Properties of Crystals*, Oxford Clarendon Press, 1985.
- [PBDN01] Peelamedu, S.M., Barnett, A.R., Dukkupati, R.V., Naganathan, N.G., "Finite element approach to model and analyse piezoelectric actuators", *JSME International, Series C*, Vol. 44, pp. 476-485, 2001.
- [Pre38] Preisach, P., "Über die magnetische Nachwirkung", *Zeitschrift für Physik*, 94, pp. 277-302, 1938.
- [RCW76] Ralls, K.M., Courtney, T.H., Wulf, J., "Introduction to materials science and engineering", Wiley., Toronto, 1976.

- [Ros56] Rosen, C.A., "Ceramic transformers and filters", Proc. Electronic Comp. Symp., pp. 205-211, 1956.
- [RMBG04] Roy, S.S., Morros, C., Bowman, R.M., Gregg, J.M., "Superior electromechanical performance over PZT, in lead zinc niobate (PZN)-lead zirconium titanate (PZT) thin films", Appl. Phys., A, pp. 339-344, 2004.
- [RK99] Rödel, J., Kreher, W.S., "Effective properties of polycrystalline piezoelectric ceramics," Journal de physique IV, pp. 239-247, 1999.
- [RK00] Rödel, J., Kreher, W.S., "Modelling of domain wall contribution to the effective properties of polycrystalline ferroelectric ceramics," Smart structures and materials, Proceeding of SPIE Vol. 3992, pp. 353-362, 2000.
- [RK00F] Rödel, J., Kreher, W.S., "Modeling of the effective linear behaviour of piezoceramic ceramics," Ferroelectrics, Vol. 241, pp. 83-90, 2000.
- [OAI91] Omura, M., Adachi, H., Ishibashi, Y., "Simulation of ferroelectrics characteristics using a one-dimensional lattice model", Japanese journal of applied physics, Vol. 30, No. 9B, pp. 2384-2387, 1991.
- [SH96] Schaeufele, A.B., Haerdtl, K.H., "Ferroelastic properties of lead zirconate titanate ceramics," Journal of Am. Ceram. Soc., 79, (10), pp. 2637-2640, 1996.
- [Sch81] Schmidt, N.A., "Coercive force and 90° domain wall motion in ferroelectric PLZT ceramics with square hysteresis loops", Ferroelectrics, Vol. 31, pp. 105-112, 1981.
- [SZY82] Sears, F.W., Zemansky, M.W., Young, H.D., University Physics, 6th Ed., Addison-Wesley, 1982.
- [SAD04] Seemann, W., Arockiarajan, A., Delibas, B., "Micromechanical simulation of piezoelectric materials using probability functions", 2004 SPIE Proc. 5387, pp. 57-64, 2004.
- [SHF03] Shieh, J., Huber, J.E, Fleck, N.A., "An evaluation of switching criteria for ferroelectrics under stress and electric field", Acta Materialia, 51, pp. 6123-6137, 2003.
- [SRM98] Shur, V., Rumyantsev, E., Makarov, S., "Kinetics of phase transformations in real finite systems: Application to switching in ferroelectrics", Journal of Applied Physics, Vol. 84(1), pp. 445-451, 1998.
- [Smi05] Smith, R.C., Smart material systems, Model development, Siam, Philadelphia, 2005.

- [SOW01] Smith, R.C., Ounaies, Z., Wieman, R., "A model for rate dependent hysteresis in piezoceramic materials operating in low frequencies," NASA/CR-2001-211062, ICASE Report No.2001-26, 2001.
- [SA04] Sun, C.T., Achuthan, A., "Domain-switching criteria for Ferroelectric materials subjected to electrical and mechanical loads", *Journal of American Ceramic Soc.*, 87 (3), pp. 395-400, 2004.
- [TWSK02] Tadmor, E.B., Waghmare, U.V., Smith, G.S., Kaxiras, E., "Polarization switching in PbTiO₃:an ab initio finite element simulation", *Acta Mater.*, 50, pp. 2989-3002, 2002.
- [Tie69] Tiersten, H.F., "Linear piezoelectric plate vibrations", Plenum Press, New York, 1969.
- [TKU01] Torii, A., Kato, H., Ueda, A., "A miniature actuator with electromagnetic elements", *Electrical Engineering in Japan*, Vol. 134, No. 4, pp. 70-75, 2001.
- [Uch00] Uchino K., "Ferroelectric Devices", Marcel Dekker AG, New York, 2000.
- [VC00] Viehland D., Chen, Y.-H., "Random-field model for ferroelectric domain dynamics and polarization reversal", *Journal of Applied Physics*, 88,11, pp. 6696-6707, 2000.
- [VL01] Viehland, D., Li, J.-F., "Kinetics of polarization reversal in 0.7Pb(Mg_{1/3}Nb_{2/3})O₃-0.3PbTiO₃: Heterogeneous nucleation in the vicinity of quenched random fields", *Journal of Applied Physics*, Vol. 90(6), pp. 2995-3003, 2001.
- [WSCLZ04] Wang, J., Shi, S.-Q., Chen, L.-Q., Li, Y., Zhang, T.-Y., "Phase field simulations of ferroelectric/ferroelastic polarization switching", *Acta Materialia*, Vol. 52, pp. 749-764, 2004.
- [YNG03] Yan, C., Nakao, M., Go, T., Matsumoto, K., Hatamura, Y., "Injection molding for microstructures controlling mold-core extrusion and cavity heat flux," *Microsystem technologies*, Vol. 9, pp. 188-191, 2003.
- [YNLBL01] Yee, Y., Nam, H.-J., Lee, S.-H., Bu, J.U., Lee, J.-W., "PZT actuated micromirror for fine-tracking mechanism of high-density optical data storage.", *Sensor and Actuators A: Physical*, 89 (1-2), pp. 166-173, 2001
- [ZR93] Zhang, X.D., Rogers, C.A., "A macroscopic phenomenological formulation for coupled electromechanical effects in piezoelectricity", *Journal of intelligent material systems and structures*, Vol. 4, pp. 307-316, 1993.

- [Zho03] Zhou, D., "Experimental investigation of non-linear constitutive behaviour of PZT piezoceramics ," Ph.D. Thesis, Forschungszentrum Karlsruhe, 2003.
- [ZK04] Zhou, D., Kamlah, M., "High field dielectric and piezoelectric performance of soft lead zirconate titanate piezoceramics under combined electromechanical loading", *Journal of applied Physics*, Vol. 96 (11), pp. 6634-6640, 2004.
- [ZKM01] Zhou, D., Kamlah, M., Munz, D., "Rate dependence of soft PZT ceramics under electric field loading," *Smart Structures and Materials.*, Proceeding of SPIE Vol. 4333, pp. 64-70, 2001.

Appendix A

Theory of piezoelectricity

In this chapter, the basic linear piezoelectric theory will be explained and the mechanism will be built on a simple one dimensional model, by which the piezoelectric linear constitutive relations are derived. Similarly, thermodynamics follows with the principle of conservation of energy for achieving linear piezoelectric equations. Lastly, piezoelectric nonlinear constitutive relations are presented after the extension of the thermodynamical principles.

A.1 One dimensional model of piezoelectricity

In this part a one dimensional model for piezoelectricity is defined by using an electrically- neutral system of charges [Aul90]. Figure A.1 illustrates the model, which can show similar electromechanical characteristics like piezoelectric solids. There are two pairs of charges with different signs in the system. Center atoms which are designated with q are connected by a rigid rod. On the contrary, outside charges ($+Q$, $-Q$) are connected to the center atoms by simple elastic springs. Figures A.2 and A.3 show the model under the application of mechanical and electrical loading, correspondingly.

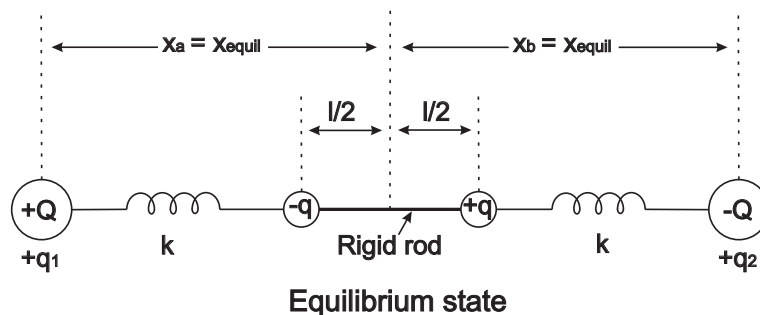


Figure A.1: Model of a piezoelectric solid [Aul90]

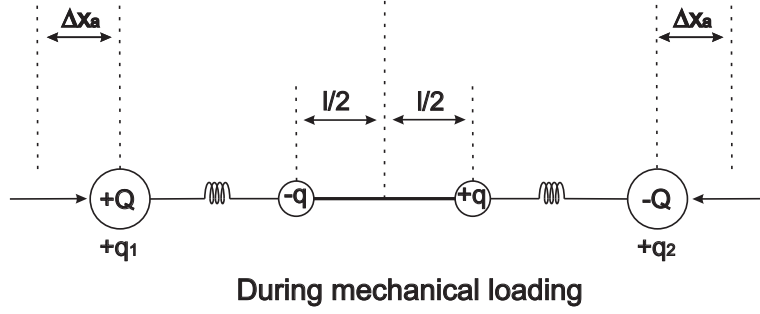


Figure A.2: Model with applied mechanical force

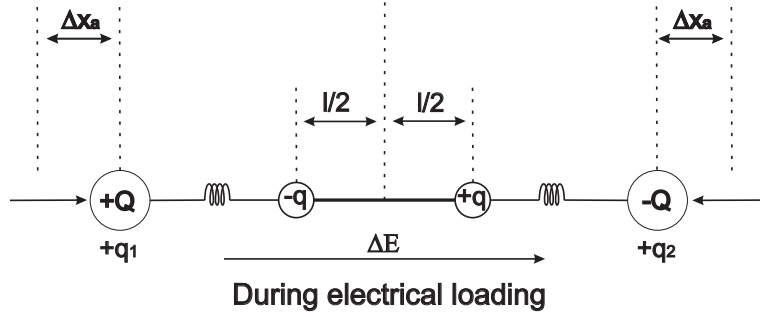


Figure A.3: Model with applied electric field

During the application of a mechanical loading the change in the displacement of outside charges is

$$\Delta X = \Delta x_{q_1} + \Delta x_{q_2} \quad (\text{A.1})$$

The dipole moment P with respect to center of the system is give by

$$P_x = \sum_n q_n x_n \quad (\text{A.2})$$

The dipole moment of the equilibrium state is

$$(P_x)_{equil} = -Qx_{equil} + ql/2 + ql/2 - Qx_{equil} = 2(ql/2 - Qx_{equil}). \quad (\text{A.3})$$

The springs are assumed to have the same elastic constants K . Then, statical forces acting on outward charges can be obtained

$$f_{q_1} = K(x_{q_1} - l/2) \quad (\text{A.4})$$

for the spring on the left hand side,

$$f_{q_2} = K(x_{q_2} - l/2) \quad (\text{A.5})$$

Electrostatic forces T acting on charges q_1 and q_2 can be calculated

$$T_{q_1} = qQ\left(\frac{-1}{(x_{q_1} - l/2)^2} - \frac{1}{(x_{q_1} + l/2)^2}\right) + Q^2\left(\frac{-1}{(x_{q_1} + x_{q_2})^2}\right) \quad (\text{A.6})$$

$$T_{q_2} = qQ\left(\frac{-1}{(x_{q_2} - l/2)^2} - \frac{1}{(x_{q_2} + l/2)^2}\right) + Q^2\left(\frac{-1}{(x_{q_2} + x_{q_1})^2}\right) \quad (\text{A.7})$$

The combined statical spring forces and electrostatic forces are

$$F_{q_1} = K(x_{q_1} - l/2) + qQ\left(\frac{-1}{(x_{q_1} - l/2)^2} - \frac{1}{(x_{q_1} + l/2)^2}\right) + Q^2\left(\frac{-1}{(x_{q_1} + x_{q_2})^2}\right) \quad (\text{A.8})$$

$$F_{q_2} = K(x_{q_2} - l/2) + qQ\left(\frac{-1}{(x_{q_2} - l/2)^2} - \frac{1}{(x_{q_2} + l/2)^2}\right) + Q^2\left(\frac{-1}{(x_{q_2} + x_{q_1})^2}\right) \quad (\text{A.9})$$

Considering the mechanical loading case, it can easily be proven from symmetry that charges q_1 and q_2 have the same absolute displacements

$$|x_{q_1}| = |x_{q_2}| \quad (\text{A.10})$$

Therefore, total change in displacement of the system given in by

$$\Delta X = 2 | \Delta x_{q_1} | \quad (\text{A.11})$$

The change in the dipole moment results in

$$\Delta P_x = -Q\Delta x_{q_1} - Q\Delta x_{q_2} = -2Q\Delta x_{q_2}. \quad (\text{A.12})$$

For the case of an electrical loading, the total forces in the system can be calculated by balance equations

$$\Delta F_{q_1} + Q\Delta E_{q_1} = 0 \quad (\text{A.13})$$

$$\Delta F_{q_2} - Q\Delta E_{q_2} = 0 \quad (\text{A.14})$$

where E_{q_1} and E_{q_2} are changes in electric field on the charges of q_1 and q_2 . For any small disturbance from the equilibrium condition, one can use the following relations

$$F_{q_1} = F_{q_1\text{equil}} + \left(\frac{\partial F_{q_1\text{equil}}}{\partial x_{q_1}}\right)_{\text{equil}} \Delta x_{q_1} + \left(\frac{\partial F_{q_1\text{equil}}}{\partial x_{q_2}}\right)_{\text{equil}} \Delta x_{q_2} \quad (\text{A.15})$$

$$F_{q_2} = F_{q_2equil} + \left(\frac{\partial F_{q_2equil}}{\partial x_{q_1}}\right)_{equil} \Delta x_{q_1} + \left(\frac{\partial F_{q_2equil}}{\partial x_{q_2}}\right)_{equil} \Delta x_{q_2} \quad (\text{A.16})$$

Since equilibrium forces are equal and have zero values and $x_{q_1} = x_{q_2}$

$$\left(\frac{\partial F_{q_1equil}}{\partial x_{q_1}}\right)_{equil} = -\left(\frac{\partial F_{q_2equil}}{\partial x_{q_2}}\right)_{equil} = A \quad (\text{A.17})$$

$$\left(\frac{\partial F_{q_1equil}}{\partial x_{q_2}}\right)_{equil} = -\left(\frac{\partial F_{q_2equil}}{\partial x_{q_1}}\right)_{equil} = B \quad (\text{A.18})$$

If (A.15) - (A.16) and (A.17) - (A.18) are substituted into eqn (A.13) - (A.14), this yields

$$A\Delta x_a + B\Delta x_b = -Q\Delta E_{q_1} \quad (\text{A.19})$$

$$-B\Delta x_a - A\Delta x_b = +Q\Delta E_{q_1} \quad (\text{A.20})$$

$$A(\Delta x_a - \Delta x_b) - B(\Delta x_a - \Delta x_b) = 0 \quad (\text{A.21})$$

Displacements of outhier charges are

$$\Delta x_{q_1} = \Delta x_{q_2} \quad (\text{A.22})$$

and the change in dipole moment is

$$\Delta P = -Q\Delta x_{q_1} - Q\Delta x_{q_2} = -2Q\Delta x_{q_1} \quad (\text{A.23})$$

Finally, one can describe the change in displacement and dipole moments of the system as follows

$$\Delta P_x = \epsilon\Delta E_x + d\Delta F_x \quad (\text{A.24})$$

$$\Delta L = d\Delta E_x + s\Delta F_x \quad (\text{A.25})$$

where s , ϵ , d are system parameters. These equations are the so-called linear constitutive piezoelectric relations.

A.2 Thermodynamical relations

The conservation of energy principle with the concept of the first law of thermodynamics for a piezoelectric material can be written by [Tie69]

$$\dot{U} = \sigma_{ij}\dot{S}_{ij} + E_i\dot{D}_i \quad (\text{A.26})$$

where, U denotes the internal energy. \dot{D}_i and \dot{S}_{ij} are the rates of change of the electric displacement and mechanical strain of the piezoelectric medium. The electric enthalpy H is defined by

$$H = U - E_i D_i \quad (\text{A.27})$$

A differentiation with respect to time gives

$$\dot{H} = \dot{U} - E_i\dot{D}_i - \dot{E}_i D_i \quad (\text{A.28})$$

Introducing this in eqn. (A.26) yields

$$\dot{H} = \sigma_{ij}\dot{S}_{ij} - \dot{E}_i D_i \quad (\text{A.29})$$

If the enthalpy H is considered to be a function of strain S and electric field E ,

$$H = H(S, E) \quad (\text{A.30})$$

and differentiating H with respect to time

$$\dot{H} = \frac{\partial H}{\partial S_{ij}}\dot{S}_{ij} + \frac{\partial H}{\partial E_i}\dot{E}_i \quad (\text{A.31})$$

and inserting in (A.31) yields

$$\left(\tau_{ij} - \frac{\partial H}{\partial S_{ij}}\right)\dot{S}_{ij} - \left(D_i + \frac{\partial H}{\partial E_i}\right)\dot{E}_i = 0 \quad (\text{A.32})$$

Since equation (A.32) is an identity, which must hold for arbitrary \dot{S}_{ij} and \dot{E}_i , which are consistent with the condition $\dot{S}_{ij} = \dot{S}_{ji}$, then

$$\frac{\partial H}{\partial S_{ij}} = \frac{\partial H}{\partial S_{ji}} \quad (\text{A.33})$$

$$\tau_{ij} = \frac{1}{2}\left(\frac{\partial H}{\partial S_{ij}} + \frac{\partial H}{\partial S_{ji}}\right) \quad (\text{A.34})$$

finally obtaining,

$$\tau_{ij} = \frac{\partial H}{\partial S_{ij}} \quad (\text{A.35})$$

$$D_i = -\frac{\partial H}{\partial E_i} \quad (\text{A.36})$$

If the enthalpy H is given by a homogeneous quadratic relation

$$H = \frac{1}{2}c_{ijkl}S_{ij}S_{kl} - d_{ijk}E_iS_{jk} - \frac{1}{2}\epsilon_{ijk}E_iE_j \quad (\text{A.37})$$

Then, from equations (A.35) and (A.36) the linear piezoelectric constitutive relations can be derived.

$$\tau_{ij} = c_{ijkl}S_{kl} - d_{kij}E_k, \quad (\text{A.38})$$

$$D_i = d_{ikl}S_{kl} + \epsilon_{ik}E_k. \quad (\text{A.39})$$

When temperature T and entropy W are taken into account and Gibbs' potential energy G [Jos92] is introduced, then G reads

$$G = U - \tau_{ij}S_{ij} - E_kD_k + TW. \quad (\text{A.40})$$

By assuming an adiabatic reversible system the differential form dU of the internal energy is given by

$$dU = \tau_{ij}dS_{ij} - E_kdD_k + TdW. \quad (\text{A.41})$$

Taking also the differential dG of Gibbs' potential

$$dG = dU - d\tau_{ij}S_{ij} - \tau_{ij}dS_{ij} - E_kdD_k - dE_kD_k - TdW - WdT. \quad (\text{A.42})$$

and Gibbs' potential after inserting into eqn. (A.41) becomes, the result is

$$dG = -\tau_{ij}dS_{ij} - dE_kD_k - WdT. \quad (\text{A.43})$$

Expressing Gibbs' potential in form of a Taylor series without having higher order terms

$$dG = \left(\frac{\partial G}{\partial \tau_{ij}}\right)d\tau_{ij} + \left(\frac{\partial G}{\partial E_k}\right)dE_k + \left(\frac{\partial G}{\partial T}\right)dT \quad (\text{A.44})$$

then, by using equation (A.43) and (A.44),

$$S_{ij} = -\left(\frac{\partial G}{\partial \tau_{ij}}\right) \quad (\text{A.45})$$

$$D_k = -\left(\frac{\partial G}{\partial E_k}\right) \quad (\text{A.46})$$

$$W = -\left(\frac{\partial G}{\partial T}\right) \quad (\text{A.47})$$

can be deduced.

When dependent variables S_{ij} , D_k , W are written as a function of the independent variables τ_{lm} , E_n and T , then

$$dS_{ij} = \left(\frac{\partial S_{ij}}{\partial \tau_{lm}}\right)d\tau_{lm} + \left(\frac{\partial S_{ij}}{\partial E_n}\right)dE_n + \left(\frac{\partial S_{ij}}{\partial T}\right)dT \quad (\text{A.48})$$

$$dD_k = \left(\frac{\partial D_k}{\partial \tau_{lm}}\right)d\tau_{lm} + \left(\frac{\partial D_k}{\partial E_n}\right)dE_n + \left(\frac{\partial D_k}{\partial T}\right)dT \quad (\text{A.49})$$

$$dW = \left(\frac{\partial W}{\partial \tau_{lm}}\right)d\tau_{lm} + \left(\frac{\partial W}{\partial E_n}\right)dE_n + \left(\frac{\partial W}{\partial T}\right)dT \quad (\text{A.50})$$

where s_{ijlm} is the elastic compliance, d_{ijn} is the piezoelectric constant, α_{ij} is the coefficient of thermal expansion, ϵ_{kn} is the dielectric constant, p_k is the pyroelectric coefficient and c is the specific heat. These material parameters can be defined as follows

$$s_{ijlm} = \left(\frac{\partial S_{ij}}{\partial \tau_{lm}}\right) \quad (\text{A.51})$$

$$d_{ijn} = \left(\frac{\partial S_{ij}}{\partial E_n}\right) = \left(\frac{\partial D_k}{\partial \tau_{lm}}\right) \quad (\text{A.52})$$

$$\alpha_{ij} = \left(\frac{\partial S_{ij}}{\partial T}\right) = \left(\frac{\partial W}{\partial \tau_{lm}}\right) \quad (\text{A.53})$$

$$\epsilon_{kn} = \left(\frac{\partial D_k}{\partial E_n}\right) \quad (\text{A.54})$$

$$p_k = \left(\frac{\partial D_k}{\partial T} \right) = \left(\frac{\partial W}{\partial E_n} \right) \quad (\text{A.55})$$

$$\frac{c}{T_0} = \left(\frac{\partial S}{\partial T} \right) \quad (\text{A.56})$$

Integrating the dependent variables finally results in constitutive equations,

$$S_{ij} = s_{ijklm} \tau_{lm} + d_{nij} E_n + \alpha_{ij} \Delta T \quad (\text{A.57})$$

$$D_k = d_{klm} \tau_{lm} + \epsilon_{kn} E_n + p_k \Delta T \quad (\text{A.58})$$

$$W = \alpha_{ij} \tau_{lm} + p_n E_n + \left(\frac{c}{T_0} \right) \Delta T \quad (\text{A.59})$$

The constitutive relations neglecting the temperature term can be written in matrix form,

$$\{S\} = [s^E] \{\tau\} + [d] \{E\} \quad (\text{A.60})$$

$$\{D\} = [d]^T \{\tau\} + [\epsilon^\tau] \{E\} \quad (\text{A.61})$$

These relations can be written in various forms like

$$\{\tau\} = [c^E] \{S\} - [g] \{E\} \quad (\text{A.62})$$

$$\{D\} = [g]^T \{S\} + [\epsilon^S] \{E\} \quad (\text{A.63})$$

or

$$\{\tau\} = [c^D] \{S\} - [h] \{D\} \quad (\text{A.64})$$

$$\{D\} = -[h]^T \{S\} - [\beta^S] \{D\} \quad (\text{A.65})$$

where the coefficients can be related to each other by

$$[c^E] = [s^E]^{-1} \quad (\text{A.66})$$

$$[g] = [c^E] [d] \quad (\text{A.67})$$

$$[\epsilon^S] = [\epsilon^\tau] - [g]^T [d] \quad (\text{A.68})$$

$$[c^D] = [c^E] + [g][\beta^S][g]^T \quad (\text{A.69})$$

$$[h] = [g][\beta^S] \quad (\text{A.70})$$

$$[\beta^S] = [\epsilon^S]^{-1} \quad (\text{A.71})$$

Nonlinear terms of spontaneous strain and spontaneous polarization (S_{0ij}, P_{0ij}) can be added to these linear constitutive relations to get nonlinear constitutive relations

$$S_{ij} = s_{ijklm}\tau_{lm} + d_{ijn}E_n + \alpha_{ij}\Delta T + S_{0ij} \quad (\text{A.72})$$

$$D_k = d_{klm}\tau_{lm} + \epsilon_{kn}E_n + p_k\Delta T + P_{0ij} \quad (\text{A.73})$$

The spontaneous strain and polarization is a nonlinear function of the mechanical stress and the electric field.

Resume

Name	Delibas
Surname	Bülent
Nationality	Turkish
Date of birth	12.06.1977, Malatya-Turkey
09/1988-06/1991	Gazi Secondary school, Malatya
09/1991-06/1995	M.A.O.L., High school Malatya
09/1995-06/2000	B.Sc. Major, Aeronautical Engineering B.Sc. Minor, Mechanical Engineering Middle East Technical University, Ankara-Turkey
09/2000-03/2002	Research Engineer in Tübitak, National Metrology Institute, Gebze-Turkey
03/2001-09/2002	M.Sc., Mechatronics Engineering Sabanci University, Istanbul-Turkey
10/2002-09/2005	Ph.D. student, Mechanical and Process Engineering DFG - Graduiertenkolleg 814 Kaiserslautern University of Technology
since 10/2005	Research Engineer in Dr. Johannes Heidenhain GmbH Research and Development (Rotary Encoders), Traunreut